1-1-2011

Photochemical treatment of organic constituents and bacterial pathogens from synthetic slaughterhouse wastewater by combining vacuum-UV and UV-C

Mauricio Barrera
Ryerson University

PHOTOCHEMICAL TREATMENT OF ORGANIC CONSTITUENTS AND BACTERIAL PATHOGENS FROM SYNTHETIC SLAUGHTERHOUSE WASTEWATER BY COMBINING VACUUM-UV AND UV-C

by

MAURICIO BARRERA

B.Eng. in Environmental Engineering

(El Bosque University, Colombia, 2005)

A thesis

presented to Ryerson University

in partial fulfillment of the

requirements for the degree of

Master of Applied Science

in the program of

Environmental Applied Science and Management

Toronto, Ontario, Canada, 2011

AUTHOR'S DECLARATION

I hereby declare that I am the sole author of this thesis.

I authorize Ryerson University to lend this thesis to other institutions or individuals for the purpose of scholarly research.

_____

I further authorize Ryerson University to reproduce this thesis by photocopying or by other means, in total or in part, at the request of other institutions or individuals for the purpose of scholarly research.

_____

ACKNOWLEDGMENTS

I would like to express my sincere gratitude to my supervisors, Dr. Mehrab Mehrvar and Dr. Kimberley Gilbride, for their guidance and support throughout the last two years of this research.

I would also like to acknowledge the principals from the NSERC Strategic Grant, Drs. Lynda McCarthy, Andrew Laursen, Vadim Bostan, and Ron Pushchak, whose comments, advice, and suggestions during our progress report meetings immensely benefitted this research. Thanks are given to PhD students, Masroor Mohajerani and Samira Ghafoori, for their help in troubleshooting and assistance in developing the kinetic model for this research as well as Masters student Shawn Clark for his valuable help with bacteria manipulation. Thanks are also due to Engineering technologist, Ali Hemmati and Daniel Boothe, from the Department of Chemical Engineering for manufacturing and assembling the experimental setup as well as Karen Terry from the Department of Chemistry and Biology for her assistance in obtaining all the materials needed during the experimental work.

I would also like to express my appreciation to my graduating cohort at Ryerson University, with whom I shared not only many times of enlightenment and entertainment, but also provided me with great support and encouragement.

I would have found this achievement much more difficult without the support of my family. I would like to specially thank my wife, Erika Rueda, for her patience, understanding, and invaluable support and encouragement throughout my graduate studies.

This research was financially supported by the Natural Science and Engineering Research Council of Canada (NSERC) through an NSERC Strategic Grant Program and Ryerson University.

This thesis is dedicated to my parents whose love, guidance, and sacrifice have made me the person I am today.

Also to my wife for her constant love, understanding, and encouragement.

ABSTRACT

Photochemical Treatment of Organic Constituents and Bacterial Pathogens from Synthetic Slaughterhouse Wastewater by Combining Vacuum-UV and UV-C

By:

Mauricio Barrera
Master of Applied Science,
Environmental Applied Science and Management
Ryerson University
2011

The reduction and degradation of total organic carbon (TOC) and bacteria inactivation efficiency using Vacuum-Ultraviolet (VUV) oxidation process, Ultraviolet-C (UV-C) photolytic process, and their combination (UV-C/VUV and VUV/UV-C) from synthetic slaughterhouse wastewater was investigated. TOC removal rates achieved during continuous mode operation were 6.2%, 5.5%, 5.8%, and 6.1%, respectively. In a second stage, H_2O_2 was added to both processes, UV-C/H_2O_2 and VUV/H_2O_2, and it was found that TOC removal rates were increased twice as much during continuous flow operation to 10.8% and 12.2%, respectively. The optimum molar ratio of H_2O_2/TOC was found to be 2.5 and 1.5 for each process respectively. Finally, it was observed that all photochemical processes achieved over 99.999% (five logs) of bacteria inactivation in a short period of irradiation time, 27.6 sec.

TABLE OF CONTENTS

LIST OF TABLES

LIST OF FIGURES

NOMENCLATURE

A	local volumetric rate of energy absorption (LVREA) (Einstein L^{-1} s^{-1})
C_i	concentration of component *i* (M)
D	diffusivity (m^2 s^{-1})
E. coli	*Escherichia coli*
f_i	fraction of photons absorbed by species i (dimensionless)
h	Planck's constant $6.62606876 \times 10^{-34}$ (J s)
k	first order reaction rate constant (s^{-1})
k'	second order reaction rate constant (M^{-1} s^{-1})
$k_{s(\lambda)}$	specific rate of light absorption by TOC (Einstein mol^{-1} s^{-1})
P. aeruginosa	*Pseudomonas aeruginosa*
Q	volumetric flow rate (L min^{-1})
q	radiant energy flux (Einstein m^{-2} s^{-1})
q_o	radiant energy flux on the sleeve wall (Einstein m^{-2} s^{-1})
r	position on r-axis for single lamp photoreactor (m)
R	photoreactor radius (m)
Re	Reynolds number, dimensionless
R_i	quartz sleeve radius (m)
$R\text{rxn},_i$	rate of reaction of component *i* (M s^{-1})
S. flexneri	*Shigella flexneri*
S. Typhimurium	*Salmonella enterica* serovar Typhimurium
u_z	axial velocity (m s^{-1})

ν	kinematic viscosity ($m^2\ s^{-1}$)
z	position on the z-axis (m)

Greek Letters

ε_i	molar absorptivity of component i ($M^{-1}\ m^{-1}$)
α	decadic absorption coefficient (m^{-1})
ϕ	quantum yield (mol $Einstein^{-1}$)
λ	wavelength (nm)
ρ	density ($kg\ m^{-3}$)
μ	dynamic viscosity ($kg\ m^{-1}\ s^{-1}$)
μ_s	solution extinction coefficient at 254 nm (m^{-1})
μ_w	water extinction coefficient at 254 nm (m^{-1})

Acronyms

AOPs	advanced oxidation processes
APHA	american public health association
BOD	biochemical oxygen demand
COD	chemical oxygen demand
CFU	colony forming unit
CFD	computational fluid dynamics
CSSs	combined sewer systems
CSOs	combined sewer overflows
DBPs	disinfection by-products
DNA	Deoxyribonucleic acid

EOP	electrical oxidation potential
GPM	gallons per minute
HAAs	haloaacetic acids
HRT	hydraulic retention time
LPM	liters per minute
LVREA	local volumetric rate of energy absorption
MPPs	meat processing plants
RNA	ribonucleic acid
TOC	total organic carbon
TDS	total dissolved solids
THMs	trihalomethanes
U.S EPA	U.S environmental protection agency
UV-A	ultraviolet range from 315 to 400 nm
UV-B	ultraviolet range from 280 to 315 nm
UV-C	ultraviolet range from 200 to 280 nm
VIS	visible light range from 400 to 700nm
VUV	vacuum-UV range from 100 to 200 nm
WHO	world health organization

CHAPTER 1

INTRODUCTION

Human activities, such as industrial, and agricultural production, as well as urbanization are the principal sources of water pollution. Globally, significant amounts of hazardous materials and pathogenic microorganisms are discharged into receiving waters daily. Currently, society is growing more aware of the importance water has for its quality of life and its very own existence, thus, increasing a mandate for clean water sources supported by new and more stringent regulations (Sullivan *et al.,* 2005). Such regulatory pressure is driving the development of new purification technologies in the water and wastewater treatment fields.

In practice, different treatment methods are applied to water and wastewater depending primarily on the nature and physicochemical properties of the effluent to be treated. For example, wastewater derived from urban areas can generally be processed efficiently through biological treatment plants by adsorption with activated carbon or by conventional chemical treatments such as chlorination, ozonation, and potassium permanganate oxidation (Tchobanoglous *et al.,* 2003; Reynolds and Richards, 1996). However, conventional technologies do not satisfy the discharge regulatory levels or subsequent reclaimed water reuse standards as these technologies fall short in overall pollutant removal efficiencies. More importantly, although the primary goal of current technologies is to purify source waters, they themselves are turning into pollution sources by

adding toxic chemicals during the purification process. For instance, disinfection chemicals, such as chlorine and ozone used to inactivate disease-causing microorganisms are responsible for the generation of hazardous compounds known as disinfection by-products (DBPs). DBPs include, but are not limited to, trihalomethanes (THMs), haloaacetic acids (HAAs), nitrosamines, and bromoform. DBPs are suspected carcinogens that may pose a potential threat to public health (Black and Veatch, 2010; Asano *et al.*, 2007).

As a result of the aforementioned issues, industrialized countries have been increasingly implementing more advanced water treatment technologies. In particular, a new type of technologies known as Advanced Oxidation Processes (AOPs), is becoming more popular due to their speed and effectiveness in the way they remove hazardous contaminants from water. AOPs comprise a set of technologies able to produce highly reactive intermediates, namely hydroxyl radicals ($^{\bullet}$OH). The dot on the radical species ($^{\bullet}$OH) indicates that an unpaired electron is present in the outer orbital. Among AOPs, the photochemical processes, which are based on ultraviolet (UV) radiation are of particular interest in the present work since they are the most simple and versatile processes to produce $^{\bullet}$OH radicals, which are oxidant species twice as powerful as common oxidants, such as chlorine or ozone. The $^{\bullet}$OH radicals are able to quickly degrade organic matter and chemical compounds in water, in some cases within seconds, depending on the wastewater being treated. Moreover, AOPs are highly effective in the disinfection processes for removing bacteria, viruses, and protozoa, while avoiding the production of toxic DBPs (Comninellis *et al.*, 2008).

Recent developments in analytical techniques have allowed the detection of a new group of hazardous contaminants present in trace amounts, which are becoming emerging contaminants of concern. This group of contaminants includes recalcitrant constituents, such as pharmaceutical active compounds and veterinary drugs, personal care products, endocrine disruptors, fluorinated surfactants, phthalates phenols, brominated diphenyl ethers, methyl tert-butyl ether (MTBE), and a group of volatile organic compounds stemming from oil derivatives such as BTEX (benzene, toluene, ethylbenzene, and xylenes), which are known to be highly toxic to human health. Their increasing presence in treated effluent reveals the incompetence of conventional treatment technologies to handle their removal (Aga, 2008; Barcelo and Petrovic, 2008; Asano *et al.*, 2007).

In the last decade, much of the literature available in water and wastewater treatment technologies focused on the potential applications of AOPs, in particular photochemical processes induced by UV radiation in the removal of not only organic matter and chemical constituents, but also the inactivation of disease-causing microorganisms from water and wastewater (Bolton and Cotton, 2008; Oppenlander, 2003). More importantly, AOPs can be used alone or in combination with conventional methods, particularly biological processes, to maximize the removal rate of organics while minimizing costs. The ability to develop effective technologies for water treatment is crucial to stop the destruction of water sources, which are vital to maintain healthy communities and prevent unwanted diseases.

For all aforementioned reason, it is paramount to test new technologies as they emerge to determine their reliability in solving real life issues. This study seeks to broaden

the information about the role AOPs can play in removing organic contaminants and waterborne infectious-disease microorganisms. Advanced oxidation processes prompted by UV radiation are technologies gaining momentum and they are establishing itself as an important and viable way for removing hazardous compounds produced in industrial processes before they are discharged to source waters not only in Canada, but all over the world.

1.1 Objectives

The goal of the present study is to test the Vacuum-UV (VUV) process effectiveness in degrading organic matter and removing bacterial pathogens from a synthetic slaughterhouse wastewater as well as to determine if the combination VUV/UV-C can result in efficiency gains for the overall process and serve as an alternative to the UV-C/H_2O_2 process. By omitting the addition of auxiliary oxidants such as H_2O_2, inefficient procedures such as monitoring and removing residual H_2O_2 concentrations after treatment may be avoided (Chelikani *et al.*, 2004; Oppenlander, 2003). More importantly, the results obtained from this investigation could reveal that processes such as AOPs, in particular VUV, can play an important role for the treatment of emerging contaminants of concern such as pesticides, herbicides, pharmaceuticals active compounds, personal care products, surfactants, and endocrine disruptors that are now the focus of health and environmental agencies around the world (IJC, 2010; Barcelo and Petrovic, 2008; Environment Canada, 2001). Consequently, the present study will shed light on how well the VUV process behaves and what features are subject to improvement as well as to where future research should be focused on.

In summary, the objectives of the present study are:

- To determine the performance of the Vacuum-UV (VUV) process in the removal of total organic carbon (TOC) and bacterial pathogens from synthetic slaughterhouse wastewater and pathogens disinfection.

- To compare TOC removal rates between the VUV process and other photochemical processes including UV-C photolysis, VUV/UV-C, UV-C/H_2O_2, and VUV/H_2O_2.

1.2 Expectations

It is hypothesized that the combination of VUV/UV-C will achieve similar TOC removal rates to that of the combination of UV-C/H_2O_2 and it could serve as a potential alternative to the UV-C/H_2O_2 process. The combination of VUV/UV-C will avoid the need to use auxiliary oxidants such as H_2O_2 and to control potential H_2O_2 residual concentrations hazardous to aquatic ecosystems, while minimizing costs and negative environmental impacts. By the combined VUV/UV-C process it is expected that both TOC and pathogens will be efficiently removed from a synthetic slaughterhouse wastewater. The VUV will produce from the water homolysis the $^{\bullet}OH$ radical species, which is highly reactive toward organic matter, while the UV-C will emit radiation at the germicidal wavelength (λ=254nm), which is highly effective in inactivating bacterial pathogens. Overall, it is expected that the combined VUV/UV-C will show potential for application in the water and wastewater treatment field.

CHAPTER 2

LITERATURE REVIEW

2.1 Introduction

The objective of the present research is to test the efficiency of VUV in the reduction of TOC from synthetic slaughterhouse wastewater and bacterial pathogens disinfection as well as its comparison with other photochemical processes. Before achieving this objective, further theoretical background information is required. The present chapter first provides a description of the main mechanisms by which photochemical process degrade organic matter, chemical compounds, and bacteria from wastewater. Then, this chapter describes and reviews the characteristics, environmental impacts, and regulatory framework of slaughterhouse wastewater as well as current technologies applied in its treatment. Finally, the need for advanced wastewater technologies is stressed as well as the opportunities created by AOPs to serve as good complementary technologies to conventional technologies, thus, maximizing treatment effectiveness and minimizing costs.

2.2 Advanced Oxidation Processes (AOPs)

AOPs consist of a set of mechanisms that produce highly reactive intermediates known as hydroxyl radicals ($^{\bullet}OH$). This species can degrade organic matter rapidly, which contrasts sharply with ordinary chemical oxidation processes that may take months and even years. This fast oxidation — in terms of seconds — of organic matter by $^{\bullet}OH$ species gave rise to the term "Advanced" (Bolton and Cotton, 2008). AOPs include photochemical degradation processes, such as UV/H_2O_2, UV/O_3, and UV/O_3/H_2O_2, in which UV radiation

plays a secondary role by initiating the photoreaction in the presence of an auxiliary oxidant to produce $^{\bullet}OH$ radicals; photocatalysis processes, such as TiO_2/UV and photo fenton reactions, in which a catalyst plays a secondary role by absorbing UV radiation to produce $^{\bullet}OH$ radicals; and chemical oxidation, such as O_3, O_3/H_2O_2 and H_2O_2/Fe^{2+} (Oppenlander, 2003; Tchobanoglous *et al.*, 2003).

AOPs have the same principles as the chemical oxidation processes associated with redox reactions, which involve the exchange of electrons between chemical species, leading to a change in the oxidation state of different compounds taking place in the process (Sawyer *et al.*, 2002). In redox reactions, the compounds gaining electrons are known as oxidizing agents, while compounds losing electrons are known as reducing agents. $^{\bullet}OH$ species, produced from different AOPs, are strong oxidizing agents, which are highly reactive toward organic matter. As McMurray and Fay (2003) illustrated, the exchange of electrons between an oxidant and a reductant is spearheaded by the difference in their electrical oxidation potentials (EOP).

Hydroxyl radical intermediates have the highest EOP (2.80V) of all the typical chemical oxidizing agents used in water purification and wastewater treatment processes. For example, the EOP value of $^{\bullet}OH$ radicals is more than twice than that of chlorine, and significantly higher than that of hypochlorite, hydrogen peroxide, ozone, chlorine dioxide, or permanganate as shown in Table 2.1 (Black and Veatch, 2010; Asano *et al.*, 2007). As a result, $^{\bullet}OH$ is the most powerful oxidant available in the water treatment field for breaking apart the carbon bonds, transforming parent compounds into either a less harmful material or into water and carbon dioxide as end products (mineralization). In some cases, the

mineralization of an organic compound cannot be reached, but the toxicity of the parent compound is reduced and eventually it can be treated by cheaper methods, such as biological treatment (Tarr, 2003; Tchobanoglous *et al.,* 2003). Because of their unpaired electron, $^{\bullet}OH$ are reactive electrophiles — electron-hunter — rapidly reacting with nearly all electron-rich organic compounds (Bolton, 2010). $^{\bullet}OH$ radicals also affect pathogens by destroying their cell wall — composed mostly of sugars and amino acids — and altering its permeability, causing cell protoplasm exposure and subsequent cell death (Oppenlander, 2003; Sosnin, 2006).

Table 2.1. Standard redox potential of selected oxidant species (adapted from Tarr, 2003).

Oxidant	E°**, V**
Fluorine	3.03
Hydroxyl radical	2.80
Atomic oxygen	2.42
Ozone	2.07
Hydrogen peroxide	1.77
Permanganate ion	1.67
Hypochlorous acid	1.49
Chlorine	1.36
Chlorine dioxide	1.27
Bromine	1.09

AOPs are usually aimed at treating organic constituents with highly toxicity profiles — endocrine disruptors, personal care products, pharmaceutical active compounds and their metabolites, pesticides, herbicides as well as carcinogenic disinfection by-products (DBPs), such as thrihalomethanes and nitrosamines — at trace levels (μg L^{-1}) (Asano *et al.,* 2007). Since typical treatment processes do not target these kinds of contaminants, AOPs are becoming a great complement to serve as a pre- or post-treatment to the usual biological

treatment (Tabrizi and Mehrvar, 2004). Thus, this technology increases the ability not only to remove organic compounds as well as refractory and toxic compounds, but also to inactivate disease-causing microorganisms.

Hydroxyl radicals are highly reactive towards organic matter and their main possible reaction types include radical addition (Reaction 2.1), hydrogen abstraction (Reaction 2.2), electron transfer (Reaction 2.3), and radical combination (Reaction 2.4) (Bolton, 2010; Asano *et al.*, 2007; Braun and Oliveros 1997; Legrini *et al.*, 1993).

1) The radical addition can be described as the $^{\bullet}OH$ addition to an unsaturated aliphatic or aromatic organic compound (R), such as $CH=CCl_2$ — trichloroethylene (TCE) — which results in the production of radical organic compounds; for example:

$$CHCl=CCl_2 + {}^{\bullet}OH \rightarrow {}^{\bullet}CHCl\text{-}C(OH)Cl_2 \qquad (2.1)$$

2) In the hydrogen abstraction mechanism, radical organic compounds are formed by the removal of a hydrogen atom — usually from the aliphatic hydrocarbons group — such as methanol (CH_3OH) under the $^{\bullet}OH$ action; for example:

$$CH_3OH + {}^{\bullet}OH \rightarrow {}^{\bullet}CH_2OH + H_2O \qquad (2.2)$$

3) Ions of higher valence are formed due to electron transfer, in which a monovalent negative ion forms either an atom or a free radical; for example:

$$I^{-} + {}^{\bullet}OH \rightarrow {}^{\bullet}I + OH^{-} \qquad (2.3)$$

4) Two radicals may combine to produce a stable product; for example:

$$^{\bullet}OH + {}^{\bullet}OH \rightarrow H_2O_2 \qquad (2.4)$$

As previously mentioned, UV radiation is able to inactivate and render bacteria harmless to human health as well as degrade organic contaminants that absorb UV radiation at different wavelengths. However, highly refractory compounds do not absorb UV radiation, whereby UV photolysis alone falls short of eliminating more complex organic compounds, such as pesticides, endocrine disruptors, detergents, and pharmaceuticals and personal care products (Oppenlander, 2003; Birkett and Lester, 2003). Nonetheless, adding auxiliary oxidants such as hydrogen peroxide (H_2O_2) and ozone (O_3), which produce the highly reactive hydroxyl radical species ($^{\bullet}OH$) under the action of UV radiation, can enhance the photolytic process.

Even though $^{\bullet}OH$ radicals are effective against a broad variety of toxic compounds, it has disadvantages that include the generation of intermediates that could be more resistant to further degradation than the parent compound, or maybe the intermediates are more toxic than the parent compound. As Tarr (2003) illustrated, the oxidation of atrazine by AOPs in some experimental studies produced intermediates more resistant to degradation than the parent compounds such as ammeline, cyanuric acid, or chlorodiaminotriazine. Although these compounds are not as toxic as the parent compound, it becomes more resistant to further degradation, hindering the final mineralization of the contaminant. For example, ammeline was reported to be produced as partial oxidation of atrazine during UV-C/H_2O_2, whereas cyanuric acid was produced during VUV irradiation (Tarr, 2003; Gonzalez *et al.*, 1994). Although both ammeline and cyanuric acid are less toxic than the parent compound, atrazine, they are harder to mineralize. However, in other studies where the experimental

conditions have been varied such as the concentration of hydrogen peroxide and pH as well as the absence of carbonates species have shown that UV-C/H_2O_2 is an effective process to degrade atrazine (De Laat *et al.,* 1997). Hence, it is important to know all the characteristics and degradation paths of the contaminants to be dealt with beforehand as well as the specific AOP technology to be used.

2.2.1 Ultraviolet Direct Photolysis

Ultraviolet radiation (UV) is a chemical process for drinking water disinfection, which does not require any additional chemicals. In the UV disinfection process, the formation of disinfection by-products (DBPs) as well as odour and taste are negligible, which are major drawbacks of chlorine and ozone (Manitoba Water Stewardship, 2005). Besides pathogen inactivation, the UV can oxidize simple organic compounds like the ones formed by carbon bonded to other key elements such as nitrogen, oxygen, hydrogen, sulphur, and phosphorus, which are the foundation of complex compounds such as proteins, amino acids, and peptides (Braun *et al.,* 1991; Maier *et al.,* 2009). The bonds that hold together organic matter absorb UV radiation resulting in bond cleavage. In this way, the energy of the photon emitted should be higher than the bond dissociation energy as shown in Table 2.2 (Luo, 2007; Maruani, 1998; Thomas and Burgess, 2008). However, the UV photolysis is innocuous against more complex compounds present in water, such as polymers, pesticides, or volatile organic compounds since they require higher energy in order to be broken down. As a result, the UV radiation alone is not enough to degrade recalcitrant compounds and therefore, it should be combined with auxiliary oxidants in order to produce more powerful oxidants such as $^{\bullet}OH$ radicals.

Table 2.2. Bond dissociation energies for common compounds (adapted from Luo, 2007).

Bond Type	Bond Energy (kJ mol^{-1})
C-H	413
C-Cl	335
C-O	356
C-N	335
C-C	346
C=C	610
C≡C	745
O-H	463

The UV-C radiation, in particular the germicidal region between 200-300 nm, as shown in Figure 2.1, has been used as an effective drinking water disinfectant since the early 1900s. The photons emitted at the germicidal region are absorbed by nucleic acids (DNA and RNA); being vital components within the cell they are adversely affected by this absorption, which causes a disruption in the genetic information transmission (Bolton and Cotton, 2008). Consequently, pathogenic agents such as bacteria, viruses, and protozoa can no longer replicate; therefore, they are no longer infectious.

2.2.1.1 Pathogen inactivation by UV radiation processes

The photons emitted by UV lamps are absorbed by the nucleic acids of the microorganisms, namely deoxyribonucleic acid (DNA) — responsible for the storage of genetic information — and ribonucleic acid (RNA) — template for the synthesis of proteins and transmission of information (Wang *et al.,* 2006a; Crittenden *et al.,* 2005). DNA and RNA can absorb radiation between 190 to 300 nm. Hence, the reproduction ability of the pathogens will be damaged and will no longer pose a risk to human health. Both purines (G and A) and pyrimidines (C, T and U) absorb UV radiation, yet the pyrimidines are more

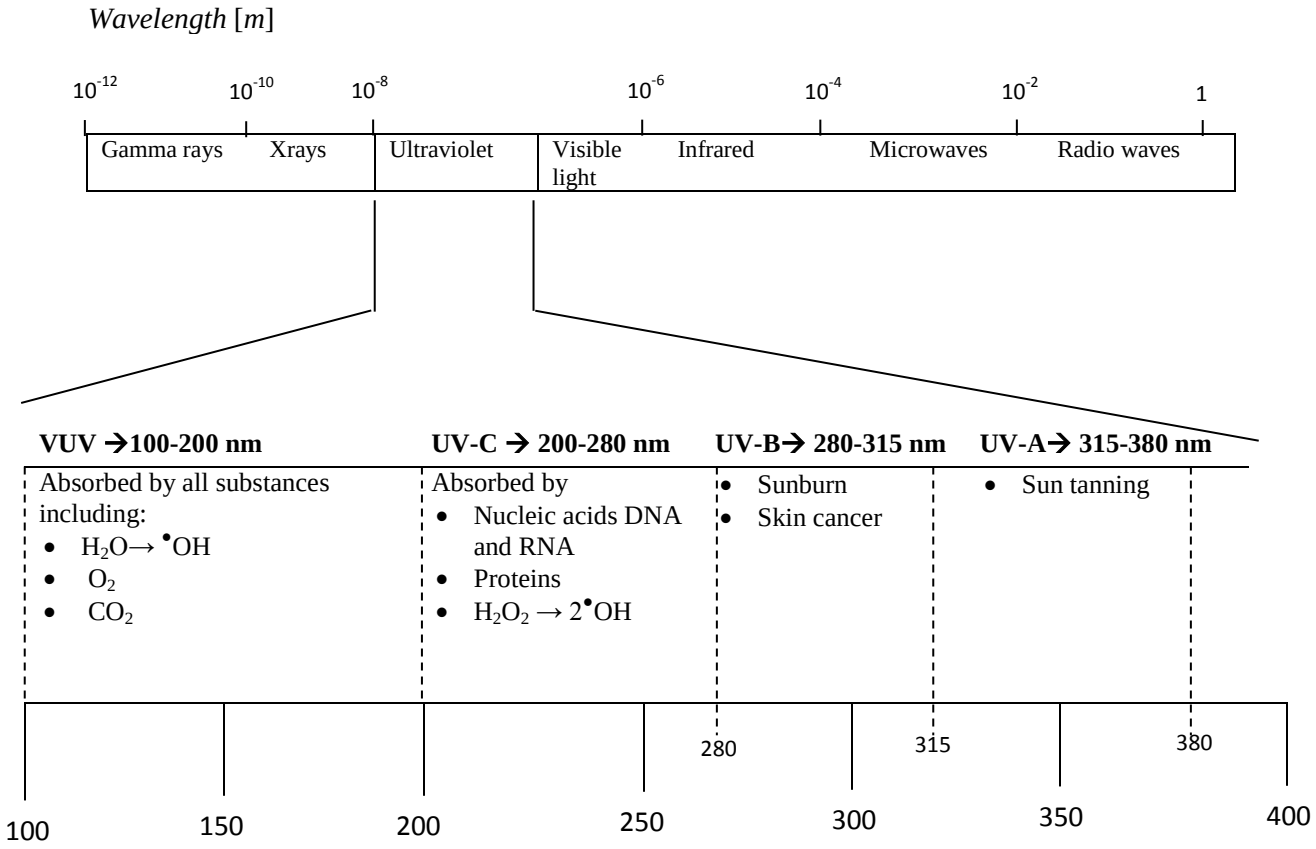

Figure 2.1. Characteristics of the sub-bands of ultraviolet radiation. Modified from Oppenlander, 2003.

susceptible to biological damage; the damage will depend on the irradiation time — usually seconds — under the UV germicidal region, usually 254 nm (Meulemans, 1987).

The major damage takes place on the nucleic bases when two adjacent thymine bases within a DNA strand, composed of base pairing (A-T, G-C), absorb UV radiation (Wang *et al.,* 2006a). Consequently, a thymine dimer is formed by a [2+2] cycloaddition reaction creating a new pair of covalent C–C single bonds, and in turn, preventing the normal pairing with the other bases (Oppenlander, 2003; Wang *et al.,* 2006a). Transcription of the genetic code from DNA to RNA relies on the correct pairing of the nucleic bases; therefore, once enough thymine dimers are formed, they will disrupt this process, thus, affecting the normal replication of the genetic code within the cell.

2.2.2 UV-C/H_2O_2 Process

Auxiliary oxidants such as H_2O_2 and O_3 are chemical compounds that can be coupled with UV radiation, usually the UV-C region from the electromagnetic spectrum between 200 to 280 nm as seen in Figure 2.1, to produce the sought-after hydroxyl radicals ($^{\bullet}OH$) species. Hydrogen peroxide is a strong oxidant that can absorb UV radiation between 180 and 440 nm, more effective in shorter wavelengths, reaching a peak near 220 nm (Oppenlander, 2003; Wang *et al.,* 2006; Tang, 2004). UV/H_2O_2 is considered as one of the most direct processes to generate $^{\bullet}OH$ among all AOPs, although H_2O_2 has a lower molar absorption coefficient of 18.6 $M^{-1}cm^{-1}$ than O_3 of 3,300 $M^{-1}cm^{-1}$ in the UV-C region (Glaze *et al.,* 1987; Tarr, 2003). The molar absorption coefficient is directly linked to the capacity for an auxiliary oxidant to absorb UV photons and produce $^{\bullet}OH$. Therefore, to offset the lower molar absorption

coefficient of H_2O_2, larger amounts of H_2O_2 should be added to the system to incentive a maximum absorption of the incident UV-C radiation (photons) by H_2O_2.

When UV radiation comes into contact with H_2O_2, it causes the homolytic cleavage of the central HO–OH bond of the H_2O_2 molecule resulting in the formation of hydroxyl radicals ($^{\bullet}OH$) as described in Reaction (2.5). $^{\bullet}OH$ species attack organic substances and it is especially efficient in oxidizing refractory and toxic constituents.

$$H_2O_2 \xrightarrow{h\nu} 2\ {}^{\bullet}OH \qquad (2.5)$$

As seen in Reaction (2.5), 2 moles of hydroxyl radicals are produced per quantum of radiation (*hv*) absorbed; however, there are other reactions to be considered such as radical-radical recombination (Reaction 2.6), which takes place when the H_2O_2 concentration is high during the oxidation process, which is responsible for the overall reduction of $^{\bullet}OH$ radicals' production. A recombination may be avoided by finding the optimum H_2O_2 concentration inherent to the specific contaminant and system configuration (Oppenlander, 2003).

$$^{\bullet}OH + {}^{\bullet}OH \rightarrow H_2O_2 \qquad (2.6)$$

In addition to radical recombination, the UV-C/H_2O_2 process effectiveness is also hindered by the H_2O_2 low molar absorption coefficient, 18.6 $M^{-1}cm^{-1}$, at 254 nm, which is responsible for large amounts of H_2O_2 being added to produce significant concentrations of

$^{\bullet}$OH within the system. By contrast, the molar absorption coefficient of ozone is 3,300 $M^{-1}cm^{-1}$ (Glaze *et al.*, 1987). Moreover, any post-treatment surplus of H_2O_2 concentration should be removed from the effluent, otherwise it could enter source waters, causing negative effects on fish and other living communities (Black and Veatch, 2010; Oppenlander, 2003). Bovine catalase is the most common compound used to remove H_2O_2 excess, which converts H_2O_2 into water and oxygen, as shown in Reaction (2.7) (Chelikani *et al.*, 2004). In particular, the low molar absorption coefficient and the use of compounds to control the H_2O_2 concentration in the effluent have a significant impact on the total cost of this AOP process.

$$2\ H_2O_2 \xrightarrow{\text{bovine catalase}} 2\ H_2O + O_2 \qquad (2.7)$$

A wide range of chemical constituents has been subjected to the UV/H_2O_2 photochemical processes such as N-nitrosodimethylamine (NDMA), trichloroethlylene (TCE), 1,4 dioxane, phenol, MTBE, and BTEX (Asano *et al.*, 2007; Oppenlander, 2003, Tang, 2004; Tarr, 2003; Wang *et al.*, 2006a) with an overall degree of mineralization over 90% (refer to Table 2.6 for details) . For a UV/H_2O_2 process to be efficient, the H_2O_2 concentration has to be in the optimum level to maximize the absorption of the incident photons, while the presence of other water compounds that may compete for the absorption of radiation must be minimized. The optimum H_2O_2 concentration also helps to minimize the recombination mechanisms as well as effluent H_2O_2 effluent concentration surpluses as previously seen in Reactions (2.6) and (2.7).

2.2.3 Photolysis of Water by Vacuum-UV (VUV)

Vacuum–UV photolysis positions itself as a very good alternative to the UV/H_2O_2 process since it avoids common drawbacks such as the need to use high amounts of H_2O_2 and to remove residual concentrations after treatment. VUV occurs within the 100 to 200 nm range of the electromagnetic spectrum and the photons emitted within this range contain a greater amount of energy than that of the photons emitted from the rest of the UV electromagnetic spectra (VIS, UVA, UVB, and UVC). For example, one mole of photons, emitted at 254 nm (UV-C), contains 471 kJ, while one mole of photons, at 185 nm (VUV), contains 647 kJ (U.S EPA, 1998). As Oppenlander (2003) explained, the water molecule starts absorbing radiation from 498 kJ/mol and higher, condition that is met by the high-energy VUV photons, which causes the cleavage of the water molecule as shown in Reaction (2.8). As a result, hydroxyl ($^{\bullet}OH$) and hydrogen ($H^{\bullet}$) radicals are generated as primary species. In addition, hydrated electrons (e_{aq}^{-}) are produced in lesser amounts shown in Reaction (2.9). Although $H^{\bullet}$ and hydrated e_{aq}^{-} play a minor role in the oxidation of organic matter, they are part of the reaction and, therefore, must be included in the oxidation cycle for the final mineralization of the organic carbon.

$$H_2O \xrightarrow{h\nu} {}^{\bullet}OH + H^{\bullet} \qquad (2.8)$$

$$H_2O \xrightarrow{h\nu} {}^{\bullet}OH + H^{+} + e_{aq}^{-} \qquad (2.9)$$

Hydrated electrons (e_{aq}^{-}) react with dissolved molecular oxygen to form superoxide radical anions ($O_2^{\bullet -}$), whose conjugated acid $HO_2^{\bullet}$ with a pK_A value of 4.8 implies that

($O_2^{\bullet-}$) is a weak base in water. The hydroperoxyl radicals ($HO_2^{\bullet}$) can disproportionate to form molecular oxygen and hydrogen peroxide, which results in a shifted equilibrium to the right of Reaction (2.11), generating an increased basicity of the superoxyl radical ($O_2^{\bullet-}$). Likewise, the hydrogen radicals formed during the VUV/H_2O photolysis are transformed into $HO_2^{\bullet}$ by a quick reaction with dissolved molecular oxygen (Reaction 2.12). Therefore, the water molecule (H_2O) can be labeled as an auxiliary oxidant (similar to H_2O_2) because of the participation of e_{aq}^- and $H^{\bullet}$ as reductive species in the oxidative cycle (Reactions 2.10 and 2.12).

$$e_{aq}^- + (O_2)_{aq} \rightarrow O_2^{\bullet-} \qquad (2.10)$$

$$(O_2^{\bullet-})_{aq} + H^+ \leftrightharpoons HO_2^{\bullet} \ (pK_A = 4.8) \qquad (2.11)$$

$$H^{\bullet} + (O_2)_{aq} \rightarrow HO_2^{\bullet} \qquad (2.12)$$

Figure 2.2 describes the general mechanisms by which an organic compound is oxidized and mineralized by different species generated during the VUV photolysis of water. The types of saturated aliphatic or aromatic organic compounds (*RH*) that can be degraded by the VUV photolysis of water include trichloromethane, $CHCl_3$, or 1,1,1-trichloroethane, CH_3-CCl_3, while unsaturated organic compounds include trichloroethylene ($CH=CCl_2$), trichloroethene, ($Cl_2C=CClH$), or tetrachloroethene, ($Cl_2C=CCl_2$). Examples of the degradation mechanisms were already shown in Reactions (2.1) to (2.4).

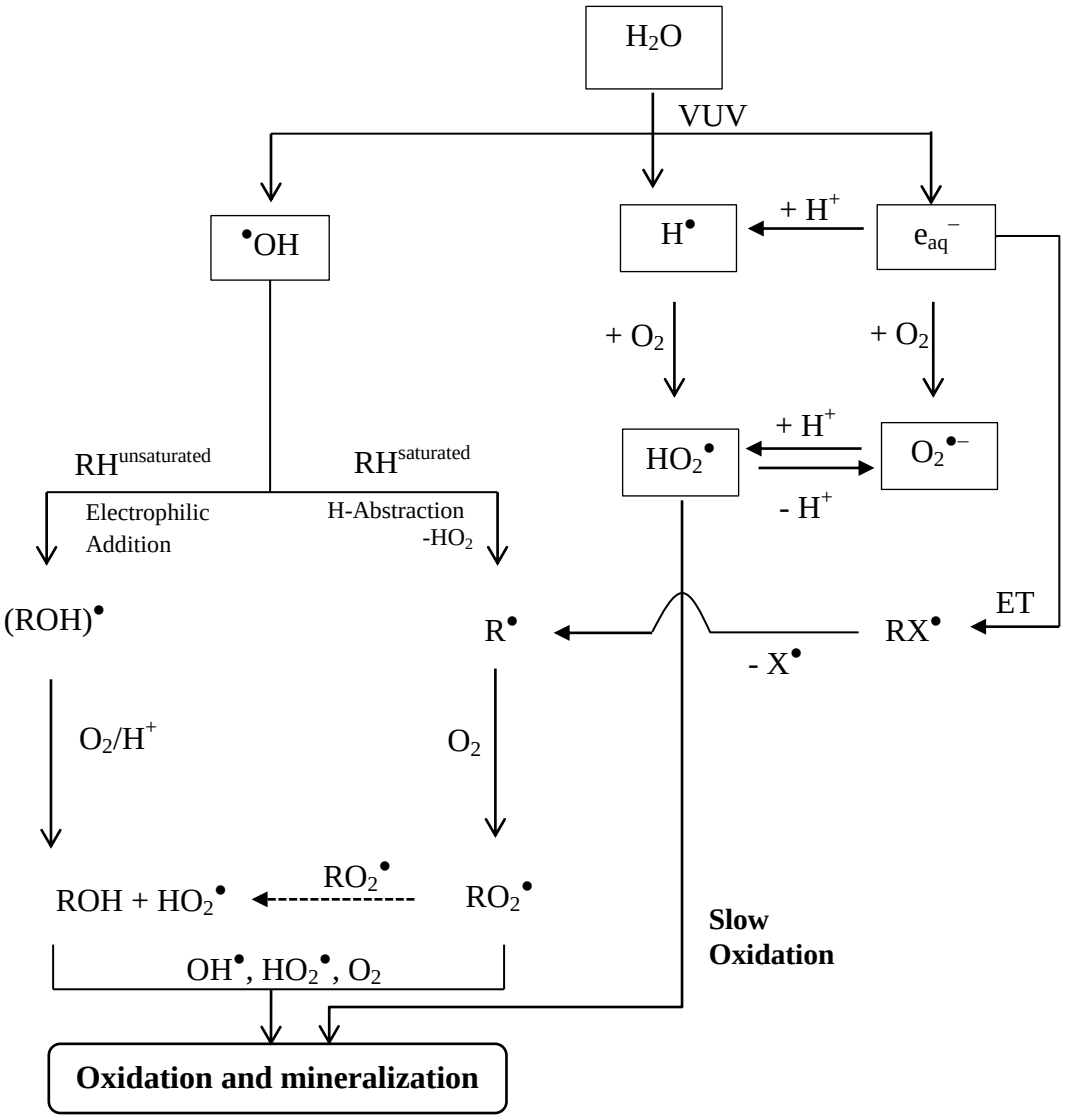

Figure 2.2. Oxidation and mineralization of organic compounds by the VUV photolysis of water. RH: Aliphatic or aromatic hydrocarbons substrate; $X^{\bullet}$: halogen radical; ET: electron transfer to an acceptor molecule (modified from Oppenlander, 2003).

A general oxidation pattern of organic matter carried out by VUV and UV/H_2O_2 photolytic processes is described in Reaction (2.13), where the parent compound is oxidized by $^{\bullet}OH$ radicals producing intermediate compounds and finally mineralized to carbon dioxide (CO_2) and water (H_2O). Intermediates include compounds such as alcohols, aldehydes, ketones, and carboxylic acids. After a C-C cleavage, these intermediates are further degraded producing formic, acetic, and oxalic acids before finally being mineralized into CO_2 and H_2O.

$$^{\bullet}OH + \text{Organic} \rightarrow \begin{array}{l}\text{Alcohols,}\\ \text{Ketones, Aldehydes,}\\ \text{Carboxylic Acids}\end{array} \rightarrow \begin{array}{l}\text{Acetic, Formic,}\\ \text{and Oxalic Acids}\end{array} \rightarrow CO_2 \text{ and } H_2O \quad (2.13)$$

According to Sawyer *et al.* (2002), alcohols such as methanol, ethanol, or isopropanol, are the primary oxidation products of organic matter. Primary and secondary alcohols are oxidized into aldehydes — formaldehyde, acetaldehyde — and ketones — acetone — respectively. Since aldehydes have a hydrogen attached to the C=O, they are easier to oxidize than. By contrast, ketones are harder to oxidize since instead of a hydrogen they have an organic chain attached to the C=O such as an alkyl group. The hydrogen present in the aldehydes is what makes them a strong reducing agent, which means they oxidize very easy. Further oxidation will lead to the formation of acids such as acetic, formic, or oxalic acids. Acids are the maximum oxidation state that an organic compound can achieve before being completely mineralized into CO_2 and H_2O. Table 2.3 shows selected organic compounds and intermediates derived from $^{\bullet}OH$ radicals oxidation such acids, alcohols,

aldehydes and ketones. Other organic compounds of environmental significance such as aromatics, ethers, and amines are also readily oxidized by the $^{\bullet}OH$ radicals.

Table 2.3. Selected organic compounds and intermediates readily oxidized by hydroxyl radical ($^{\bullet}OH$) species (adapted from Bigda, 1995).

Group	Representative compounds
Acids	Formic, gluconic, lactic, malic, propionic, tartaric
Alcohols	Benzyl, tert-butyl, ethanol, ethylene glycol, glycerol, isopropanol, methanol, propenediol
Aldehydes	Acetaldehyde, benzaldehyde, formaldehyde, glyoxal, isobutyraldehyde, trichloroacetaldehyde
Ketones	Dihydroxyacetone, methyl ethyl ketone
Ethers	Tetrahydrofuran
Aromatics	Benzene, chlorobenzene, chlorophenol, creosote, dichlorophenol, hydroquinone, p-nitrophenol, phenol, toluene, trichlorophenol, xylene, trinitrotoluene
Amines	Aniline, cyclic amines, diethylamine, dimethylformamide, EDTA, propanediamine, n-propylamin

Currently, there are different ways to produce VUV radiation: via low pressure (LP) and medium pressure (MP) mercury lamps as well as excimer lamps. LP mercury lamps emit mostly monochromatic radiation at 254 nm, yet some radiation is also emitted at 185 nm. As Oppenlander (2003) explained, the wavelength at 185 nm can be harnessed by using high purity quartz sleeves (known as suprasil quartz) with a relative VUV output efficiency of about 10% of that of the 254 nm emissions. By contrast, emissions at 254 nm could reach efficiencies of about 60%. Low-pressure mercury lamps are usually limited to less than 300 W of electric input. Another type of lamps is a MP mercury lamp that can emit polychromatic radiation at different emission regions, including UV-C (15-23%), UV-B (6–7 %), UV-A (~ 8%), VIS (~15%), and IR (47–55%). By using a suprasil quartz sleeve, the

VUV (185 nm) can be also harnessed obtaining efficiencies of around 20% of that of the UV-C output. Most recently, xenon excimers (Xe_2*) lamps have been gaining appeal for VUV production, as they produce VUV at 172 nm, a stronger wavelength, and may reach efficiencies of about 60%. Excimers refer to "dimers consisting of two atoms of the same structure" (Oppenlader, 2003). Consequently, xenon excimer lamps are becoming a great alternative in the VUV production that is efficient and more powerful wavelength (172 nm) in comparison to LP and MP mercury lamps.

2.3 Factors Limiting the Efficiency of AOPs

Certain factors affect the effectiveness of photochemical processes in water purification; they are mainly related to the presence of carbonate ions, the absorbance/transmittance of water, and pH.

2.3.1 Alkalinity in terms of the Bicarbonate and Carbonate Ions

Carbonate (CO_3^{-2}) / bicarbonate (HCO_3^-) ions are important factors influencing the efficiency of the hydroxyl radicals ($^{\bullet}OH$) in oxidizing contaminants present in water. The total carbonate concentration of elements such as calcium, magnesium, sodium, potassium, and ammonia can be measured as alkalinity, which is the ability of water to neutralize an acid and it depends on the concentrations of CO_3^{-2}, HCO_3^-, and OH^-. Calcium and magnesium are the most common elements responsible for carbonate concentrations (Tarr, 2003; Tchobanoglous *et al.,* 2003). In fact, alkalinity is usually measured as calcium carbonate [$CaCO_3$] in mg L^{-1}.

Carbonate and bicarbonate ions are the most efficient scavengers of hydroxyl radicals (Oppenlander, 2003; Tarr, 2003). According to Reynolds and Richards (1996), carbonate concentrations are relevant in waters with pH measurements of 8.5 and above. Carbonate and bicarbonate species compete for $^{\bullet}OH$ to produce carbonate radicals ($CO_3^{\bullet-}$); thus, the system will suffer a loss in availability of reactive species ($^{\bullet}OH$) intended to degrade the organic matter present in water, which leads to a loss of the system's efficiency.

$$^{\bullet}OH + HCO_3^- \rightarrow H_2O + CO_3^{\bullet-} \qquad (2.14)$$

$$^{\bullet}OH + CO_3^{2-} \rightarrow CO_3^{\bullet-} + OH^- \qquad (2.15)$$

As Reactions (2.14) and (2.15) show, the negative impact of carbonate/bicarbonate alkalinity on hydroxyl radicals is mostly due to carbonate radicals, which are produced at the high pH range (Oppenlander, 2003; Tarr, 2003). In this regard, reducing the water pH to 7 or lower can minimize alkalinity. As a result, the predominant species will be CO_2, which will not scavenge the valuable hydroxyl radicals needed in the system.

2.3.2 Chloride Ions

Chloride ions may hinder the production of $^{\bullet}OH$ to a lesser extent than the carbonate and bicarbonate ions, yet it should be taken into account when designing AOPs for water treatment processes. According to Liao *et al.* (2001), by maintaining the water at a neutral to slightly alkaline pH, the interference of chloride ions are minimized. Reaction (2.16) describes how the chloride ion scavenges hydroxyl radicals to produce $HOCl^{\bullet-}$. Additionally,

Reaction (2.16) illustrates how $HOCl^{\bullet-}$ is rapidly converted back into $^{\bullet}OH$ and Cl^{-}. Furthermore, the $HOCl^{\bullet-}$ can be protonated to form chlorine radicals and water as shown in Reaction (2.17). The p*K* value for the deprotonation reaction (reverse Reaction 2.17) is 7.2. Thus, at pH > 7.2, the $HOCl^{\bullet-}$ is dominant, whereas at pH < 7.2, the $Cl^{\bullet}$ is the dominant species, in turn, reducing the $^{\bullet}OH$ radicals available in the system (Liao *et al.*, 2001).

$$^{\bullet}OH + Cl^{-} \leftrightharpoons HOCl^{\bullet-} \qquad (2.16)$$

$$HOCl^{\bullet-} + H^{+} \leftrightharpoons Cl^{\bullet} + H_2O \qquad (2.17)$$

2.3.3 Absorbance (A) / Transmittance (T)

In a solution, it is important to determine the amount of light in a specific wavelength that can be absorbed since it determines how fast the oxidation of pollutants will be within the photoreactor (Christensen and Linden, 2003). The well-known Beer–Lambert law of absorption describes the solution capacity for the absorption of UV/VIS radiation as a function of the wavelength (λ) (Oppenlander, 2003). Equation (2.18) describes the absorbance as the logarithm to the base 10 of the ratio of the spectral radiant power of incident radiation P_{λ}^{0}, essentially monochromatic, to the radiant power of transmitted radiation (P_{λ}^{trans}):

$$A_{10} = \log\frac{P_{\lambda^0}}{P_{\lambda^{trans}}} = \log\frac{1}{T} = -\log T = \varepsilon_{\lambda} cl \qquad (2.18)$$

where,

A_{10} the (decadic) absorbance of a beam of collimated monochromatic radiation in a homogeneous isotropic medium;

P_λ^0 the incident spectral radiant power;

P_λ^{trans} the transmitted spectral radiant power;

ε_λ the molar (decadic) absorption coefficient in L/mol.cm (SI unit: m^2/mol)

c the concentration of the substrate in mol L^{-1};

l the thickness of the solution transverse by the UV radiation (also called pathlength of irradiation) in cm.

The absorbance is generally measured through a spectrophotometer using a specified wavelength, usually 254 nm, and a fixed path length (l =1cm). Thus, contrasting the spectral radiant power of light transmitted through the reference sample to that of the light transmitted through the solution, the ratio P_λ^0 / P_λ^{trans} can be obtained. The logarithm to the base 10 of this ratio represents the absorption of energy per unit depth, or absorbance of the solution to be treated (Oppenlander, 2003).

T is the (internal) transmittance, which assumes that all light is either transmitted or absorbed; reflection and scattering are neglected. The (internal) transmittance, which comprises the energy loss by absorption, is inversely related to the absorbance as shown in Equation (2.19), thus, it is the ratio of the transmitted spectral radiant power (P_λ^{trans}) to that incident on the sample (P_λ^0) (Asano *et al.*, 2007; Oppenlander, 2003).

$$T = \frac{P_{\lambda} trans}{P_{\lambda 0}} \quad \text{or} \quad T\,(\%) = \frac{P_{\lambda} trans}{P_{\lambda 0}} \times 100 \qquad (2.19)$$

The parameter commonly used to determine the suitability of the UV radiation for disinfection is % transmittance *T* (%) as described in Equation (2.20).

$$T = 10^{-A} \text{ or } T\,(\%) = 10^{-A} \times 100 \qquad (2.20)$$

2.3.4 pH

The impacts of the pH on the AOPs efficiency were previously mentioned in Sections 2.3.2 and 2.3.3. Since carbonate concentrations are relevant in water with pH ranges of 8.5 and above, by reducing the water pH to 7 or below, the alkalinity can be minimized; thus, the predominant species will be CO_2, which will not scavenge the valuable hydroxyl radicals needed in the system. Similarly, by maintaining the water at a neutral to slightly alkaline pH, the interference of chloride ions are minimized. In the present research, the neutral pH was used.

2.4 Wastewater Used to Test the Photochemical Processes

The present study focused on testing photochemical processes based on UV radiation, which are becoming a promising technology to deal with current water and wastewater treatment requirements. In particular, this work attempted to evaluate the viability for applying the VUV (λ=185 nm) as a photochemical process as well as its potential combination with UV-C (λ=254 nm), to remove organic matter from synthetic slaughterhouse wastewater and pathogens in water, such as *Escherichia coli (E. coli)* O157:H7, *Shigella flexneri*, *Salmonella enterica*, and *Pseudomonas aeruginosa.* The findings

will serve to determine the efficiency of the processes and its potential uses in removing a broader set of organic compounds, in particular emerging contaminants of concern. This specific wastewater was chosen based on a previous study, in which an anaerobic biological treatment was coupled with a UV/H_2O_2 process (Cao, 2009; Cao and Mehrvar, 2010). The results showed that UV/H_2O_2 is a good complementary treatment to biological processes by improving the general ability of the system to remove the TOC concentration. The present study attempted to go further by testing the VUV photolytic process and its combination with UV-C to see if the use of auxiliary oxidants (H_2O_2) can be omitted from the process. Consequently, additional costs related to monitoring and removal of excess H_2O_2 concentrations could be avoided.

2.5 Slaughterhouse Wastewater Occurrence

Meat processing plants, also known as slaughterhouses, are facilities where a wide variety of animals including cattle, hogs, and poultry are slaughtered for both human consumption and animal feeding operations — processed by-products (Wang *et al.*, 2010). The meat processing industry is one of the major consumers of fresh water among industrial food processing facilities as shown in Table 2.4, which makes it a significant producer of wastewater effluents. According to the World Bank (1999), a slaughterhouse plant, which is a meat processing facility, may consume between 2.5 and 40 m^3/ ton of water per metric ton of beef produced.

Table 2.4. Water consumption in different sectors of the US food and beverage manufacturing (adapted from Wang *et al.*, 2010).

Food Industry	Water consumption (%)
Fruits and vegetables	10.1
Grain and oilseeds	9.0
Meat processing	23.9
Seafood	1.6
Animal food	4.9
Beverages	12.7
Sugar and confectionary	5.2
Dairy	12.1
Bakery and tortilla products	9.6
Other food	10.9

The production of beef has been growing steadily in recent years and some authors predict this trend is likely to continue due to income increases in some countries such as India and China, which are shifting toward a western-like diet rich in proteins (Halweil, 2008). In 2002 the global annual production of beef was around 50 million tonnes, whereas in 2007 the annual production reached 64.7 million tonnes, representing an increase of 29% over 8 years (FAO, 2010; Wang *et al.*, 2006b). As a result, it can be inferred that the number of slaughterhouse facilities will get bigger, resulting in more volume of high-strength wastewater (high concentration of organic matter) to be treated. Consequently, this growing industry will demand reliable and effective technologies to properly treat these effluents before being discharged into source waters to minimize negative environmental impacts.

The present study intended to assess the reliability of combining Vacuum-UV (VUV) and UV-C to serve as complementary post-treatment processes to conventional biological processes in the degradation of organic loads as well as the elimination of pathogenic agents

(bacteria) derived from cattle slaughtering such as *E. coli* O157:H7, *Shigella flexneri*, *Salmonella enterica* serovar Typhimurium, and *Pseudomonas aeruginosa*

2.5.1 Slaughterhouse Wastewater Composition

Slaughterhouse facilities use vast volumes of fresh water mostly for cleaning procedures, including carcass blood washing, equipment sterilization and cleaning before and after killing operations as well as work area cleaning (Wang *et al.*, 2006b). Apart from cleaning procedures, water is also used for watering and washing livestock before slaughtering in order to remove any accumulated dirt and manure. In fact, more than 65% of the water used in slaughterhouses can be attributed to three activities: cleaning, spraying, and rinsing activities. The remaining 35% is associated with personal hygiene, cooling water scald tank, tool sterilization, animal handling facilities, and vehicles washing (Wang *et al.*, 2005).

The washing and cleaning procedures bring about high loads of organic content inherent to the meat processing operations. For example, large amounts of blood, fats and oils, body tissue, nitrogen (from blood), phosphorus, detergents from cleaning products, and salts (sodium) from protein recovery products such as sodium lignosulfonate, are released after washing and cleaning activities. According to Wang *et al*. (2006), the typical amount of blood derived from a single animal (450 kg live weigh) may be around 16 kg. Blood is one of the major contributors to Chemical Oxygen Demand (COD), which can reach values up to 400,000 mg L^{-1}. The carcass and evisceration washing procedures are the main providers of organic content at slaughterhouse plants (Wang *et al*., 2006b; U.S EPA, 2002).

Apart from high amounts of organic loads, pathogenic microorganisms such as *E coli* O157:H7, *Shigella* spp. and *Salmonella* spp. are released during the slaughtering (Water Environment Federation, 2009). It is well known that these bacteria genera live in the cattle's gastrointestinal tract, eventually mixing with the rest of residues in the effluent. These pathogens are usually released during the cutting and splitting of the viscera, also known as the evisceration process. Table 2.5 shows a summary of the different organic and microbiological constituents produced when slaughtering a commercial steer. It becomes of vital importance to rely on proper on-site technology to effectively remove not only organic constituents, but also pathogenic agents from the effluent generated from the slaughtering process. The degree of removal required will depend on each jurisdiction's regulatory framework, with the overall goal of removing over 85% of organic load (Wang *et al.*, 2010).

Table 2.5. Typical raw material breakdown from a commercial steer (450 kg live weight).

Item	Weight in *kg*	References
Commercial sale:		
Edible meat	160	Wang *et al.* (2006b)
Edible offal	15	Wang *et al.* (2006b)
Hide	32	Wang *et al.* (2006b)
Byproducts for rendering:		
High-grade Fat	45	Wang *et al.* (2006b)
Bone and meat trim	50	Wang *et al.* (2006b)
Waste:		
Nonedible offal and gut fill	112	Wang *et al.* (2006b)
Blood	16	Wang *et al.* (2006b)
BSE suspect material[b]	20	Wang *et al.* (2006b)
Bacterial Pathogens	**Cells/gram[a]**	
Escherichia .coli O157:H7	10^{7}-10^{9}	Gyles *et al.* (2010)
Salmonella	10^{5}-10^{8}	Gyles *et al.* (2010)
Campilobacter	10^{7}-10^{9}	Water Environment Federation (2009)
Shigella	10^{7}-10^{9}	Water Environment Federation (2009)
Pseudomonas. aeruginosa	N.A	Gyles *et al.* (2010)

N.A = Not Available

a. Cells per gram of feces

b. BSE – stands for Bovine Spongiform Encephalopathy known as "mad cow" disease

2.5.2 Environmental Effects in Source Waters

The presence of organic constituents in natural source waters may cause a variety of environmental impacts, such as eutrophication, temperature changes, and dissolved oxygen depletion, which will undoubtedly have a severe impact on the ecosystem (UNEP, 2000). For example, organic matter will consume the oxygen intended for fish and other benthic organisms, leading to such problems as reproduction and developmental abnormalities. Moreover, by killing the individuals most sensitive to a lack of dissolved oxygen, which is vital to support life, could trigger biodiversity losses. Likewise, hot water and steam used for sterilizing and cleaning are responsible for thermal pollution, which may become a major issue for organisms that have a narrow tolerance to temperature changes in water. Finally, high concentrations of nitrogen and phosphorus stimulate algal growth (a phenomenon known as eutrophication). Once algae are dead, they sink to the bottom of the waterbody, where bacteria start the process of biodegradation. Vast amounts of oxygen are employed by bacteria to biodegrade dead algae, and when this is add to the oxygen required to degrade high concentrations of organic matter derived from blood, and fat proteins, it could rapidly render source waters anoxic. This problem is already visible in East Asia with the *red tide* phenomenon, where algal blooms are affecting fisheries and some of the most valuable aquatic biodiversity, such as the coral reefs of the South China Sea (World Bank, 2005).

Several studies show the damage wastewater effluents loaded with high amount of organic constituents may exert on source waters. For instance, the Bogota River is one of the most important rivers in Colombia, which flows through the capital city, Bogota. The Bogota River daily receives an estimated 500 tons of organic matter, including approximately 1,350

tons of suspended solids (Rietbergen-McCracken, and Abaza, 2000). Different sources, including slaughterhouses, upstream municipalities, horticultural- facilities, and coal yards, are responsible for the production of this high-strength (high concentration of organics) wastewater (Rietbergen-McCracken and Abaza, 2000). As a result, the Bogota River has several sections in which life no longer exists as well as exhibits a putrefaction odour derived from the hydrogen sulfide, which is produced by the anaerobic biodegradation processes being carried out in its waters.

Similarly, the Ikpoba River, located in Nigeria, Africa, has seen the quality of its water being affected by high coliform concentrations stemming from discharged slaughterhouse plant effluent. As Benka-Coker and Ojior (1995) illustrated, the pathogenic bacteria concentration, including species such as *Escherichia coli* spp., *Shigella* spp., *Salmonella* spp., *Klebsiella* spp., *Streptococcus* spp., and *Staphylococcus* spp., was increased to 10^7 from 10^4 CFU/100 mL due to an untreated slaughterhouse effluent being discharged upstream. Adverse health effects, such as gastrointestinal upset, bloody diarrhea, liver malfunction, and, in some cases, even death, are associated with these pathogenic agents (Percival *et al.*, 2004). In addition to disease-causing microorganisms, the concentration of suspended solids, biological oxygen demand (BOD), nitrates, and phosphates was increased leading to a reduction of the concentration of dissolved oxygen from 7.2 to about 2.4 mg L^{-1}. Therefore, the water quality of the receiving water was severely affected by not having a proper treatment technology for the reduction of the organic content derived from the slaughterhouse plant in place.

Regulatory frameworks that deal with slaughterhouse effluents vary from country to country and the selection of a particular treatment will depend both on the characteristics of

the wastewater to be treated as well as the regulations which must be complied with. For instance, some meat processing plants (MPPs) are allowed to discharge their effluent into the municipal sewer system provided that adequate treatment has previously reduced BOD loads. Typical BOD values for effluents to be allowed into municipal sewer systems are around 250 mg L^{-1}. In other cases, MPPs are required to conduct on-site treatment prior to direct discharging into receiving waters (Tchobanoglous *et al.,* 2003; U.S EPA, 2002). The main factors determining whether a plant can discharge into the municipal sewer system or not have to do with the plant size as well as the volume and organic concentration of the wastewater produced.

2.5.3 Aging Infrastructure

There is an additional problem specifically related to aging infrastructure, which may add to the potential risk of untreated wastewater reaching receiving waters. According to the International Joint Commission (2009), the collection systems in some part in North America, which are responsible for transporting wastewater to sewage treatment plants, dated back to the mid-19th century and many of them have not been upgraded and are beyond the capacity for which they were originally intended. These collection systems have been designed to work as combined sewer systems (CSSs), where domestic, commercial, industrial, and storm water are all transported via a single pipe connected to the water treatment facility. The problem lies in that sometimes during wet-weather periods of heavy rainfall and snowmelt, the pipes cannot handle the large volumes of water being pumped into the system and their capacity is exceeded. During these events, termed Combined Sewer Overflows (CSOs), the excess of wastewater, a combination of raw sewage and stormwater,

running through the system is directly dumped into the receiving waters without any treatment. Consequently, huge loads of organic constituents and disease-causing microorganisms, not to mention chemical constituents, pharmaceutical and personal care products as well as other hazardous compounds from commercial and industrial sources end up in source waters without any treatment (Nemerow, 2007; Stoddard, 2002).

A large number of the remaining CSSs in North America are located in the Northeast of the continent, particularly within the Great Lakes region (International Joint Commission, 2009). In fact, around 70% of the US CSSs are located in the states surrounding the Great Lakes. Meanwhile in Canada, specifically the province of Ontario, around 20% of the total municipalities have CSSs posing a potential risk for combined sewer overflows events to occur. As the International Joint Commission (2009) stated, several CSO events have been reported in recent years near the great lake communities in Ontario; in total, 107 known CSOs, with 1,544 releases of raw or partially treated sewage occurred in 2006 alone. For example, a recent report stating the hot spots (pollution sources) affecting the Great Lakes shows that the CSO events are a major problem to the Saint Clair River, which is constantly receiving raw sewage discharges from the Sarnia sewer system during CSO events (Jackson, 2006). On the American side, a major event occurred in September 2008, when the metropolitan water reclamation system of Chicago decided to release 11 billion gallons of raw sewage water to Lake Michigan. This measure was taken to protect the waterway systems' structure due to a high-flow event caused by 6.8 inches of rainfall received across the metropolitan area (a record at that time). Consequently, these kinds of events combined with an aging infrastructure pose a significant threat to the Great Lakes communities, in particular the Ontario's source water ecosystems and, most importantly, the people living in

these communities due to untreated water discharges containing poisonous cocktails of hazardous constituents (International Joint Commission, 2009).

It can be perceived that the main problem with CSSs has to do with the overflow events, which are a mixture of all sort of hazardous contaminants, and in which slaughterhouses may play a significant role by contributing high-strength effluents with significant concentrations of highly resistant pathogenic agents. Only in southern Ontario, there are several slaughterhouses (Figure 2.3) that can process a certain number of animals per day. On-site treatment would be the best option to treat and disinfect the effluent, so it could then be discharged safely into receiving waters. Thus, the transportation of the water through the sewer system to the municipal wastewater treatment facilities would be avoided, minimizing the risk of raw water releases during overflow events.

2.5.4 Regulatory Standards for Slaughterhouse Effluents

The major concern with meat processing plants (MPPs) effluent has to do with the discharge into receiving waters of oxygen demanding constituents, which are derived mainly from blood, fatty tissues, and different salts and detergents used in cleaning procedures. Organic constituents in high concentrations may deplete oxygen in a body of water, thereby causing irreversible alterations to aquatic ecosystems and wildlife (Wang *et al.,* 2010; U.S EPA, 2006; Tchobanoglous *et al.,* 2003). Regulatory agencies in North America such as the U.S EPA, Canadian Environmental Agencies, such as Environment Canada and provincial Ministries of Environment, namely in the province of British Columbia as well as the European Environment Agency (EEA) are directing efforts at outlining standards to limit maximum concentrations of oxygen demand compounds, as BOD and COD concentrations,

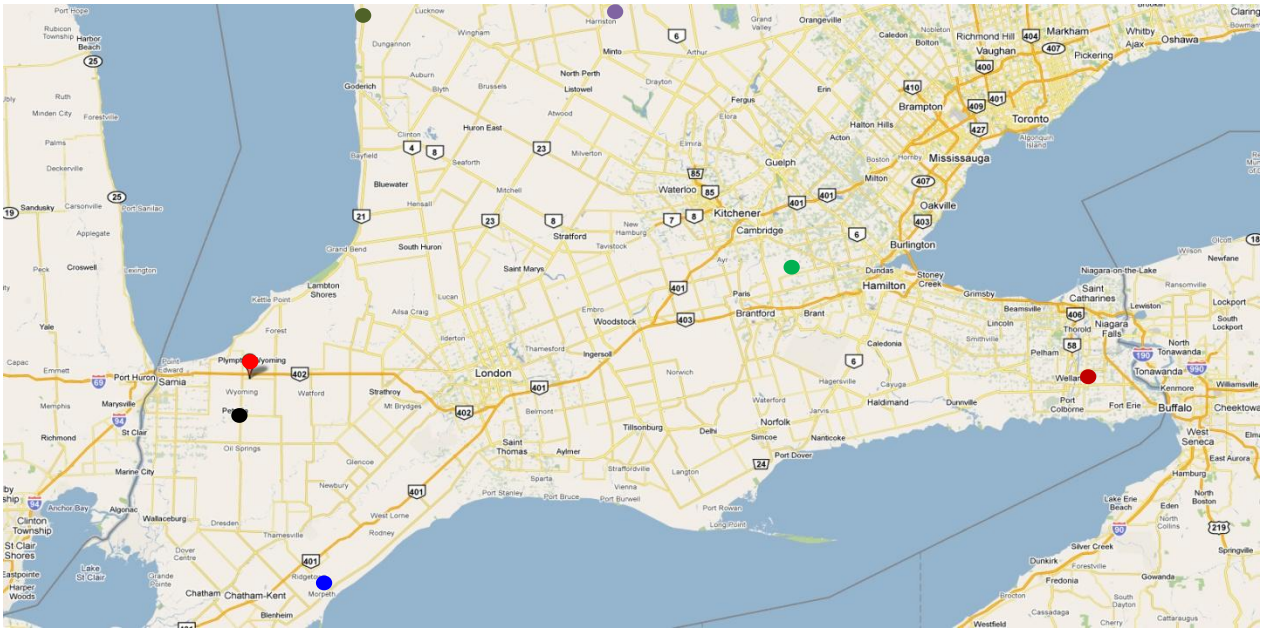

Legend:		
Plant's Name	**Address**	**Map convention**
Lambton Meat Products	5814 Minielly Road, Wyoming, N0N 1T0	
Niagara Sausage & Meat Products Limited	Ridge Road RR 4, Welland, L3B 5N7	
Willie's Meats Ltd	2387 4th Conc West RR 1, Troy, L0R 2B0	
Whitmore Meat Packers Ltd	340 Centre Street, Petrolia, N0N 1R0	
Walkerton Meat Market	RR 2, Walkerton, N0G 2V0	
The Beef Way (1997)	RR 2, Kincardine, N2Z 2X4	
Town & Country Meats & Abattoir	19950 Hill Road, Ridgetown, ON N0P 2C0	

Figure 2.3. Meat processing plants located in southern Ontario licensed by the Ontario Ministry of Agricultural and Rural Affairs (OMAFRA) — Map obtained from Google maps.

derived from MPPs that are discharged directly or indirectly into watercourses (U.S EPA, 2002; Council of the European Communities, 1991).

Direct effluent discharges require an on-site wastewater treatment; whereas indirect discharges require a pre-treatment of the effluent before being sent to the municipal sewage treatment facilities. Thus, high-strength effluents will be prevented from being discharged into source waters without proper treatment. Standard levels described in Table 2.6 include concentration limits to organic constituents recommended by different agencies to be discharged for the sector in general.

Table 2.6. Comparison of wastewater discharged standards for meat processing plants in different jurisdictions.

Parameter	Canadian Standards[a] (mg L^{-1})	U.S EPA Standards[b] (mg L^{-1})	EU Standards[c] (mg L^{-1})	Ontario Standards[d] (mg L^{-1})	British Columbia Standards[e] (mg L^{-1})	World Bank[f] (mg L^{-1})
Biochemical Oxygen Demand (BOD_5)	Freshwater lakes, slow-flowing and streams 5; Rivers, Streams and estuaries 20; Shoreline 30	30	25	25	45	50
Chemical Oxygen Demand (COD)	N.A	N.A	125	N.A	N.A	250
Total Suspended Solids (TSS)	Freshwater lakes, slow-flowing and streams 5; Rivers, Streams and estuaries 20; Shoreline 30	30	35	25	60	50

N.A =Not Available
[a] Correctional Service Canada, 2003
[b] 40 *CFR* 133.102
[c] Council of the European Communities. (1991).
[d] Environmental Commissioner of Ontario (2010)
[e] Environmental Management Act (2007)
[f] International Finance Corporation, IFC (2007)

It can be seen that Canadian standards are very stringent in comparison to their European and American counterparts. Even though the discharge standards are very stringent, they are not specific for each industry. Recently, some regulatory agencies have been trying to enact tailored-regulation specifically for the meat and poultry processing industry. For instance, the province of British Columbia is attempting to create a set of guidelines to specifically address meat processing plants effluents by creating a code of practice that has been incorporated into the provincial *Environmental Management Act*, brought into force on July 4, 2004. Therefore, British Columbia has given a legally binding character to the specific effluents produced at MPPs, which leads the way among the other provinces in Canada (Environmental Management Act, 2007).

In addition to establishing concentrations limits of organic loadings, the U.S EPA is attempting to take an integral approach where individual measures stipulated are not only relying upon the end-of-pipe treatment, but also on a broader strategy ensuring a multiple barrier approach. For example, concepts such as Best Practicable Control Technology Currently Available (BPT), Best Conventional Pollutant Control Technology (BCT), Best Available Technology Economically Achievable (BAT), New Source Performance Standards (NSPS) as well as Pretreatment Standards for Existing Sources (PSES) are all being incorporated into the process to act in conjunction with each other to help industrial production gain efficiencies, reduce cost as well as integrate the best technologies available at the minimum costs (Water Environment Federation, 2008; U.S EPA, 2002). Therefore, industry and regulatory bodies are taking steps to act in coordination to achieve the same goal of abating hazardous and deleterious compounds entering waterways.

2.6 Waterborne Pathogens in the Present Study

The present research addressed the problems caused by pathogenic bacteria representative from the cattle slaughtering process, including *Escherichia coli* O157:H7, *Salmonella enterica* serovar Typhimurium*, Shigella flexneri, and Pseudomonas aeruginosa* (Water Environment Federation, 2009). The presence of these bacteria in source waters has been labelled by Health Canada as being of utmost concern due to their virulence, which poses a serious threat to Canadian public health (Health Canada, 2006). As Kumar *et al.* (2005) stated, pathogenic bacteria derived from the cattle gastrointestinal tract are usually exposed to high doses of veterinary antibiotics, furthering resistance to them. As a result, it becomes necessary to remove these bacteria from any wastewater effluent before being discharged to source waters, since they might pose an extra threat due to their developed resistance to medical treatment by antibiotics.

2.6.1 Escherichia coli (E. coli)

E. coli is a facultative anaerobe, gram-negative bacteria which forms rod-shaped cells 2.0–6.0 µm in length and 1.1–1.5 µm in width; cells may vary from coccal to long filamentous rods (Percival *et al.,* 2004). There are more than 200 strains of *E. coli* identified to date. Pathogenic *E. coli* can be classified into six different groups based on serological and virulence characteristics: enteropathogenic, enterotoxigenic, enterohaemorrhagic, enteroinvasive, enteroaggregative, and diffusely adherent (Percival *et al.,* 2004; Health Canada, 2006).

The enterohaemorrhagic strain, *E. coli* O157:H7, is capable of causing bloody diarrhea. It is of a particular importance, since it has a low-infection dose of just 10 cells needed to cause illness in humans (Bitton, 2005; Lemarchand *et al.*, 2004; Salvato *et al*, 2003). *E. coli* O157:H7 may destroy mucosal cells by attaching to them and producing toxins (verotoxins). Eventually, it may cause several symptoms such as abdominal pain, bloody diarrhea, and haemolytic-uremic syndrome (HUS). According to Health Canada (2006), the incubation period of *E. coli* O157:H7 ranges between 3 and 4 days, and the symptoms occur over a period of 7 to 10 days. Furthermore, an important number of infections (about 2–7%) caused by *E. coli* O157:H7 result in HUS, which is responsible for the destruction of erythrocytes leading to complications such as thrombocytopaenia, microangiopathic, haemolytic anaemia, and acute renal failure. According to the Ontario Drinking Water Standards, Objectives and Guidelines (2003), the maximum allowable concentration of *E. coli* in a drinking water supply system in Ontario must be "not detectable" in 100 mL of a water sample. Therefore, it becomes of greatest interest to guarantee that different water sources are free of these bacteria.

In recent years, several outbreaks of *E.coli* O157:H7 have occurred in different cities throughout North America and Europe, which resulted in considerable diseases and even deaths among communities. As Percival *et al*. (2004) illustrated, this strain was responsible for an outbreak in Missouri in 1990, which affected the drinking water system, causing the illness of 243 people, around 7.7% of a total population of 3,126. As a result, 86 cases developed bloody diarrhea, 36 were hospitalized, and four died. Similarly, an outbreak in Scotland in the summer during the same year caused haemorrhagic colitis in four people. The root of the problem was linked to two subsidiary reservoirs used for the water supply system,

which were apparently contaminated by cattle slurry. A highly publicized outbreak of *E. coli* O157:H7 associated with drinking water occurred in Walkerton, Ontario, during May 2000 (Percival *et al.,* 2004). The drinking water came from a number of wells and there was strong evidence suggesting that one of the wells had become contaminated with cattle manure following heavy rains and flooding. As a result, around 2,300 people became ill, 1,346 people were treated, 65 were hospitalized, and 7 people died. It was established that 179 illness cases were due to *E. coli* O157:H7, 97 to *Campylobacter jejuni*, and 37 people were diagnosed with other bacteriological infections (Greenbaum and Wellington, 2008). Twenty-seven of these patients developed haemolytic uraemic syndrome (HUS) with six fatalities. The fatality rates are very high in the elderly and very young, with 10% of children under 10 years developing a combination of haemolytic anaemia, thrombocytopaenic purpura, and acute renal failure (Bitton, 2005; Percival *et al.,* 2004). As a result, Health Canada, which is the federal government agency responsible for monitoring and controlling potential public health's threats, has classified the specific serotype *E.coli* O157:H7 as a current pathogen of concern (Health Canada, 2006).

2.6.2 Salmonella enterica

Salmonella can be described as gram-negative bacilli, which are non-spore-forming facultative anaerobes. These types of bacteria are around 2–5 μm long and 0.8–1.5 μm wide. They move by peritrichous flagella, which is the main characteristic of *Salmonella* (Percival *et al.,* 2004). These bacteria represent a very pathogenic collection of species that cause infections to a broad range of animals. Different serotypes of *Salmonella* are commonly found in the intestines of humans, animals, and birds. As Percival *et al.* (2004) illustrated, the

genus *Salmonella* is comprised of two species, *Salmonella enterica* and *Salmonella bongori*. There are six subspecies of *S. enterica*, the most important of which is *S. enterica* subsp. *enterica* (subspecies I), which includes the *typhoid* and *paratyphoid* bacilli.

The ingestion of water contaminated with *Salmonella enterica* is responsible for different diseases in humans, including gastroenteritis, enteric fever and septicaemia (Percival *et al.,* 2004). It was shown that gastroenteritis, which affects the colon, usually develops between 18 to 48 h after ingestion of *Salmonella,* and can last from 2 to 5 days. The general symptoms are diarrhea, fever, and abdominal pain. *S.* Typhimurium (typhoid fever) or the paratyphoid bacilli, *S. paratyphi* A, B, and C are responsible for causing enteric fever, which in the case of *S.* Typhimurium can last longer and be more severe than paratyphoid fever, it may even cause death. Symptoms include sustained fever, diarrhea, and abdominal pain as well as fatal liver, spleen, respiratory, and neurological damage. Typhoid fever symptoms may persist for 2 or 3 weeks. As for *Salmonella* septicaemia, chills, high remittent fever, anorexia, and bacteremia comprise the main symptoms. These microorganisms can be found in any organ in the body and produce focal lesions, resulting in meningitis, endocarditis, pneumonia, or osteomyelitis. The incubation period for human salmonellosis, which is a kind of gastroenteritis caused by *Salmonella* spp., is usually between 12 and 36 h, yet incubation periods of 6 h or less have been recorded in cases where people have consumed a large number of cells (Percival *et al.,* 2004).

Salmonella infections are associated with untreated water consumption, as well as water supply systems, contaminated with sewage waters and fecal pollution. Other important

sources of waterborne contamination include agricultural runoff, leaking domestic drains, and septic tanks seepage (Percival *et al.,* 2004). It is worth noting that most *Salmonella* serotypes are capable of surviving for long periods of time in water and are able to grow in heavily polluted water during warmer months. Although disinfection procedures used in drinking water treatment are effective at removing *Salmonella*, there is evidence that they are more resistant to inactivation than coliforms (Percival *et al.,* 2004). Hence, the absence of coliform bacteria (including *E. coli*) from treated drinking water is not a reliable indicator for the absence of *Salmonella.*

2.6.3 Shigella flexneri

The genus *Shigella* is associated with waterborne disease-causing microorganisms that have been targeted by the World Health Organization (WHO) as a major concern in drinking water quality due to its virulence and hazard to human health. As WHO (2008) described, the four main genera of *Shigella* include *S. dysenteriae, S. flexneri, S. boydii, and S. sonnei*. Several gastrointestinal illnesses are associated with the most virulent strains, including, abdominal colic, watery diarrhea frequently complemented by fever and malaise. The most important intestinal upset includes dysentery, which causes inflammation of the lower part of the bowels that can develop into bloody diarrhea (Lemarchand *et al*. 2004). Shigellosis, another type of dysentery, is another infection derived from the ingestion of this group of bacteria. A very low dose of *Shigella* from 10^0 to 10^4 cells is needed to cause infection in comparison to other enteric bacteria.

The main route on exposure for *Shigella* is through ingestion, mainly in the form of the fecal-oral route. As Percival *et al*. (2004) asserted, infected individuals may excrete between 10^5–10^9 *Shigella* cells per gram of wet feces, whereas asymptomatic individuals may excrete in the range of 10^2–10^6 per gram. This can be inferred for cattle, which can hold around the same amount of cells in their gastrointestinal tract. It has been reported that after treatment and recovery, patients can continue excreting significant amount of cells for months, and in some cases, even up to a year (Percival *et al.*, 2004).

WHO (2008) has estimated that around 2 million people are infected each year, causing around 600,000 deaths, mostly in developing countries. General symptoms caused by *Shigella* spp. can become noticeable between 24–72 h after ingestion and in most cases their manifestations are mild in adults. However, infant fatalities have been reported in several countries, particularly in children less than 10 years of age (WHO, 2008; Percival *et al.*, 2004).

2.6.4 Pseudomonas aeruginosa

Even though there are around 200 species that comprised the *Pseudomonas* genus, the most important strain is *Pseudomonas aeruginosa* (Percival *et al.*, 2004). This specific strain is considered an opportunistic pathogen and may become a major concern to people with vulnerable immune systems as well as individuals hospitalized under diverse afflictions (Percival *et al.*, 2004). For example, *P. aeruginosa* may cause severe infections to patients with burn injuries or respiratory afflictions. Likewise, individuals with lung infections may develop serious complications, including sepsis, pneumonia, and pharyngitis. If these

complications are not properly cared for, they may lead to blood stream contamination, or bacteremia, which may result in organ failure or even death.

According to Percival *et al*. (1994), *P. aeruginosa* can be easily found in drinking water sources. In fact, some surveys of tap water have shown concentrations between 1 and 2300 CFU mL^{-1} (Maier *et al.,* 2009). *Pseudomonas* spp. are usually transmitted by direct contact, especially if there are open skin injuries. For example, this strain is responsible for about 10% of hospital-acquired infections, which can be easily transmitted through tap and shower water. As Maier *et al.* (2009) noted, *P. aeruginosa* present in surface water sources usually stem from human fecal contamination. The main issue regarding *P. aeruginosa* exposure is that once infection has developed, it becomes very difficult to treat. Only a few antibiotics are effective against it, which include fluoroquinolone, gentamicin, and imipenem, whose availability could be scarce in some developing countries. Therefore, timely detection and subsequent disinfection could prevent further health deterioration in vulnerable individuals, in particular those with immuno-compromised systems.

2.7 Slaughterhouse Wastewater Treatment Technologies

Wastewater treatment technologies employed in slaughterhouse plants are very similar to the ones employed in municipal wastewater treatment and may include primary, secondary, and in some cases, tertiary treatment (Flynn, 2009; Wang *et al.,* 2010). Biological treatment is the most commonly applied process as secondary treatment and is comprised of aerobic and anaerobic digestion; these could be used alone or in combination depending on the characteristics of the wastewater being treated (Baruth, 2005). With regards to

slaughterhouse wastewater, anaerobic digestion is the preferred treatment to apply due to the high-strength (high organic content) effluents derived from slaughterhouse facilities (Cao, 2009; U.S EPA, 2006; Wang *et al.,* 2004; Tchobanoglous *et al.,* 2003).

Primary treatment is aimed at reducing large particles such as grit, tree branches, rags as well as easily removable constituents such as floatables and grease, and settable suspended solids (sand, clay, minerals), which can impact the proper functioning of the water treatment plant. This physical treatment, namely filtering and sedimentation, removes suspended solids and BOD in the slaughterhouse effluents (Spellman, 2009; Weissman, 2007). The unit processes used in this stage include screening, catch basin, dissolved air flotation (DAF), and flow equalization. As a result, primary treatment effluents will produce water that is almost clear with a reduced BOD concentration, with organic and inorganic matter removal ratios between 60 to 80% (Tchobanoglous *et al.,* 2003; U.S EPA, 2002; Reynolds and Richards, 1996).

The present study does not provide an in-depth description of primary or biological treatment since the focus is on tertiary or complementary treatment, namely Advanced Oxidation Processes (AOPs), coupled with the biological treatment. Biological processes are proven technologies able to reduce organic matter (biodegradable part) effectively up to 90%; nonetheless, these technologies are innocuous against recalcitrant compounds resistant to biodegradation (Wang *et al.,* 2008; Tchobanoglous *et al.,* 2003; U.S EPA, 2002).

Secondary treatment is aimed at reducing BOD concentration by removing the soluble organic compounds either in solution or suspension (colloidal), which remain after primary treatment (Tchobanoglous *et al.,* 2003; Qasim *et al.,* 2000). The size of the particles in solution is less than 0.1 µm, whereas colloidal particles can range from 0.1 to 1.0 µm. Biological treatment may include different combinations of various processes, such as anaerobic lagoons, aerobic lagoons, facultative lagoons, any activated sludge process, and other biological treatments like trickling filters (U.S EPA, 2002). These processes can achieve organic matter removal rates of up to more than 90% and bacteria removal rates between 90 to 98% at typical retention times of around 20 days (Wang *et al*, 2006a; Del Pozo and Diez, 2005; Tchobanoglous *et al.,* 2003; Kiepper, 2001).

Anaerobic digestion is the preferred process in Meat Processing Plants (MPPs) due to its effectiveness in treating high-strength (high concentration of organic matter) wastewaters with COD concentrations between 3,000 and 30,000 mg L^{-1} (Tchobanoglous *et al.,* 2003). Anaerobic processes do not require air generators to provide bacteria with sufficient concentrations of oxygen for their metabolic activity, as in the case of aerobic treatment (Wang *et al*, 2004; U.S EPA, 2002). Air generators may have significant capital costs additions, which will render aerobic treatment not viable for this kind of wastewaters. However, aerobic and anaerobic processes can be coupled by employing the anaerobic process as a pre-treatment stage to remove the bulk of organic constituents, followed by an aerobic process to remove the remaining BOD. Ultimately, the selection of the appropriate process depends on the wastewater characteristics as well as the regulations to be complied with (Wang *et al.*, 2006b).

2.7.1 Water Quality Analytical Parameter

The total organic carbon (TOC) analysis provides a more accurate appraisal of the total organic compounds present in a water or wastewater sample than BOD and COD, which are typical tests used in wastewater sampling. In the TOC test, the organic matter corresponds to the organic carbon — in its various oxidation states — that is contained in a water sample; the TOC can be quantified by measuring the CO_2 generated when the organic compounds are oxidized (U.S EPA, 2002; Henry and Heinke, 1996). The TOC analysis excludes the inorganic carbon compounds in order to obtain more accurate results of the organic contamination in source waters (Zhang, 2007; Oppenlander, 2003). A more accurate analysis gives a more accurate measure of the potential oxygen demand a certain effluent can exert on receiving waters as well as enhances the ability to take accurate measures aimed at minimizing the possible negative effects.

As the American Public Health Association (APHA, 1998) described, the TOC method may be more suitable for the determination of the organic matter since it takes into account all of its different oxidation states. Other analytical methods, such as BOD and COD, only oxidize some of the compounds depending on their state decreasing the accuracy of the results. In addition, the aforementioned analytical test may take from 3 h to 5 days to produce any result, whereas the TOC analysis can provide results in 15 min. As a result, the TOC analysis is a versatile tool that allows accurate and rapid measures of the carbon content derived from organic compounds in a wastewater sample (Tchobanoglous *et al.,* 2003; APHA, 1998).

2.7.2 Wastewater Disinfection Technologies

Wastewater disinfection is applied in the last stage of the treatment process, just before discharging the effluent previously treated into receiving waters. At this point, primary and secondary treatments have already removed 90-98% of microorganisms from water during filtration, flocculation, coagulation, and biological treatment stages, yet a significant number of pathogens are still present (Tchobanoglous *et al.*, 2003). The main goal of disinfection is to prevent large concentrations of infectious-disease microorganisms from reaching waterways, intended for human consumption (Crittenden *et al.*, 2005; Spellman, 2009).

There is a whole gamut of alternatives used to disinfect wastewater, including chlorine, chlorine dioxide, and ozone, which are all chemical compounds that should be added to water. All aforementioned technologies are capable of inactivating bacteria by either one or several mechanisms, such as damaging the cell wall, changing the nature of the protoplasm, affecting the DNA and RNA structure as well as hindering enzyme activity (Tchobanoglous *et al.*, 2003). However, the production of toxic disinfection by-products (DBPs) has been identified as a major disadvantage due to their toxicity to humans and aquatic life (Tchobanoglous *et al.*, 2003). In addition to DBPs, chlorine has been proved ineffective against protozoan pathogens, particularly *Cryptosporidium parvum* (WHO, 2008). The most representative cryptosporidium outbreak took place in 1994 in Milwaukee, Wisconsin, where 403,000 people became ill, 4400 were hospitalized and 54 died (Bitton, 2005). *C. parvum* stems from human and animal feces and an infected individual may excrete approximately 10^9. The minimal infective dose is 10^1 cells cysts (WHO, 2008; Bitton, 2005). Hence, the benefits derived from the low costs of chlorine disinfection and its derivative

compounds (chloramines or chlorine dioxide) are overshadowed by the production of toxic DBPs and its infectivity against certain waterborne pathogens, particularly *C. parvum.*

Disinfection by-products (DBPs) are formed when some of the disinfectants react with certain constituents, such as natural organic matter (humic and fulvic acids) as well as bromide, which are present in the water being treated. DBPs are suspected carcinogens and a potential threat to human health. For example, chlorine has the ability to form disinfection by-products (DBPs), such as trihalomethanes (THMs) and other halogenated DBPs, which are suspected carcinogens (Tchobanoglous *et al.,* 2003; Nieuwenhuijesen *et al*, 2000). Some THMs that occurred in drinking water supplies include chloroform ($CHCl_3$), bromodichloromethane ($CHBrCl_2$), dibromochloromethane ($CHBr_2Cl$), bromoform ($CHBr_3$), dichloroiodomethane ($CHCl_2I$), and bromochloroiodomethane (CHIBrCl). DBPs produced during chlorination may cause birth defects, reproduction impairment, and are suspected carcinogens (Nieuwenhuijesen *et al*, 2000). Apart from THMs, another important DPB, namely *N*–nitrosodimethylamine (NDMA), is formed in the presence of nitrites in water and wastewater. NDMA is among the most potent suspected carcinogens known (Asano *et al.*, 2007). As a result, the use of chlorine compounds for the disinfection of drinking water can pose serious risks to public health by the production of deleterious substances (Black and Veatch, 2010; Bolton, 2010; Manitoba Water Stewardship, 2005).

Even though ozone is effective against all waterborne pathogens, including *C. parvum,* it also forms disinfection by-products (DBPs) such as aldehydes, aldo- and keto-acids, which are formed in the presence of organic and inorganic elements. Furthermore,

inorganic DBPs, such as bromated ion, bromoform, brominated acetic acid, bromopicrin, brominated aceto nitriles, and cyanogens bromide are formed in the presence of bromide, (Tchobanoglous *et al.,* 2003). Brominated DBPs are suspected carcinogens and highly toxic to human health.

Chlorine dioxide does not impart any flavor or chlorine-like taste to water, unlike chlorine, its major disadvantage is the production of chlorite and chlorate ions, which are toxic DBPs as well as its inability to inactivate *C. parvum* (WHO, 2008; Tchobanoglous *et al.,* 2003).

Contrary to the aforementioned disinfection technologies, UV radiation does not produce significant alterations on the chemistry of water nor does it significantly interact with any of the chemicals within the water (Black and Veatch, 2010; U.S EPA, 1999). UV radiation does not alter the natural physiochemical features of the water being treated as no chemical agents are added. As a result, the formation of THMs or other DBPs with UV disinfection is minimal. In addition, UV radiation has been proved effective in inactivating *C. parvum* and it may reach 4 log (99.99%) inactivation rates in no more than one minute of exposure time (Rose and O'Connel, 2009; U.S. EPA, 2006).

2.7.2.1 Disinfection Regulatory Requirements

After organic mater have been treated from water a last stage before being discharge to a water body is the pathogen disinfection (Black and Veatch, 2010). The goal of sufficient drinking water disinfection may vary, but the most stringent regulation, like the one from Germany, set it at 4 log reduction (99.99%) concentration for bacterial pathogens and 3 log reduction (99.9%) for viral pathogens as well as protozoa (Oppenlander, 2003; U.S EPA, 1989). The annual infection risk must not exceed 1 infection per 10,000 consumers, which is

assumed as an acceptable risk for infectious agents acquired through potable water (Sommer *et al.,* 2008). According to the Ontario Drinking Water Standards (2003), the maximum allowable concentrations for both *E. coli* and total coliform should be not detectable (zero cells) in a 100 mL of water sample.

Water quality characteristics and log removal requirements of specific locations are determinants for the irradiation time required for achieving effective pathogenic inactivation. As the U.S EPA (1999) implied, the survival of microorganisms can be calculated based on a first order kinetics, as a function of UV irradiation time and is not dependent on the initial microorganism's density. Equation (2.21) states the bacteria inactivation efficiency (*I*) of the system is as follows:

$$I = log\frac{N_0}{N_t} \qquad (2.21)$$

Where N_0 is the initial concentration of microorganisms and N_t is the concentration of microorganisms after treatment. Hence, a 4 log-unit inactivation, which is the regulation requirements for bacterial pathogens, means that the initial number of microorganisms (100%) is reduced by 99.99% (Oppenlander, 2003).

2.8 Need for Advanced Treatment Application

Having done a general review of the most common treatment technologies applied in meat processing plants, the question is whether or not it is justified to complement biological treatment with a pre-treatment or post-treatment process carried out by AOPs. The answer

can be directly linked to factors such as biodegradability, form (colloidal, suspended, or dissolved), and toxicity or inhibitory characteristics of the organic and inorganic constituents specific to each wastewater (Eckenfelder, 2009; Tabrizi and Mehrvar, 2004). A variety of organic compounds toxic to bacteria include aromatic compounds, halogenated compounds, oils, lipophilic solvents, and anionic surfactants (Gerardi, 2006). For instance, aromatic compounds, such as benzene, toluene, and xylenes are also highly toxic to bacteria. Similarly, compounds such as chloroform, trichloromethane, tetrachloromethane, and methylene chloride as solvents halogenated compounds used in manufacturing dyes, pharmaceuticals, and plastics are highly toxic to bacteria used in wastewater treatment. All the aforementioned compounds have a common characteristic in that they are non-ionic in charge or structure, thus, causing them to dissolve rapidly into the cell wall exerting toxicity. As a result, undesired effects such as treatment efficiency losses, discharge permit violations, and operational cost increments may arise if these sorts of compounds are not removed before biological treatment. In this case, a pre-treatment process by AOPs should be conducted in order to eliminate these recalcitrant and toxic compounds, maximizing the efficiency of the biological treatment stage.

Table 2.6 summarizes recent studies conducted on AOPs, namely UV-C/H_2O_2 and VUV, alone and combined with biological treatment and its effectiveness in removing organic compounds from slaughterhouse wastewater as well as so-called emerging contaminants, such as bisphenol A (BPA), pharmaceutical active compounds (PhACs), personal care products, perfluorinated surfactants, and other contaminants from surface waters. Conventional biological processes do not target these kinds of contaminants,

Table 2.6. Selected studies on AOPs effectiveness in removing recalcitrant compounds from water and wastewater.

Target Compound	AOP Process	Analytical parameter	Results	References
Aromatic compounds in slaughterhouse wastewater	UV-C/H_2O_2	COD and Color	The H_2O_2/UV treatment was 5.2 times faster than simple UV in removing aromatic compounds >95%	Luiz *et al.*, 2009
Organic content as TOC from slaughterhouse wastewater	Combined biological/ UV-C/H_2O_2	TOC, TN, COD, and BOD	Molar Ratio of $[H_2O_2]$ /[TOC] of 3.5; pH neutral; 95% TOC removed	Cao and Merhvar, 2010
Nonbiodegradable toxic compounds from nonionic/anionic textile surfactant	Combined Biological/ UV-C/H_2O_2	COD	Good removal rates of COD after 120 min of irradiation time	Arslan-Alaton *et al.*, 2007
Thiacloprid (insecticide)	UV-C/H_2O_2	[Substrate] by HPLC	Molar ratio of $[H_2O_2]$ /[TOC] of 220 and pH 2.8. Under these conditions, 97% of the thiacloprid was removed in about 120 min.	Abramovic *et al.*, 2010
Pharmaceuticals: Dilantin carbamazepine, Atenolol, Meprobamate, trimethoprim	UV-C/ H_2O_2	[Substrate] by liquid chromatography/mass spectrometry	Removal rates between 0 and >99%	Rosario *et al.*, 2010
Pharmaceuticals: 12 antibiotics and 10 analgesics	UV-C/H_2O_2	[Substrate]	Removal rates between 86–100%	Kim *et al.*, 2009a
Pharmaceuticals and personal care products	UV-C/H_2O_2	[Substrate]	$[H_2O_2]$ = 8.2 mg L^{-1} Removal rates > 90%	Kim *et al*, 2009b
Tetracyclines	UV-C/H_2O_2	[Substrate] and TOC	$[H_2O_2]$ = 0.02–2 mmol L^{-1}, 100% removal in 6 min	Lopez at al., 2010
Perfluorinated Surfactants	UV-C/H_2O_2	TOC and COD		Quinete *et al.*, 2010
Neurotoxins: Anatoxin-a	VUV	[Substrate] by HPLC	$[H_2O_2]$ = 30 mg L^{-1} is added to 0.6 mg L^{-1} of anatoxin-a >70% degradation	Afzal *et al*, 2010
Trichloroethene	UV-C/H_2O_2	[Substrate]	Complete mineralization in 30 min	Li *et al.*, 2007
Bisphenol A (BPA)	UV-C/H_2O_2	[Substrate	Effectively removed from the system	Yongqiang, 2010
Atrazine	VUV	TOC	[ATZ]= 30 mg L^{-1}. mineralization achieved	Gonzalez *et al.*, 1994
NOM	UV-C/H_2O_2	[Substrate]	Reduction of NOM 94%	Goslan *et al*, 2006

Notes:

[Substrate]= pollutant concentration removal measured by analytical methods such as HPLC and GC/MS
NOM= Natural Organic matter
TOC= Total Organic Carbon
COD= Chemical Oxygen Demand

whereby AOPs are becoming more appealing to serve as complementary treatment either in a pre- or post-treatment stage, to current biological processes. Additionally, AOPs may inactivate bacteria without adding any additional chemicals to the water, unlike the chlorination or ozonation disinfection processes, thereby avoiding the formation of hazardous disinfection by-products (Wang *et al.*, 2006a; Tchobanoglous *et al.*, 2003).

In summary, it is evident that conventional wastewater treatment processes, mainly biological processes, are good for achieving organic matter removal. However, toxic compounds derived from industrial processes, such as manufacturing of pharmaceuticals, dyes, or plastics are noxious to bacteria used to digest the pollutants and inhibit their ability to properly digest the target pollutants. More importantly, conventional processes do not remove trace concentrations of emerging contaminants such as PhACs, BPA, personal care products, trichloroethene, neurotoxins, and perfluororinated surfactants. Therefore, the combination of conventional wastewater treatment with other technologies, among which AOPs are gaining momentum, is being strongly considered by policy-makers in regulatory agencies as well as decision–makers in different industry sectors to comply with regulatory standards and enhance wastewater treatment processes (Water Environment Federation, 2008; U.S EPA, 2002).

2.9 Concluding Remarks

AOPs are becoming a promising technology used in both water and wastewater treatment processes. It has been shown that photochemical processes are one of the most

efficient processes among AOPs to produce $^{\bullet}OH$, which is the most powerful oxidant in the water treatment field. In particular, the vacuum-UV photolysis process is turning into an excellent option to purify water. The many advantages of the VUV process include the production of $^{\bullet}OH$ from the homolysis of the water molecule without the addition of auxiliary chemicals, which ideally is the main purpose of purification: removing rather than adding more chemicals. The VUV process does not require monitoring of the residual H_2O_2 after treatment or the addition of even more chemicals, such as catalase, to remove it.

Even though producing VUV radiation is more expensive than UV-C radiation, the lighting industry is developing fast and is producing new lamps, which convert electric energy into VUV at higher efficiency rates, thereby reducing the costs (Oppenlander, 2003). Consequently, VUV is becoming one of the outstanding members belonging to the AOPs group, which could produce the coveted $^{\bullet}OH$ in a simple manner becoming a feasible alternative to UV-C/H_2O_2. Another important advantage of the photochemical processes in general is that they do not generate the highly toxic disinfection by-products (DBPs) during the disinfection stage, unlike other chemical disinfectants such as chlorine, ozone, chloramines, or chlorine dioxide. As shown in the literature review, DBPs pose an extra risk to public health apart from the compounds being targeted by the process itself. When looking at literature, it can be noticed that there are few studies that look at the combination of VUV/UV-C as an alternative to the UV-C/H_2O_2 photolytic process.

A recent study on slaughterhouse wastewater treatment by combining anaerobic treatment and UV-C/H_2O_2 (Cao and Mehrvar, 2010) served as guideline to the present study,

which seeks to further the results obtained in the aforementioned work by looking at the feasibility to use a combination of VUV/UV-C for TOC removal from slaughterhouse wastewater. In addition, the present study conducts experiments on batch recirculation and continuous mode to observe any differences in TOC removal efficiencies. The results obtained from this work will help to broaden the information about AOPs' behaviour and effectiveness in removing TOC from slaughterhouse wastewater, particularly in the VUV photolytic processes, and its potential applications to purify water. VUV is emerging as an important AOP, which is of interest for the academic community and society in general due to its versatility in oxidizing organic compounds without using auxiliary oxidants.

CHAPTER 3

MATERIALS AND METHODS

3.1 Introduction

This study focused in establishing the efficiency of VUV, in comparison to other photochemical process, including UV-C photolysis, UV-C/VUV and VUV/UV-C combined as well as UV-C/H_2O_2 and VUV/H_2O_2, to remove organic matter (as TOC) and bacteria from synthetic slaughterhouse wastewater. To that end, experiments were conducted and results were analyzed to assess the applicability of such processes. The present chapter first reviews the materials required to conduct the experiments. This review then leads to a description of the methods and procedures associated with TOC quantification and analysis as well as bacteria quantification. Finally, kinetic modeling and electrical energy per order, which serves to evaluate the treatment efficiency for each of the photochemical processes, are explained.

3.2 Materials

3.2.1 Synthetic Wastewater Composition

Synthetic slaughterhouse wastewater was generated according to a previous study conducted by Stephenson and Lester (1985). The individual components and concentrations consisted of: commercial meat extract powder (Oxoid Lab Lemco LP0029, Oxoid Ltd.), 1950 mg L^{-1}; glycerol ($C_3H_8O_3$), 200 mg L^{-1}; ammonium chloride (NH_4Cl), 360 mg L^{-1}; and sodium chloride (NaCl), 50 mg L^{-1}. An initial TOC concentration of ~140 mg L^{-1} was used in

this study. Eventually concentrations of 30 and 230 mg L^{-1} were used to observe the behaviour of the system for different molar ratios of $[H_2O_2]$ / [TOC].

3.2.2 Bacteria Strains

Four bacteria strains were used to test different photochemical processes, including *Escherichia coli O157:H7* ATCC 700927, *Salmonella enterica* serovar Typhimurium ATCC 14028, obtained from Dr. Dae-Young Lee (University of Guelph, Guelph, Ontario, Canada) *Shigella flexneri* ATCC 12022, and *Pseudomonas aeruginosa* ATCC 27853, obtained from Liberty Victorio-Walz (Ryerson University, Toronto, Ontario, Canada). All bacteria strains were grown overnight in 3 g/L Tryptic Soy (CASO) Broth (TSB) (EMD Chemicals Inc., Mississauga, ON, Canada) with shaking (250 rpm) at incubation temperatures of 37°C, except for the *P. aeruginosa* strain, which was grown at 30°C to an approximate cell density of 10^9 CFU mL^{-1}, which was confirmed by optical density (O.D).

3.2.2.1 Plates for the Enumeration of Microorganisms

Heterotrophic plate counting was used to enumerate bacterial cells. Tryptic soy agar (TSA) was prepared by adding 3 g of TSB and 15 g of agar to 1 L distilled water. The solution was autoclaved at 121°C for 30 minutes and then was cooled for 15 minutes. The agar was poured into petri dishes (sterile VWR® Petri Dishes from VWR, Mississauga, Ontario, Canada). The pouring procedure was performed within a laminar flow fume hood in order to prevent any contamination from the surrounding air. The plates were left inside the fume hood overnight to let them solidify.

3.2.2.2 Dilution media

Sodium chloride (saline, NaCl 0.9%) was the solution used in the serial dilution. NaCl prevented the bacteria from lysing while the plating spread procedure took place (Benson, 2001). One litre of stock solution was prepared by adding 9 g of NaCl to 1 L of distilled water. The solution was sterilized by autoclaving it at 121°C for 30 min.

3.2.3 Experimental Setup

Two stainless steel photoreactors model SL-LAB 2 (Siemens Inc.) were used for the treatment of the synthetic wastewater. Each photoreactor had a capacity of 7.57 liter per minute (LPM) (2 gallons per minute (GPM)), a length of 305 mm, and a diameter of 51 mm. According to the manufacturer, the capacity of 7.57 LPM is dependent on a 40 mJ cm^{-2} UV dosage at the end of lamp life and a UV transmittance of 98% (254 nm; 1 cm cell).

UV-C Low-pressure Hg lamp at 14 W and a VUV LP Hg lamps high output at 14 W (LP4130 and LP4135 obtained from Siemens Inc.) were used. UV emission peaks were at 254 nm (UV-C output of 4 W) and 185 nm (VUV output of 3.90 W). A quartz sleeve was used to protect the lamps from fouling formation — dirt arising from the solution being treated — that may interfere with the UV radiation emission as shown in Figure 3.1. The effective volume of the photoreactor (obtained by subtracting the volume of the quartz sleeve from the total photoreactor volume was 0.46 L. The volume was confirmed by filling the photoreactor with water resulting in the same volume of 0.46 L.

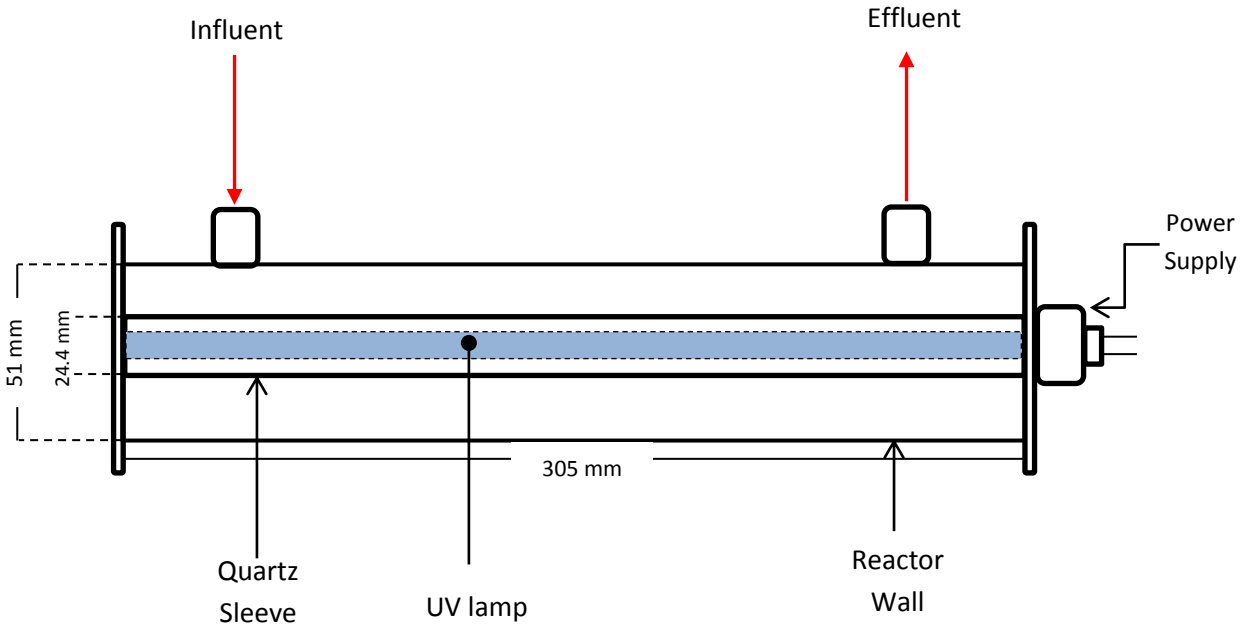

Figure 3.1. Schematic diagram of an individual UV photoreactor.

Figure 3.2 illustrates the photochemical wastewater treatment system comprised of two photoreactors, (a) front view shows the UV-C (254 nm) and (b) rear view shows the VUV (185 nm) photoreactor; a centrifugal magnetic pump with a maximum capacity of 4.6 GPM and maximum head of 36.1 ft. (Model RK-72012-10 obtained from Cole-Parmer); and an acrylic in-line flowmeter (model R-32477-00 Cole-Parmer) with a flow-rate range between 0.1 and 1 L min^{-1} used to control the water flow-rate during the continuous operation. The system was also equipped with a by-pass valve to control the flow-rate and provide the relief to the pump pressure. In addition, the system was supplied with a set of valves that allowed using both processes UV-C and VUV individually as well as the two processes combined. The experimental setup can be also seen in more detail on Figure 3.3(a) front view and 3.3(b) rear view, which provide an actual image of the experimental setup.

3.3 Experimental Procedures

3.3.1 Synthetic Slaughterhouse Treatment by UV-C and VUV

To obtain the kinetic parameters of all six processes: UV-C photolysis, VUV oxidation, UV-C/VUV and VUV/UV-C combined as well as UV-C/H_2O_2 and VUV/H_2O_2, experiments with synthetic wastewater were run in a batch recirculation operation. The wastewater was exposed to each one of the photochemical processes for a total of 2.5 h. Initially, both processes UV-C and VUV individually were tested for the TOC removal from the synthetic wastewater slaughterhouse. It was then exposed to the combined processes UV-C/VUV and VUV/UV-C. Finally, hydrogen peroxide was used as an auxiliary oxidant added UV-C/H_2O_2 and VUV/H_2O_2. It is worth noting that batch experiments are only with the purpose to find the kinetic parameters. In real life is unpractical and impossible to

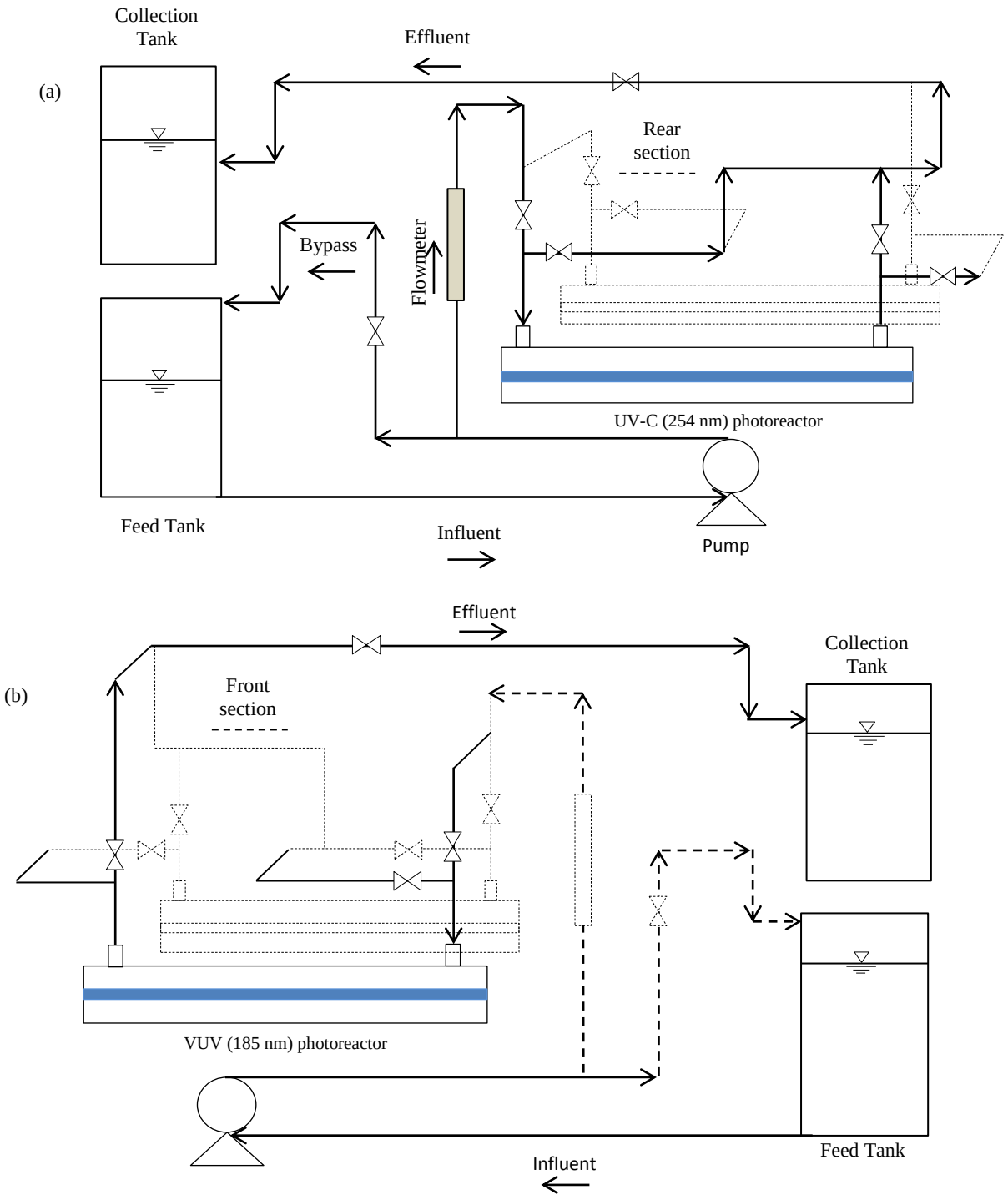

Figure 3.2. Schematic diagram of the combined UV-C and VUV photochemical processes experimental setup (a) front view and (b) rear view.

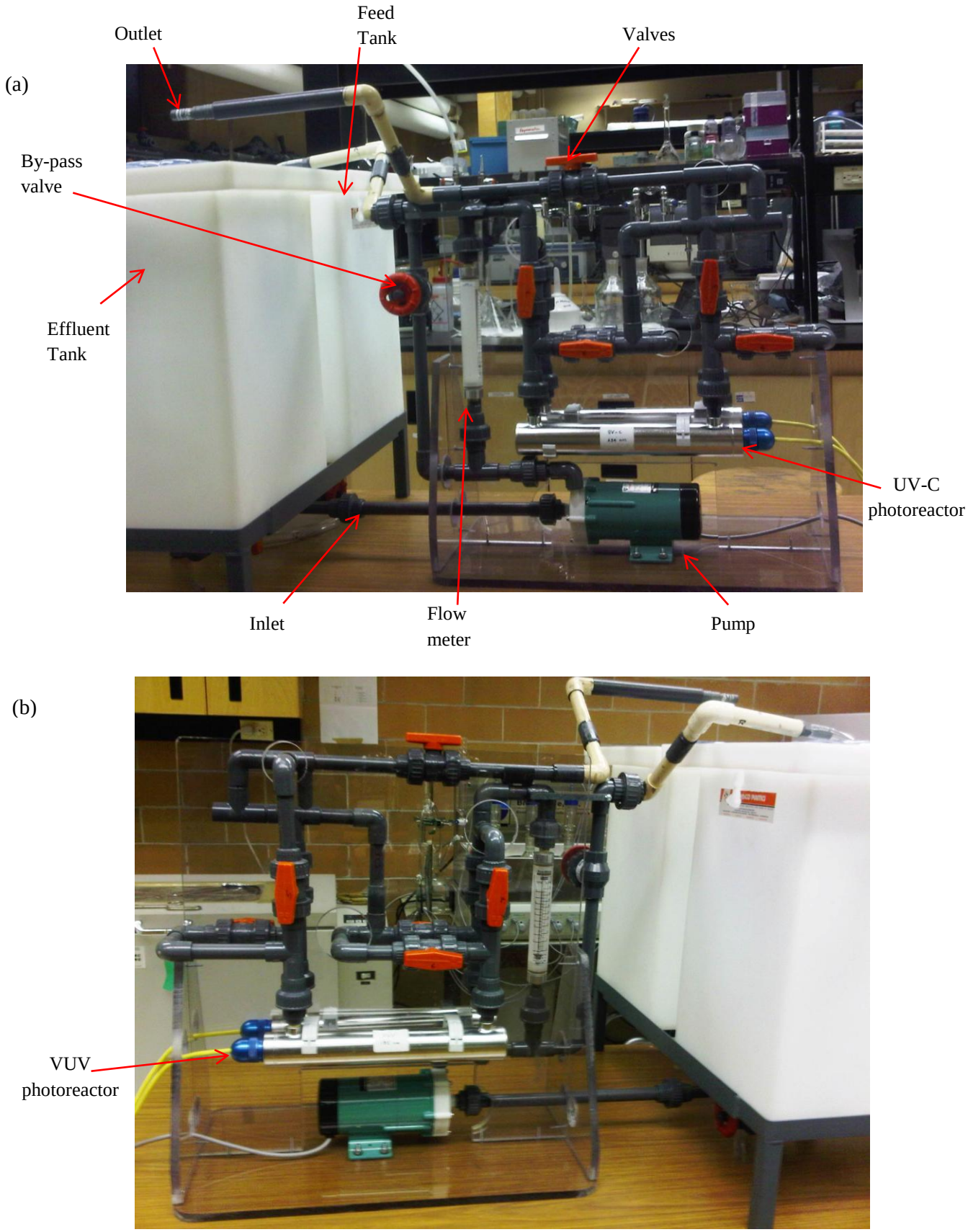

Figure 3.3. VUV and UV-C experimental setup (a) Front view (b) Rear view.

implement a water treatment plant using batch recirculation processes due to the huge volumes used. Therefore the goal is to test the system in continuous flow operation to resemble field conditions.

The volumetric flow rate was set at 0.3 L min^{-1}, which provided a total hydraulic residence time of 0.92 min (55.2 sec). According to Oppenlander (2003), a batch recirculation should be operated such that not more than 5% of the contaminant is degraded at each pass through the photoreactor, because it will reduce the overall efficiency of the batch recirculation process. Since preliminary tests with a flow rate of 0.1 L min^{-1} removed more than 5% (see results section), it was assumed that 0.3 L min^{-1} would be an ideal flow rate to perform the recirculation experiments, causing less than 5% of pollutant depletion by every pass-through the photoreactor. Experiments using higher flow rates were conducted; however, the TOC degradation efficiency was unnoticeable. At higher flow rates, the irradiation time was reduced, thereby reducing the TOC degradation effectiveness of the process. Therefore, the results showed in this study refer to TOC reduction performed in a continuous system at a flow rate of 0.1 L min^{-1} only.

TOC removal rates were then assessed in a continuous-flow operation to compare any change on TOC removal efficiencies with respect to the results obtained during the batch recirculation mode. Experiments were conducted in the same fashion: first, the two processes UV-C and VUV were tested individually and then, the two processes were combined. Finally, hydrogen peroxide was added to each process. A flow-rate of 0.1 L min^{-1}, which determined a hydraulic residence time of 4.6 min, was employed during flow-through

operation. A flow rate of 0.2 L min^{-1} was used for the combined treatment in order to guarantee a total residence time of 4.6 min, 2.3 min in each photoreactor.

3.3.1.1 TOC analysis

Samples were taken at the effluent of each photoreactor in the individual processes as well as at the effluent of the combined processes at t = 0, 30, 60, 90, 120, 150 min (2.5 h of total irradiation time) in the case of the batch recirculation operation. For the continuous operation mode, samples were taken at the effluent tank, after one-pass of the sample through the photoreactor. The samples were analysed by an Apollo 9000 Combustion TOC analyser (Apollo 9000, Teledyne Tekmar Co.), which was previously calibrated using potassium hydrogen phthalate (KHP). The KHP was dried in an oven at 105°C during 2 h and let to cool in a desiccator to remove any moisture absorbed from the atmosphere. The calibration of the TOC analyzer was performed by preparing a set of working standard solutions within the range expected for the TOC values, namely 1- 400 mg L^{-1}. A 1,000 mg L^{-1} KHP stock solution was prepared by dissolving 2,125 mg of KHP into 1 L of distilled water. Then, working solutions of 1, 25, 50, 100, and 400 mg L^{-1} were prepared from the stock solution using distilled water. Equation (3.1) illustrates how the TOC removal efficiency was calculated:

$$TOC\% = \frac{TOC_{in} - TOC_{out}}{TOC_{in}} \times 100 \qquad (3.1)$$

where, TOC_{in} is TOC concentration in the inlet, $mg\ L^{-1}$, and TOC_{out} is TOC concentration in the outlet, $mg\ L^{-1}$.

3.3.2 Bacteria Inactivation Experiments

Experiments for the inactivation of bacteria were conducted on a continuous operation mode using different exposure times which were controlled by varying the flow rate, including 0.1 0.5, 1, 6, 6.5, and 7 L min^{-1} in the photoreactors. These flow rates were chosen based on the minimum and maximum values allowed by the pump specifications. To test the efficiency of each process in inactivating bacteria, two types of working solutions were employed. Volumes of 70 L, prepared with distilled water to simulate clear and transparent water, were spiked by adding equal volumes 1:1:1:1 (25 mL) a mixed culture of the bacterial strains (see Section 3.1.2), which had been grown overnight and reached a stationary phase. Tryptic Soy Broth (TSB) media in which the bacteria were grown was removed by washing them to prevent any interference to the TOC concentration readings derived from additional organic compounds. For the washing procedure the bacteria suspended in TSB solution were centrifuged at 5,000 rpm for 15 min (in a Thermo Scientific Heraeus Multifuge X1**).** The TSB solution was removed and the bacteria pellets were re-suspended using saline solution. Bacteria concentrations in the working solution were approximately 10^5 CFU mL^{-1}, comprised of a mixed culture 1:1:1:1 of the targeted strains. The inlet concentration in the working solution was measured by heterotrophic plate counting. The solution was then exposed to UV-C and VUV radiation in a continuous mode operation at different residence times (provided by the aforementioned flow rates) ranging from 4.1 to 288 s for 7 and 0.1 L min^{-1} flow rates, respectively.

In the second stage, 5 L working solutions of synthetic slaughterhouse wastewater were prepared and sterilized by autoclaving them at 121°C for 1 h to prevent any background bacteria contamination. After, the solution was spiked with the targeted bacterial strains following the same procedures of the experiments conducted with distilled water, obtaining initial concentrations of 10^5 CFU mL^{-1}.

3.3.2.1 Heterotrophic plate counting

Ten mL samples were collected in sterile falcon tubes. To obtain a viable cell number between 30 and 300 colonies per plate, several tenfold dilutions were performed by diluting 0.1 mL of sample into 0.9 mL of saline as shown in Figure 3.4. Each aliquot was vortexed to ensure a uniform concentration. Samples of 0.1 mL were subsequently spread plated in duplicate on tryptic soy agar. The plates were incubated overnight (in a C25KC classic incubator, New Brunswick Scientific Co. Edison, NJ, USA) at 37°C.

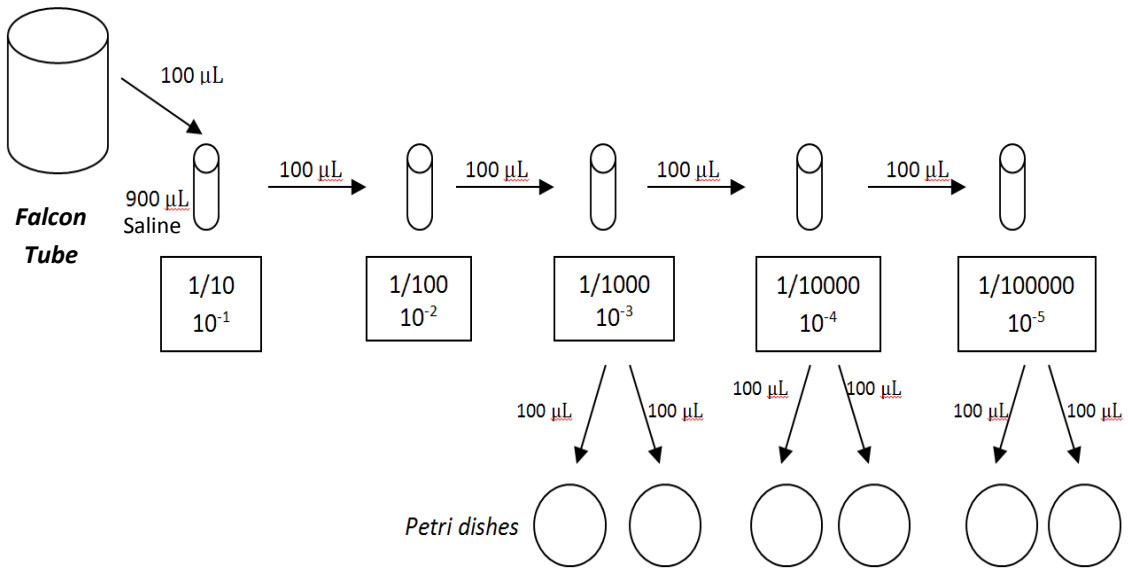

Figure 3.4. Schematic representation of the serial dilution procedure.

Colonies formed in 24 h were counted with the naked eye. Each colony or cluster of bacteria represented an agglomeration of millions of cells of bacteria theoretically originating from a single cell. For this reason, colony forming units (CFU) is the parameter that best fits in measuring the population size of bacteria (APHA, 1998; Batzing, 2002). Equation (3.2) shows how to determine the bacteria concentration by dividing the number of colonies observed by the sample volume:

$$\text{CFU/mL} = \frac{no.\ of colonies\ counted \times dilution factor}{volume\ of\ sample\ inoculated\ (mL)} \qquad (3.2)$$

CHAPTER 4

RESULTS AND DISCUSSION

4.1 Introduction

This chapter shows the results obtained during the experimental work. This chapter first provides the TOC removal rates obtained during the batch recirculation mode for all photochemical processes evaluated: UV-C photolysis, VUV oxidation, combined UV-C/VUV and VUV/UV-C as well as UV-C/H_2O_2 and VUV/H_2O_2, followed by an outline and discussion of the results obtained for TOC removal rates achieved during continuous mode operations. This leads to the discussion of the optimum H_2O_2 concentration for the UV-C/H_2O_2 and VUV/H_2O_2 obtained for the specific operating conditions associated with the experimental setup employed in this study as well as the analysis from a molar ratio [H_2O_2]/[TOC] point of view. This chapter concludes with a discussion of the overall performance of the photochemical treatment of the synthetic slaughterhouse wastewater in the presence of bacteria.

4.2 Batch Recirculation Mode Experiments

A series of experiments in batch recirculation mode was conducted in order to establish the TOC removal efficiency. First, a set of controlled experiments was performed in order to determine the loss of organic matter through adsorption into the reactor walls or by volatilization. The synthetic slaughterhouse wastewater was recirculated within the system with the UV lamps turned off for 2.5 h. Samples were collected every 30 min at the effluent. Figure 4.1 describes the variation of the TOC concentration after 2.5 h of UV exposure.

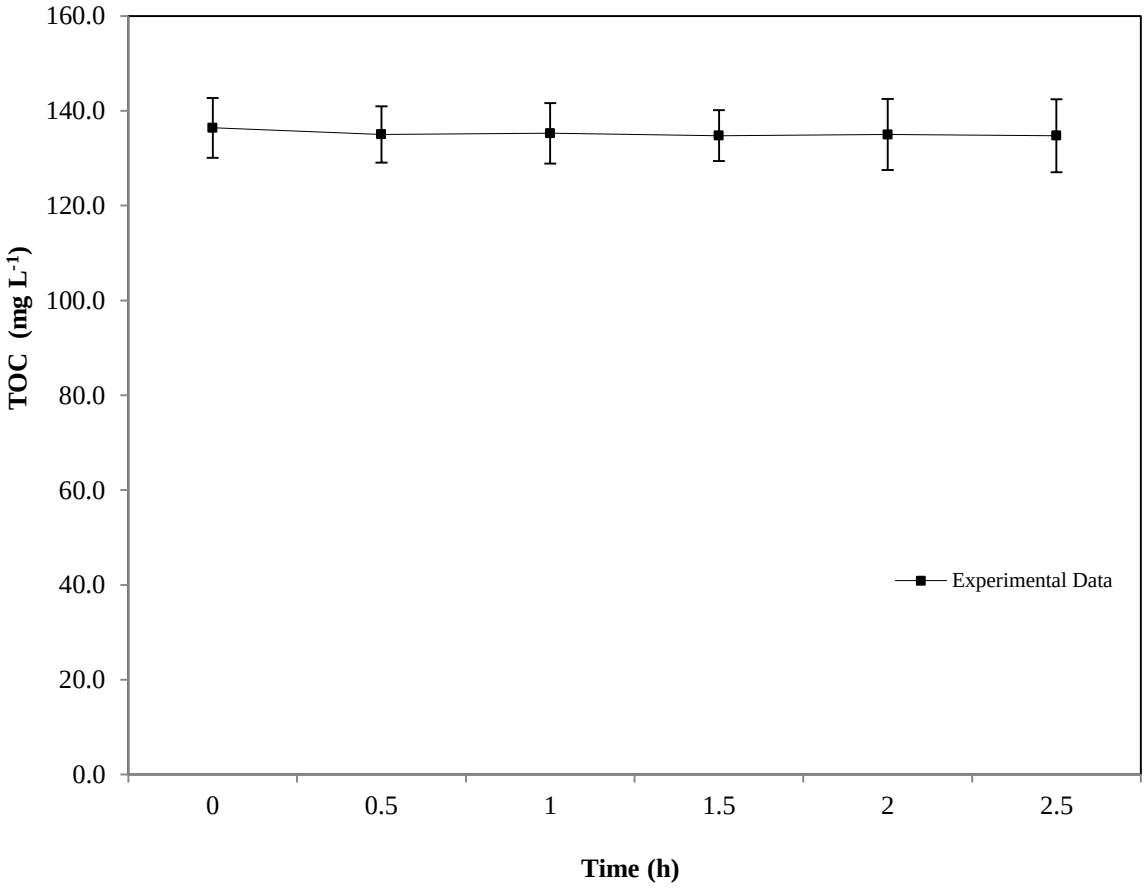

Figure 4.1. Dark reaction (No UV radiation and no H_2O_2 present) for TOC removal of a synthetic slaughterhouse wastewater during batch recirculation mode. Error bars represent the standard deviation for three experimental replicates.

After 2.5 h, the dark reaction showed that the TOC concentration remained almost constant with only a 1.23% TOC reduction. Therefore, it appeared that no significant organic material adsorption to the reactor walls or material losses due to volatilization occurred. Any TOC reduction in subsequent experiments can therefore, be attributed to the action of either UV-C or VUV radiation.

No attempt to control the temperature was made. The temperature of the system ranged between 26 and 28°C. A fan to cool down the pump was the only source of cooling the system employed to avoid pump overheating. The pH was between 7.0 and 7.2 measured by a portable pH meter (230A plus, Thermo Orion).

4.2.1 UV-C and VUV Direct Photolysis

To evaluate the total organic carbon (TOC) removal rates achieved by different photochemical processes, the synthetic slaughterhouse wastewater was exposed to both photolytic processes, UV-C and VUV, individually as well as the combined processes UV-UV-C/VUV and VUV/UV-C. The UV-C photolysis consisted of direct absorption of UV radiation at peak maxima of 254 nm by the target pollutants, while VUV consisted of the water photolysis (bond cleavage) to produce $^{\bullet}OH$ and oxidize the pollutants present in the water sample.

The TOC removal from synthetic slaughterhouse wastewater was studied in a batch recirculation mode for four processes. Figure 4.2 shows the TOC removal trend for all four photolytic processes including UV-C, VUV, and combined UV-C/VUV and VUV/UV-C photolytic processes. In the first stage, the UV-C and VUV individually irradiated the synthetic slaughterhouse wastewater for 2.5 h. TOC removal rates reached a total of 48.1% and 55.4% for UV-C and VUV, respectively, as shown in Figure 4.3.

Eventually, a slaughterhouse wastewater sample was irradiated by the combined processes, UV-C/VUV as well as VUV/UV-C. The arrangement of the processes was varied in order to observe any possible differences in the final removal efficiency. The combined processes UV-C/VUV and VUV/UV-C achieved removal rates of 57.6 and 55.1% respectively as shown in Figure 4.3. It is noticed that a slightly higher removal rate of 57.6% for the combined processes than for the VUV alone, of 55.4%. A possible explanation to this result can be the formation of different intermediates during the oxidation process. From the general AOPs oxidation pattern of organic matter (see Reaction 2.13) It could be inferred that compounds, which are faster to degrade such as alcohols or aldehydes, were formed during the combined UV-C/VUV process, whereas harder-to-degrade compounds like ketones and carboxylic acids were formed during the VUV and VUV/UV-C. Therefore, the position in which UV-C or VUV in the combined process come first might have altered the oxidation pathway. This could only be determined by very specific analytical procedures such as gas chromatography-mass spectrometry (GC/MS), or a high-performance liquid chromatography (HPLC) analysis, which are highly sensitive procedures and can identify the kinds of intermediates that are formed during the oxidation process (APHA, 1998).

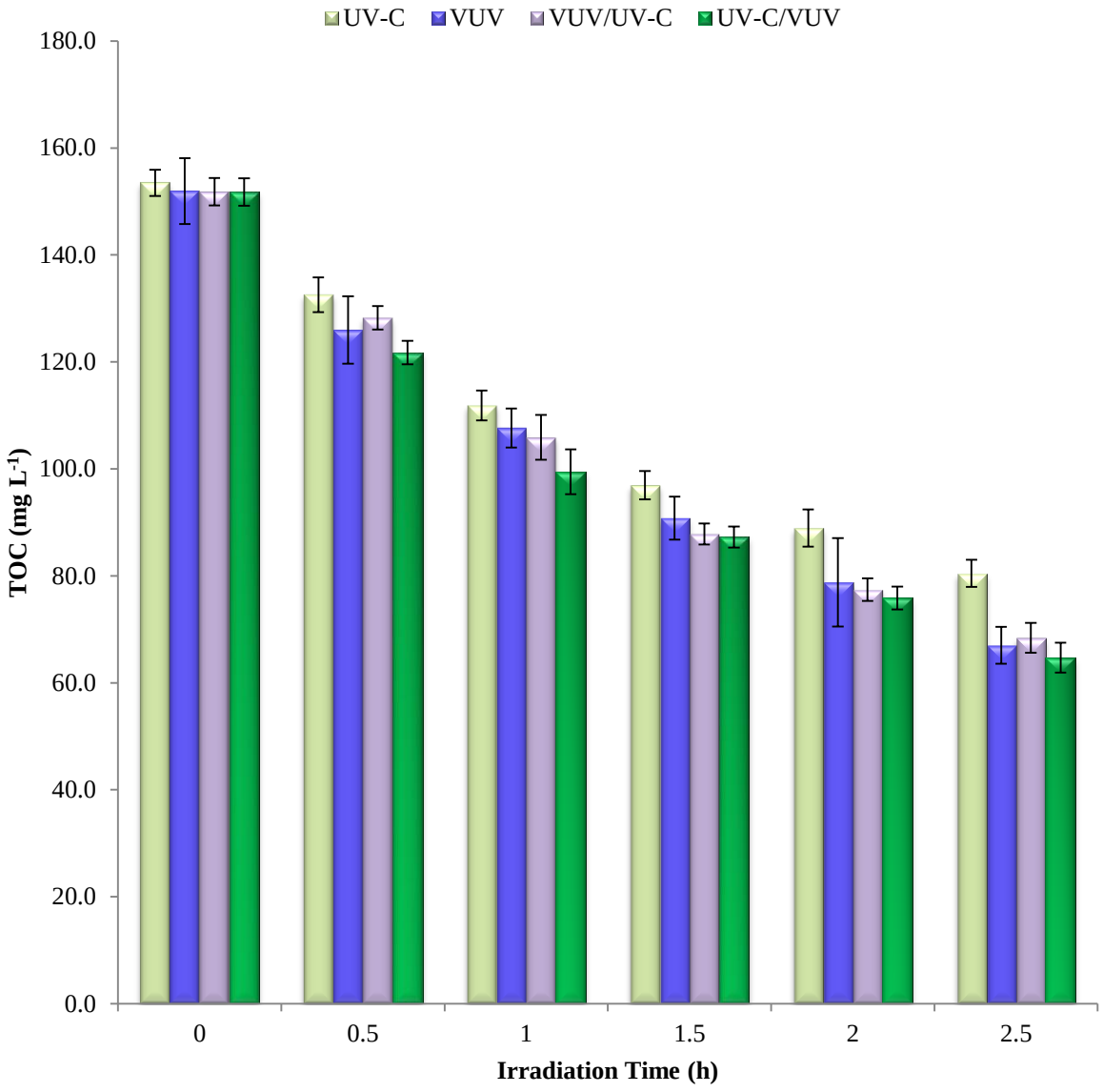

Figure 4.2. TOC removal for the different photochemical processes UV-C (254 nm) and VUV (185 nm) and their respective combinations UV-C/VUV and VUV/UV-C in batch recirculation mode. Error bars represent the standard deviation for three experimental replicates.

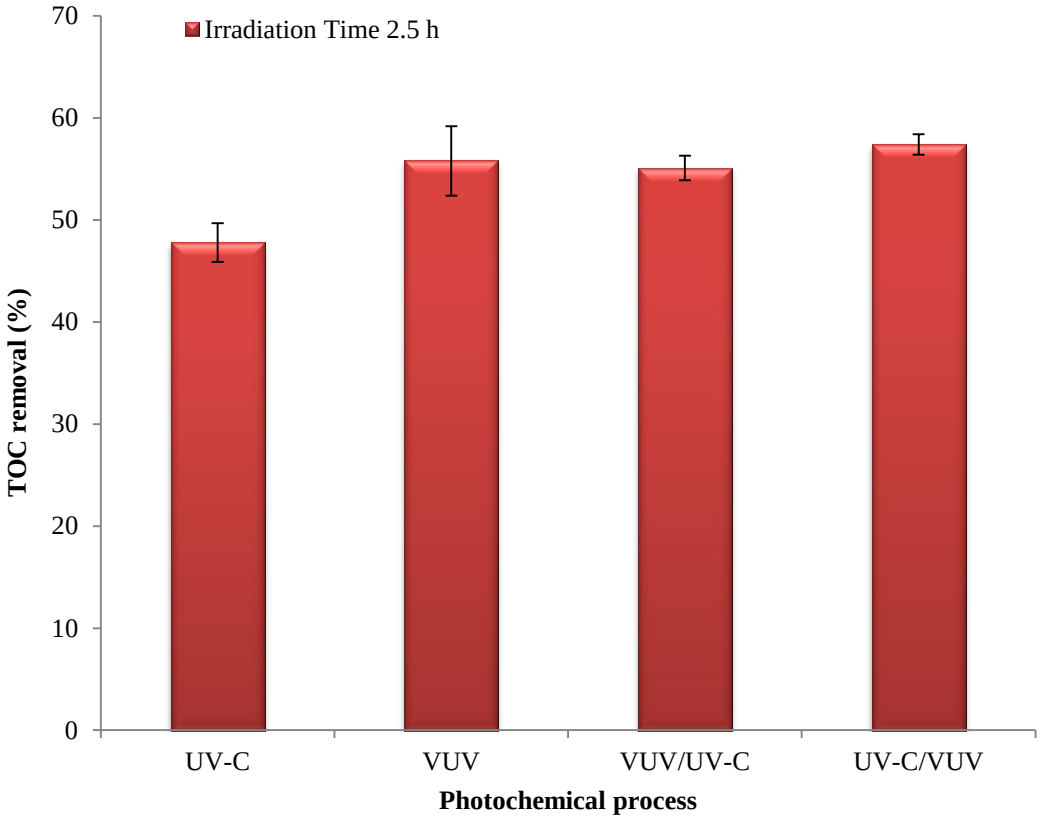

Figure 4.3. TOC removal (%) for the different photochemical processes UV-C (254 nm) and VUV (185 nm) and their respective combinations UV-C/VUV and VUV/UV-C in batch recirculation mode. Error bars represent the standard deviation for three experimental replicates.

The least efficient process was the UV-C photolysis alone, 48.1%, which can be attributed to the different degradation mechanisms. For example, while the VUV oxidation process is carried out by the production of highly reactive $^{\bullet}OH$ radical species, the UV-C process is carried out by direct photolysis of the organic molecules, which is less efficient in TOC degradation. It should be also noted the difference in the lamps' conversion efficiencies. While UV-C lamp has an efficiency of 28%, the VUV lamp conversion efficiency is about 5% that of the UV-C output achieved by using a suprasil quartz sleeve (high purity). As a result, the VUV process achieved higher TOC degradation rates with just a fraction of the conversion efficiency of that of the UV-C lamp. It would be interesting to see results using lamps with higher efficiencies, such as excimer lamps, which can reach efficiencies of about 60% of VUV output at 172 nm.

4.2.2 UV-C/H_2O_2 and VUV/H_2O_2 Photo-initiated Oxidation in Batch Recirculation Mode

To establish any benefits in TOC removal derived from the addition of hydrogen peroxide into the system, experiments were conducted by UV-C/H_2O_2 and VUV/H_2O_2. Hydrogen peroxide absorbs UV radiation in a wide range from 180 to 480 nm (Tang, 2004). The shorter the wavelength, the better the absorption, therefore, producing more $^{\bullet}OH$, which becomes available to the oxidation process.

A dark reaction experiment with H_2O_2 in the absence of UV-C and VUV radiation was conducted to determine the extent of TOC removal achieved by this oxidant alone. Then, experiments were conducted in the presence of UV-C and VUV radiation. Figure 4.4 shows

the difference in TOC removal rates achieved by both UV-C and VUV combined with H_2O_2 as well as H_2O_2 in the absence of UV radiation. TOC removal rates of 50.9% and 48.6% were achieved by UV-C/H_2O_2 and VUV/H_2O_2, respectively, as shown in Figure 4.4(a). Optimal doses of H_2O_2 were obtained for each process, 1000 mg L^{-1} for UV-C and 600 mg L^{-1} for VUV — optimal doses were obtained according to Section 4.3.1.1. TOC removal rates by H_2O_2 alone in the absence of UV radiation for the optimal doses of 600 and 1000 mg L^{-1} were 12.5% and 14.0%, respectively, as shown in Figure 4.4(b). As a result, it can be implied by looking at the results from figure 4.4(a) and 4.4(b) that the final TOC removal was due to the $^{\bullet}OH$ species created during the H_2O_2 photolysis under the action of both UV-C and VUV radiation. Also, it is suggested that the VUV/H_2O_2 was more efficient in terms of hydrogen peroxide dose required, only 600 mg L^{-1}, to degrade TOC in comparison with 1,000 mg L^{-1} required for the UV-C/H_2O_2 process. This result can be explained by the fact that the shorter the wavelength, the more energy it has, thus, the better it is absorbed by the H_2O_2 producing more $^{\bullet}OH$ radicals. As a result, the ability of the system to degrade organic matter is substantially improved.

On the other hand, when comparing these results with those obtained during individual processes, UV-C and VUV, showed no improvement with regards to TOC degradation from the system. Figure 4.5 shows that TOC removal rates of both processes UV-C/H_2O_2 and VUV/H_2O_2 were very similar to that of the UV-C photolytic process alone, 48.1%. Moreover, the TOC removal rates were lower than the VUV oxidation process itself, 55.4%, which in practice has a similar organic matter oxidation mechanism to that of UV-C/H_2O_2 and VUV/H_2O_2 photo-initiated processes via $^{\bullet}OH$ radicals. This result can be attributed to the fact that the hydrogen peroxide was a one-time addition at the beginning of

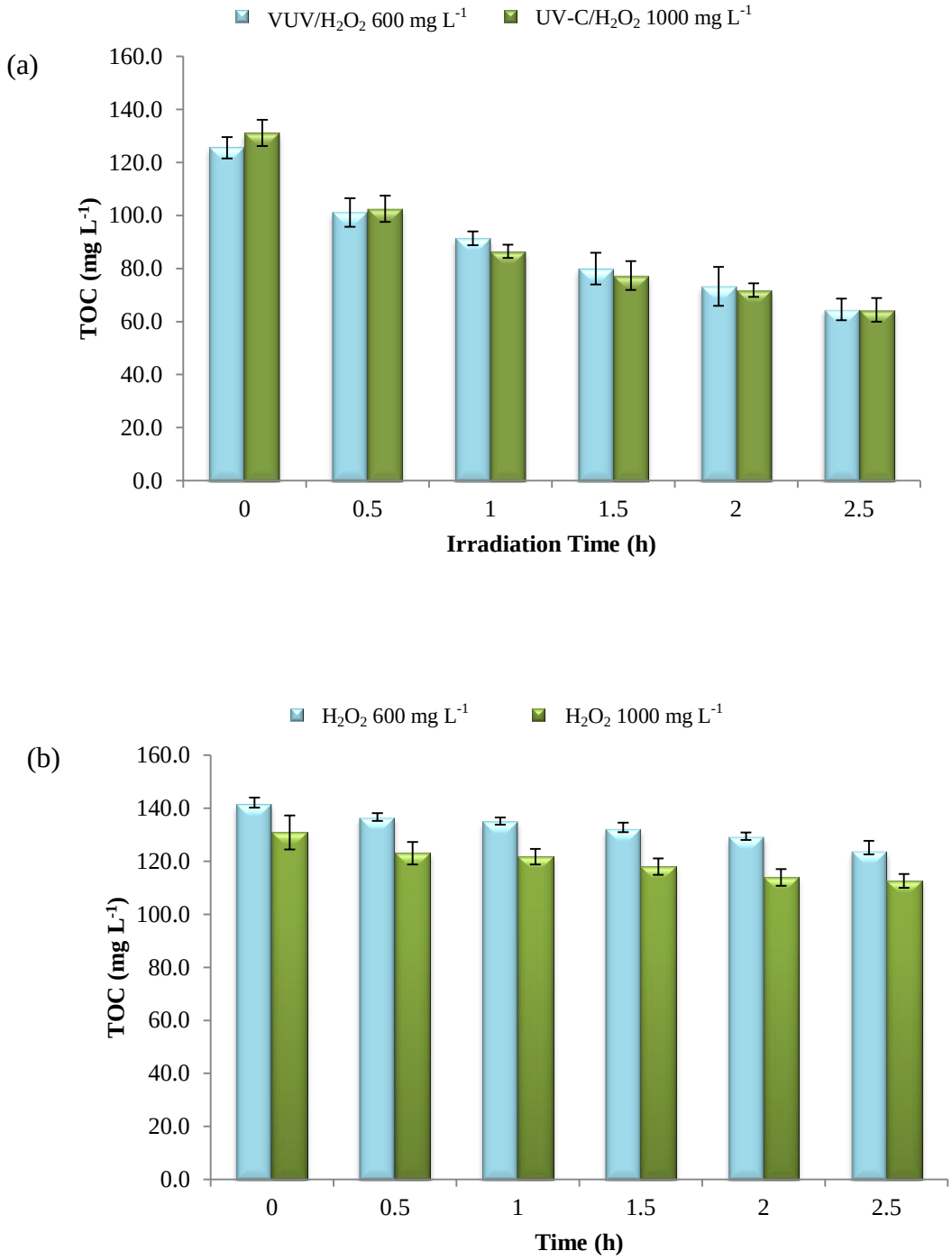

Figure 4.4. Comparison between the organic matter degradation efficiency in batch recirculation mode by (a) UV-C/H_2O_2 and VUV/H_2O_2 at optimal doses of 1,000 and 600 mg L^{-1} and (b) H_2O_2 Optimal doses tested alone (No UV irradiation). Error bars represent standard deviation of three replicates.

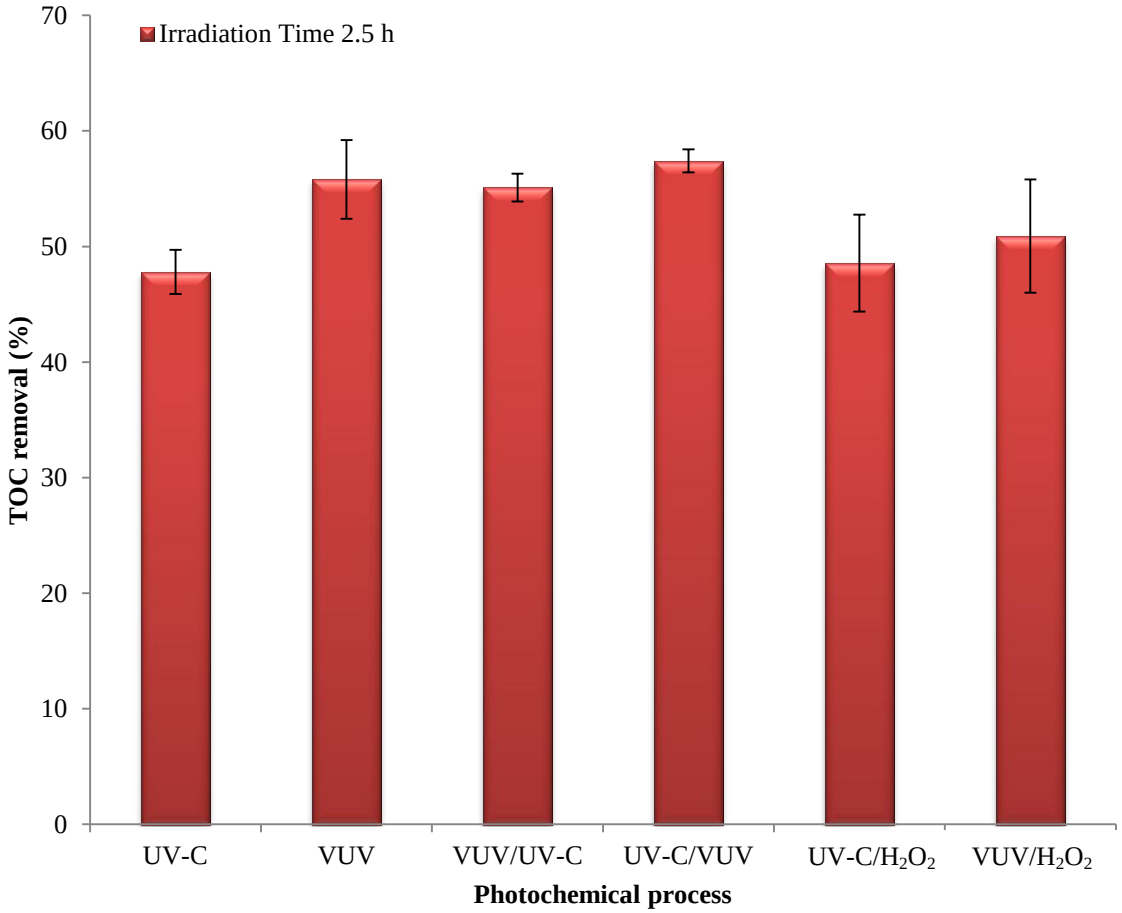

Figure 4.5. TOC removal rates (%) for UV-C/H_2O_2 and VUV/H_2O_2 at optimal doses of 1,000 and 600 mg L^{-1}, respectively, in batch recirculation mode and their comparison with the other photochemical processes: UV-C, VUV, UV-C/VUV and VUV/UV-C. Error bars represent standard deviation of three replicates.

the process and it is known that after a period of time, the H_2O_2 concentration decays during the photolytic mechanism prompted by the UV-C and VUV irradiation. Thus, the production of hydroxyl radicals was set back, suggesting that the main mechanism of TOC removal rate constants were mainly due to the direct photolysis action on both processes, UV-C and VUV, instead of $^{\bullet}OH$ oxidation. Consequently, the final TOC reduction rates were lower than that of the VUV process alone and its combination with UV-C in the batch recirculation mode.

4.3 Experiments in Continuous Mode Operation

To evaluate the results obtained during the batch recirculation mode, experiments in continuous–flow mode were conducted. The procedures followed the same steps performed during batch recirculation mode, but with an additional variable comprised of a flow-rate of 0.1 L min^{-1}, which provided a hydraulic residence (HRT) time of 4.6 min (HRT was obtained by dividing the reactor volume, 0.46 L, by the flow rate). The hydraulic residence time refers to the time the solution being treated remains in the photoreactor under UV radiation exposure. The water transmittance of the synthetic slaughterhouse wastewater solution was about 75%. The transmittance was measured with a spectrophotometer (Ultrospec™ *1100 pro* UV/visible) at 254 nm.

Dark reaction experiments conducted showed no significant loss of organic constituents through wall adsorption to the reactor or the pipeline occurs as shown in Figure 4.6. These results are in accordance with the results observed during the batch recirculation operation. As was expected, TOC removal rates under VUV photolysis were slightly higher

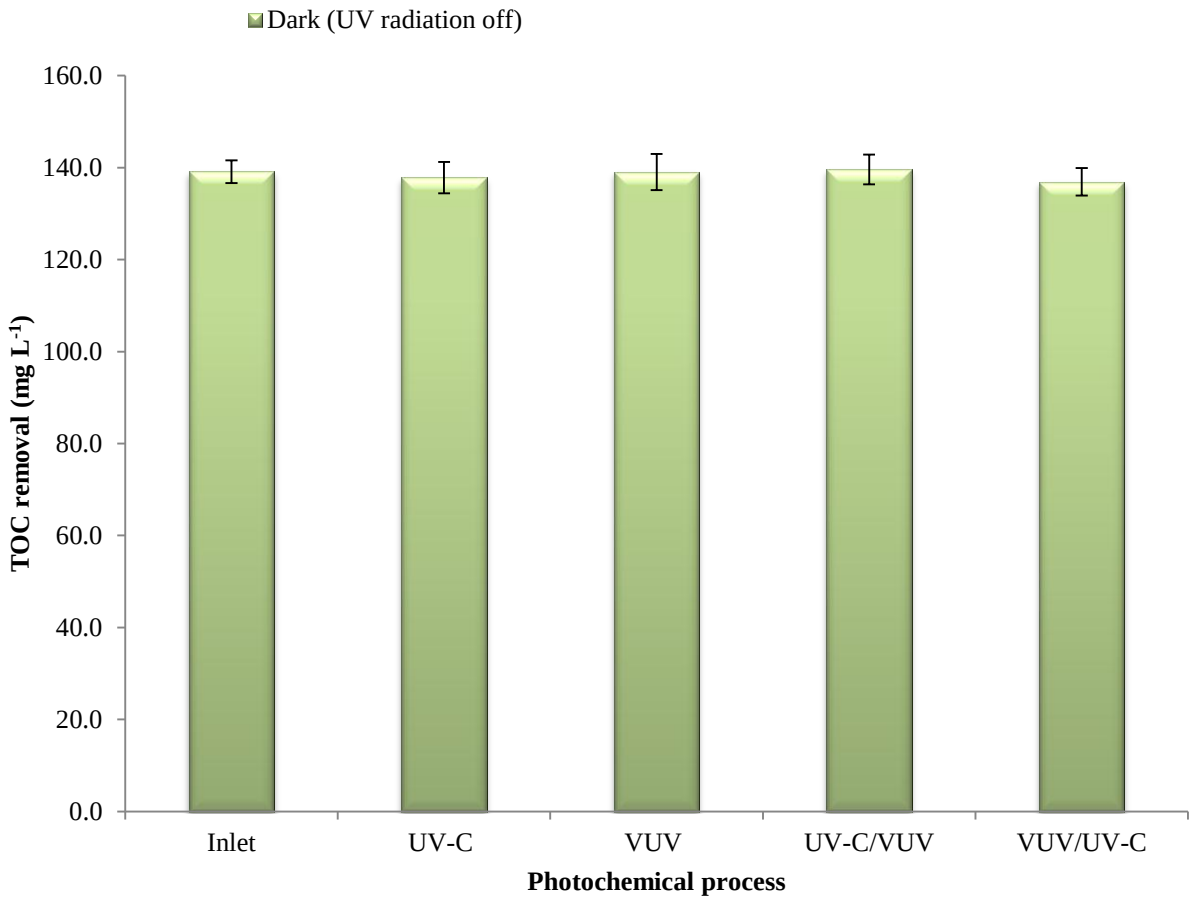

Figure 4.6. Dark reaction for TOC removal for the different photochemical processes during continuous mode: VUV (185 nm) and UV-C (254 nm), UV-C/VUV, and VUV/UV-C. Continuous mode operation; flow rate=0.1 L min^{-1}; HRT = 4.6 min. Errors bars represent the standard deviation for three experimental replicates.

6.2%, than that of UV-C, 5.5%, showing a same pattern to that of batch recirculation mode. As for combined UV-C/VUV and VUV/UV-C, TOC removal efficiency were higher than that of UV-C alone, 5.8% and 6.1%, respectively, but very similar to that of VUV alone as shown in Figure 4.7.

4.3.1 UV-C/H_2O_2 and VUV/H_2O_2 in Continuous Mode Operation

The next stage was to combine both processes, UV-C (254 nm) and VUV (185 nm), with an auxiliary oxidant, namely hydrogen peroxide (H_2O_2). As previously described in the literature review, hydrogen peroxide absorbs UV radiation in a broad spectrum from around 180 to 440 nm (Tang, 2004). It will be interesting to see TOC removal rates from more efficient VUV lamps as they become available in the marketplace, which some authors suggest may reach efficiencies of 60 to 65% (Sosnin, 2007; Oppenlander, 2003).

4.3.1.1 H_2O_2 dose optimization

An auxiliary oxidant such as H_2O_2 considerably improves the single UV-C radiation efficiency as well as the organic content removal rates. However, it was important to optimize the dose added since an overdose of H_2O_2 will negatively affect the organic removal by $^{\bullet}$OH recombination (As shown in Reaction (2.4) in Section 2.1). Conversely, a lower dose will reduce the $^{\bullet}$OH radical production available to the system.

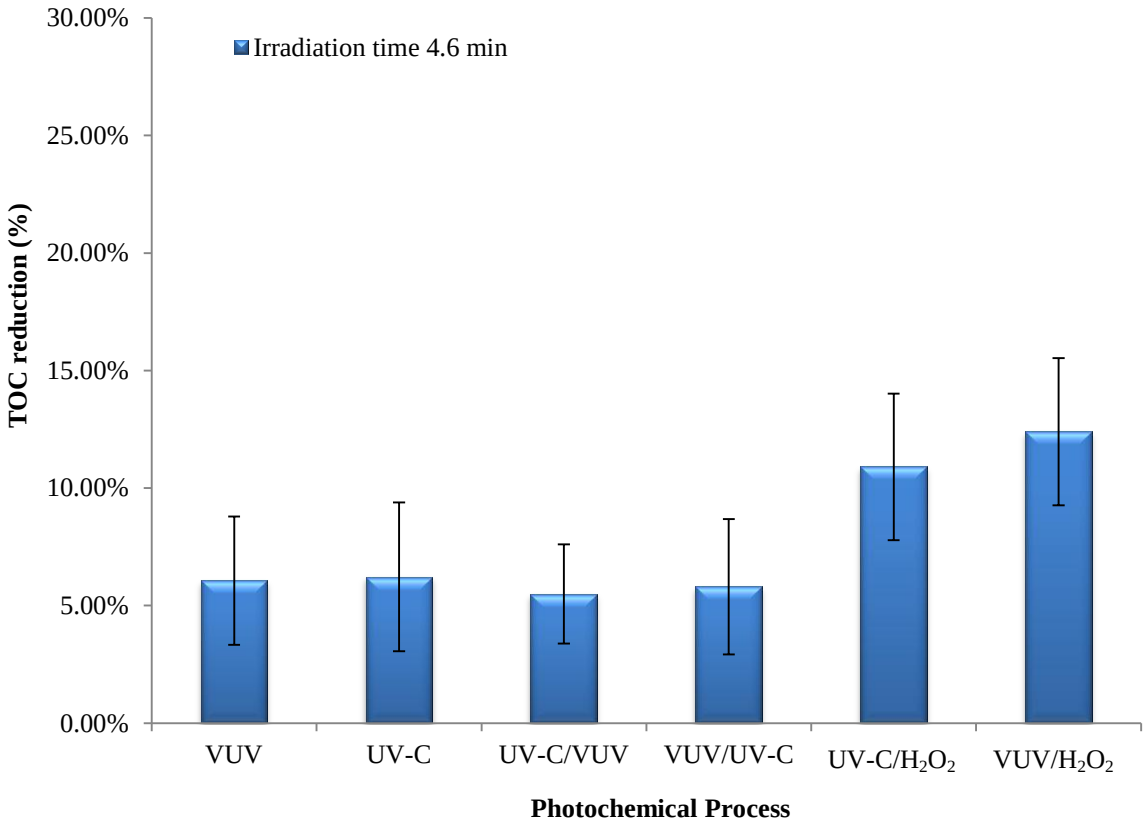

Figure 4.7. TOC removal (%) efficiency from synthetic slaughterhouse wastewater for all the photochemical processes evaluated: VUV, UV-C, UV-C/VUV, VUV/UV, UV-C/H_2O_2, and VUV/H_2O_2. Continuous mode operation; flow rate = 0.1 L min^{-1}; HRT = 4.6 min. Errors bars represent the standard deviation for three experimental replicates.

Different authors have pointed out that the H_2O_2 concentration may vary from 100 to 5,000 mg L^{-1}. Tabrizi and Mehrvar (2004a) reported that 720 mg L^{-1} of H_2O_2 was the optimum concentration needed to degrade linear alkylbenzene sulfonate by UV-C/H_2O_2. Likewise, Bali *et al.* (2004) noted that 340 and 850 mg L^{-1} of H_2O_2 were the optimum doses for achieving a complete removal of two dyes, namely reactive black 5 and direct yellow 12. Shu and Chang (2005) expressed that approximately 130 mg L^{-1} of H_2O_2 was required for the decolourization of a synthetic azo dye in wastewater. In addition, in a recent work on synthetic slaughterhouse wastewater treatment by combining anaerobic treatment and UV-C/H_2O_2, 1,371 mg L^{-1} was the optimum dose of H_2O_2 concentration (Cao and Mehrvar, 2010; Cao, 2009). The present study used the same composition for the synthetic wastewater as Cao and Mehrvar (2010); thus, the H_2O_2 concentration used in such work served as guideline for the system employed in the present study. The H_2O_2 dose varies based on the contaminant being treated; it also requires a customized optimization for each specific system and experimental set-up.

In the present work, different concentrations of H_2O_2 were used while the organic matter concentration (expressed as TOC) was kept constant. The lowest H_2O_2 concentration started at 300 mg L^{-1} and was increased by 100 mg L^{-1} increments until 1,300 mg L^{-1}. Figure 4.8 shows that for the combination of UV-C/H_2O_2, a dose of 1,000 mg L^{-1} resulted in the highest TOC removal, whereas 600 mg L^{-1} H_2O_2 resulted in the highest TOC removal for the combination of VUV/H_2O_2. Since VUV emits radiation with higher energy (185 nm), a lower concentration of H_2O_2 was required to produce a significant amount of $^{\bullet}OH$ when compared with UV-C. In both cases, a sizeable variation from the optimal concentrations beyond 1,000 and 600 mg L^{-1}, respectively, proved to be negative since the TOC removal rates decreased.

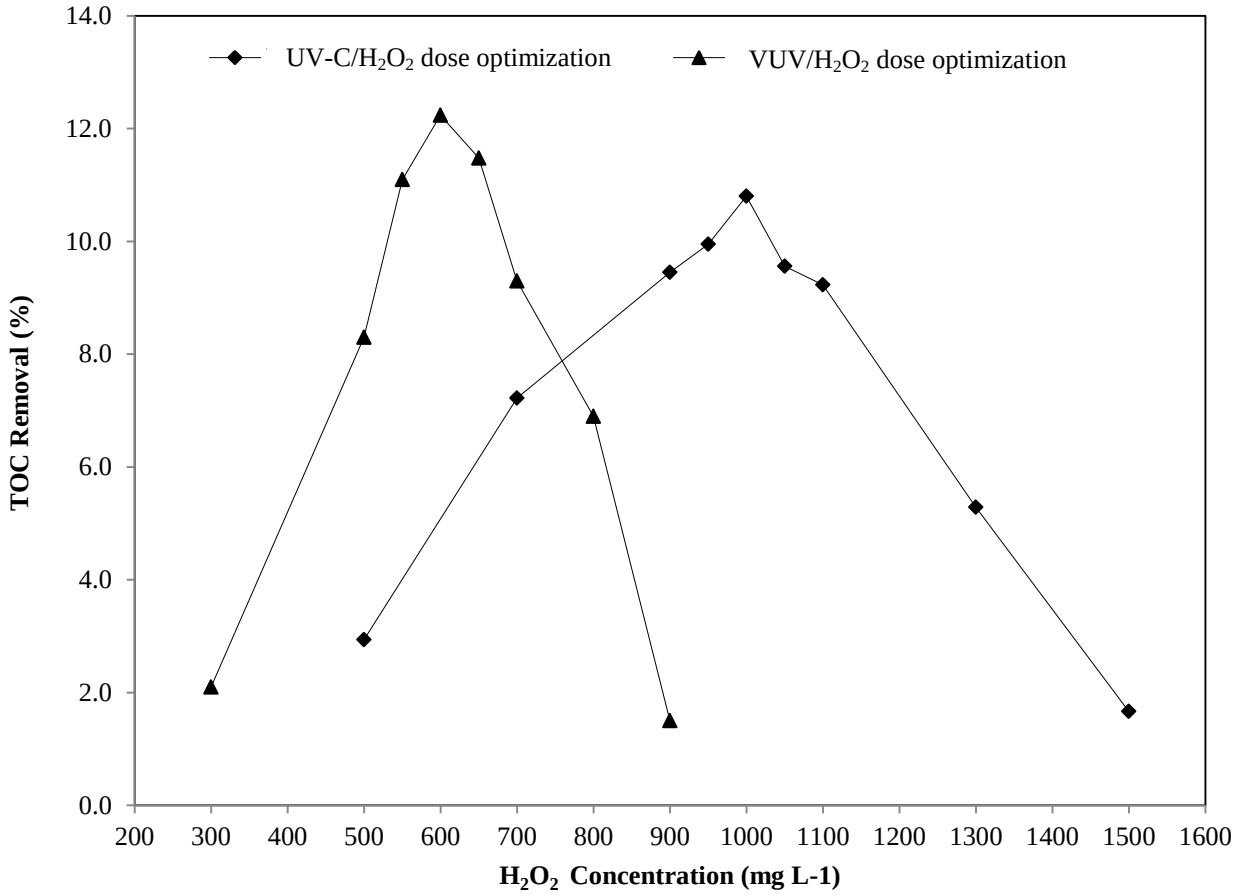

Figure 4.8. Optimal concentration of H_2O_2 for TOC removal under UV-C radiation (λ=254 nm) = [H_2O_2] 1000 mg L^{-1} and VUV radiation (λ=185 nm) = [H_2O_2] 600 mg L^{-1}. Continuous mode operation; flow rate 0.1 L min^{-1}. HRT= 4.6 min.

Once the optimum doses were established, these values were used to conduct experiments with both processes, UV-C/H_2O_2 and VUV/H_2O_2.

Based on the H_2O_2 optimization profile from Figure 4.8, experiments with the optimum concentration doses of H_2O_2, namely 600 and 1000 mg L^{-1} for the VUV and UV-C respectively, were conducted. In the UV-C/H_2O_2 process, with an optimum H_2O_2 concentration of 1000 mg L^{-1}, a 10.8% TOC removal was achieved in just 4.6 min of irradiation time. Likewise, the VUV/H_2O_2 process, with an optimum concentration of 600 mg L^{-1}, a 12.2% TOC removal was achieved in 4.6 min of irradiation time as previously shown in Figure 4.7. Therefore, there was a significant increase in TOC removal rates when H_2O_2 was added as an auxiliary oxidant by duplicating the efficiency of the system when combined with VUV, from 6.2%, and improving the efficiency by 1.9 times when combined with UV-C, from 5.5%, in the continuous mode operation as shown in Figure 4.7.

These results contrast sharply with those obtained during the batch recirculation mode (shown in Figure 4.5), which suggested no difference from the addition of hydrogen peroxide. As previously explained, this might be due to the fact that the hydrogen concentration should be kept constant during the entire irradiation procedure. In the batch recirculation experiments, the hydrogen peroxide was a one-time addition at the beginning of the experiments, so the concentration of H_2O_2 could have decayed after the first couple of passes.

A uniform concentration of TOC and bacteria present in the sample at the time of VUV and UV-C irradiation was guaranteed by mixing the sample at the feed tank above a

stirring power of 2000 rpm (provided by the pump). By contrast, during the batch operation, the H_2O_2 was added at the beginning, but it was not possible to keep a constant optimum concentration inside the photoreactor at all times. As a result, the TOC removal rates observed on the continuous operation was superior to the one observed during batch recirculation mode.

4.3.1.2 Molar Ratio of [H_2O_2] / [TOC] in Continuous Mode

The ratio of [H_2O_2]/[TOC] is an important parameter to optimize the wastewater treatment and adjust the H_2O_2 concentration accordingly to specific TOC concentrations present at any given time. As a result, an optimum molar ratio will maximize the efficiency and minimize the costs associated with electric power consumed. Figure 4.9 shows the optimum dose required to obtain in the best TOC removal rate in terms of molar ratio of H_2O_2 concentration to TOC concentration ([H_2O_2]/[TOC]) for: (a) the UV-C/H_2O_2 photolytic process, and (b) the VUV/H_2O_2 photolytic process. It can be noticed that the optimum molar ratios were found to be 2.5 and 1.5 for UV-C/H_2O_2 and VUV/H_2O_2, respectively. Consequently, the VUV/H_2O_2 process requires less addition of H_2O_2 than the UV-C/H_2O_2 process to achieve similar, and even higher, TOC removal rates.

Further experiments, this time varying the TOC concentration, while keeping the H_2O_2 concentrations constant, were conducted to confirm whether these molar ratios were correct or not. H_2O_2 concentrations of 1000 mg L^{-1} or 0.0294 mol L^{-1} and 600 mg L^{-1} or 0.0176 mol L^{-1} were used for UV-C and VUV, respectively. Working solutions of slaughterhouse wastewater containing TOC concentrations of 22, 140, and 230 mg L^{-1}

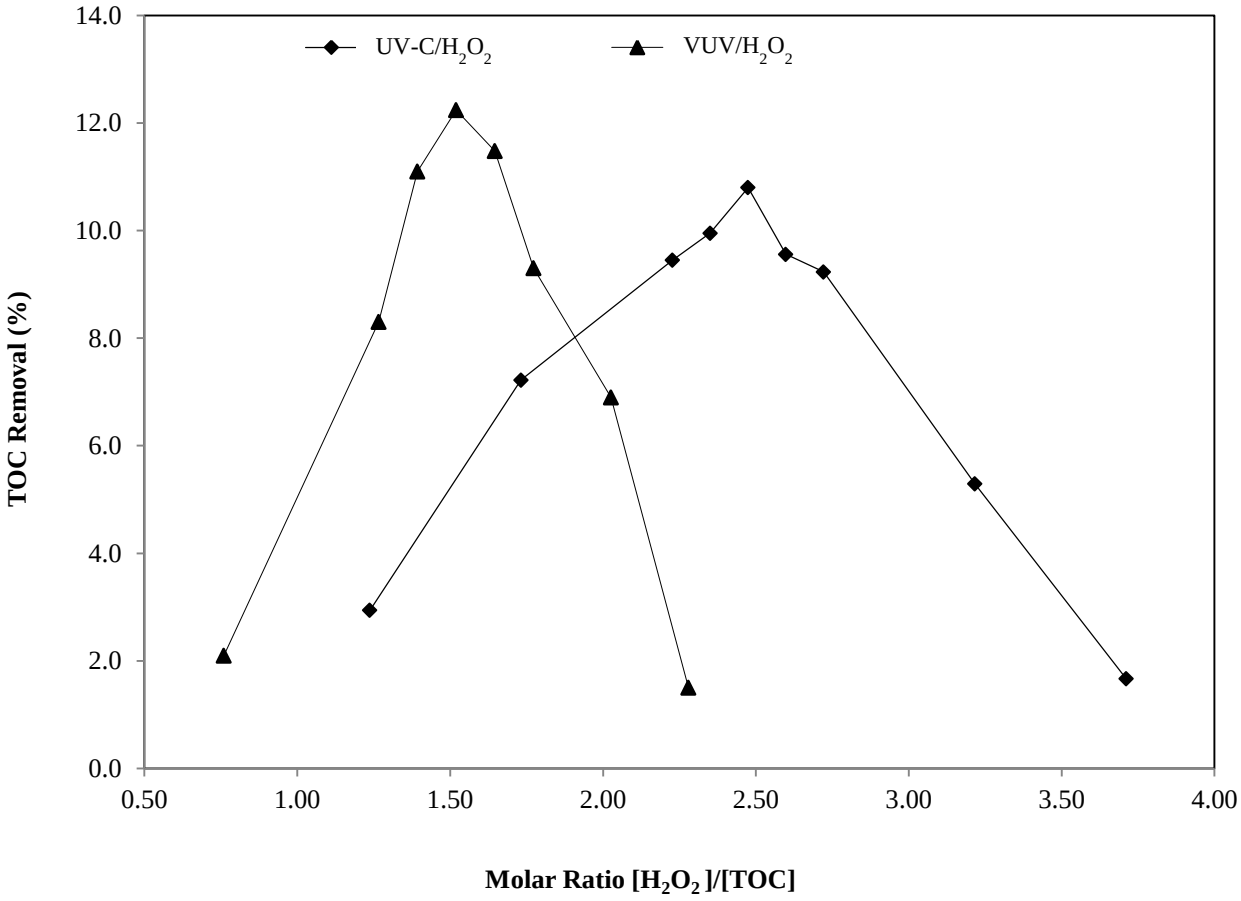

Figure 4.9. Relation of molar ratio of $[H_2O_2]$/[TOC] for different TOC molar concentrations of synthetic slaughterhouse wastewater by UV-C/H_2O_2 and VUV/H_2O_2 in continuous mode operation; flow rate 0.1 L min^{-1}. HRT= 4.6 min.

(0.0018, 0.116, and 0.0191 mol L^{-1}) respectively, were used. Figure 4.10 shows that for initial TOC concentrations of 22, 140, and 230 mg L^{-1} (a) in the UV-C/H_2O_2 process, the molar ratios were of 16, 2.5, and 1.5, achieving TOC removals rates of 5.6%, 10.8% and 6.8%, respectively and (b) in the VUV/H_2O_2 process the molar ratios were 9.6, 1.5, and 0.9, achieving TOC removals rates of 5.3%, 12.2%, and 8.7%, respectively. It can be noticed that lower molar ratios — low [H_2O_2] in contrast to [TOC] — as well as higher molar ratios — higher [H_2O_2] in contrast to [TOC] — compromised the ability for the system to remove TOC because of the $^{\bullet}OH$ radicals recombination resulting in H_2O_2 residual concentrations, increasing the costs of treatment. By contrast, an optimum molar ratio may maximize the TOC removal rates achieved by the system. As shown in Figure 4.10, molar ratios of 2.5 for UV-C and 1.5 for VUV, achieved the best TOC removal rates of 10.8% and 12.2%, respectively.

The optimum molar ratios obtained in this study are in accordance with the literature that states optimum molar ratios should be between the 0-100 (Vilhunen *et al*., 2010; Tabrizi and Mehrvar, 2006; Baeza *et al*., 2003). It is worth noting the results presented in Figure 4.10 considered only three different TOC concentrations, whereby it is recommended that additional experimental work — testing more TOC concentrations — be conducted to generate additional data points in order to further confirm the optimum molar ratios.

4.4 Bacteria Inactivation Experiments in Continuous Mode Operation

To determine the effectiveness of different photochemical processes in inactivating bacteria, several experiments were conducted in continuous mode operation using UV-C photolysis and VUV oxidation, combined UV-C/VUV and VUV/UV-C as well as

(a)

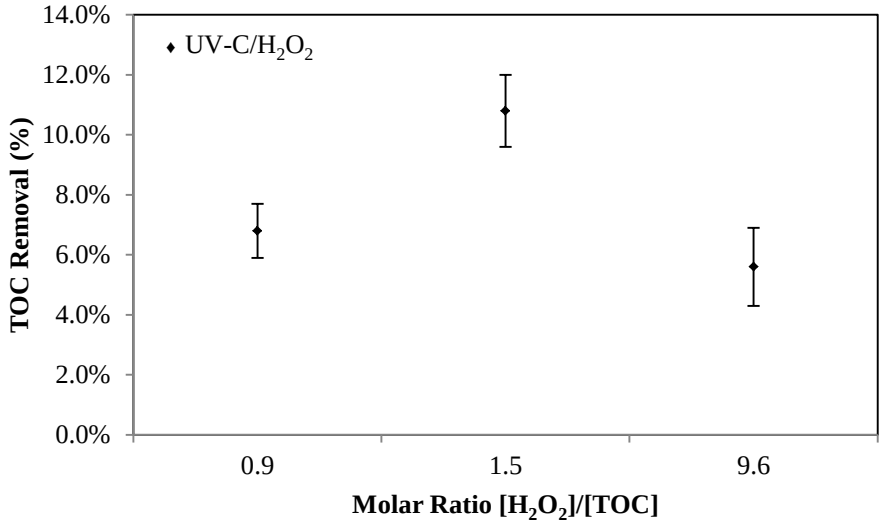

(b)

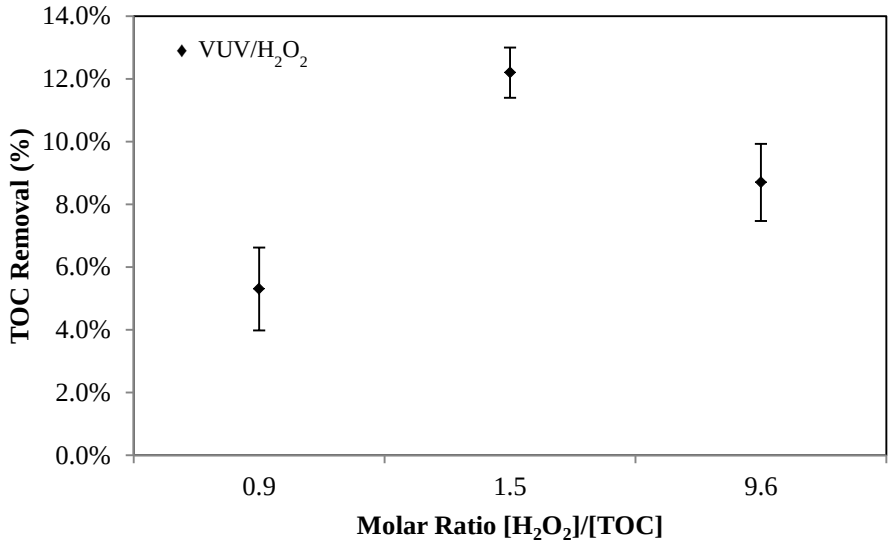

Figure 4.10. Relation of molar ratio $[H_2O_2]/[TOC]$ for three TOC molar concentrations of synthetic slaughterhouse wastewater by (a) UV/H_2O_2 and (b) VUV/H_2O_2. $[TOC]_{in}$ = 0.0191, 0.0116, 0.0018 mol L^{-1} respectively. $[H_2O_2]_{in}$ = 0.0176 and 0.0294 mol L^{-1}, for UV/H_2O_2 and VUV/H_2O_2 respectively. Continuous mode operation; flow rate 0.1 L min^{-1}. HRT= 4.6 min. Errors bars represent the standard deviation for three experimental replicates.

UV-C/H_2O_2 and VUV/H_2O_2. First, experiments with the bacterial strains of concern: *S.* Typhimurium, *E.coli O157:H7, S. flexneri, and P. aeruginosa*, inoculated into distilled water, were performed. The distilled water provided ideal UV transmittance conditions (clear waters) in order to test the behaviour of the system in ideal condition (minimal turbidity and particles). Then, synthetic slaughterhouse wastewater inoculated with the bacteria strains of concern was used to determine the effect that a reduction in transmittance due to soluble organic matter might have on the inactivation effectiveness of the selected bacterial pathogens. Varying the volumetric flow rate controlled the exposure time. Various flow rates, including 0.1, 0.5, and 1 L min^{-1} as well as 6, 6.5, and 7 L min^{-1} in the higher region were used. The maximum capacity of the pump was 7 L/ min.

4.4.1 Bacteria Inactivation in Transparent Waters (> 98% transmittance)

To assess any adsorption of bacteria through the walls of the photoreactor and pipe system, experiments in the absence of UV radiation (dark reaction) were carried out. There was no reduction of bacteria concentration in the absence of UV radiation as shown in Figure 4.11: (a) in clear (distilled) water, and (b) in synthetic slaughterhouse wastewater in the presence of bacterial pathogens. This suggested that any reduction in bacteria concentration in future experiments would be due to the UV radiation only. This statement was confirmed by experiments done in the presence of UV radiation, confirming the effectiveness of both UV-C photolysis and VUV oxidation in inactivating bacteria. A maximum flow rate that provided an exposure time ~4 seconds was achieved. This was the lowest exposure time at which the wastewater solution was exposed, meaning that any exposure time higher than this will automatically eliminate all bacteria concentrations in the system.

(a)

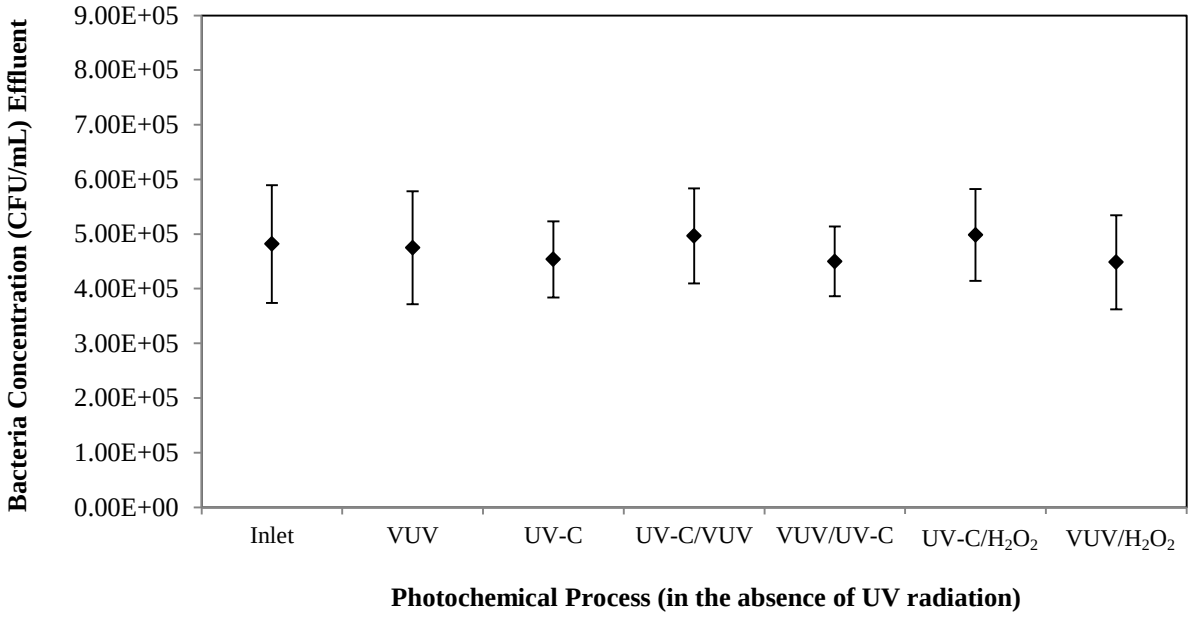

(b)

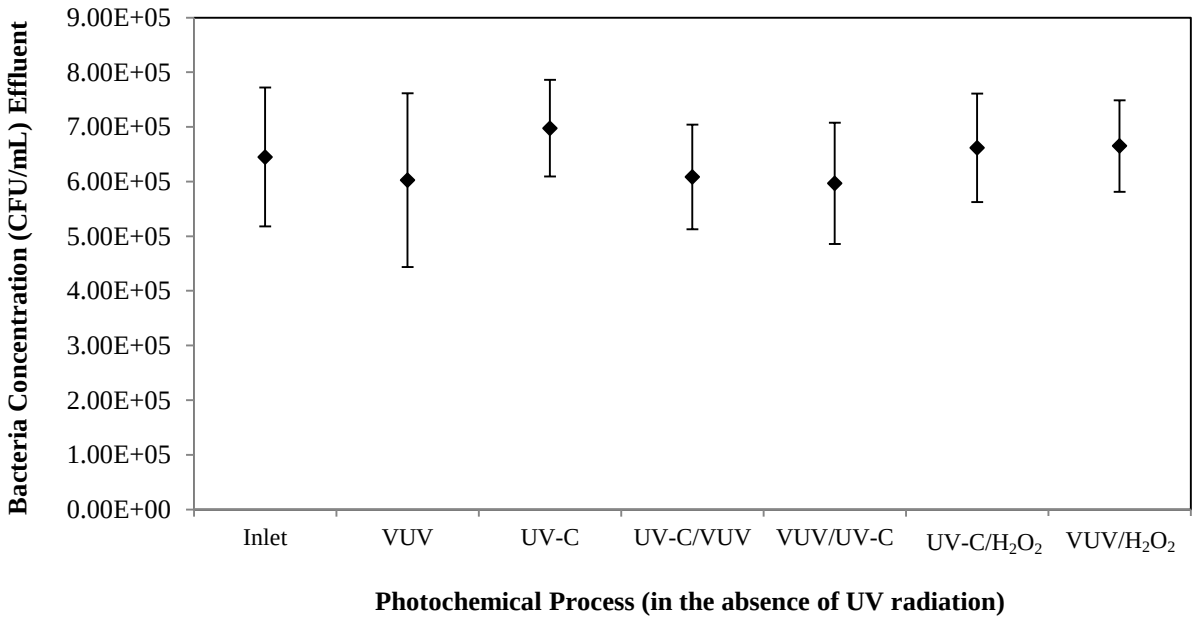

Figure 4.11. Inactivation of bacteria under dark conditions (in the absence of UV) in continuous mode operation by the different photochemical processes for (a) a residence time ~4 s in clear (distilled) water and (b) a residence time ~27 s for synthetic slaughterhouse in the presence of bacterial pathogens.

Mixed culture bacteria concentrations with an initial population density — all together — of 10^5 CFU mL^{-1} were treated in continuous mode operation by each photochemical process and effectively reduced to non-detectable levels. Logarithmic viability reduction values were on the order of 5 logs as shown in Table 4.1. Experiments at lower flow rates (higher exposure times) were conducted and the results were as expected (non-detectable bacteria cells).

Table 4.1. Logarithmic viability reduction of mixed culture bacterial strains: *S.* Typhimurium, *E. coli O157:H7, S. flexneri, and P. aeruginosa*, in clear (distilled) water after photochemical treatment in continuous mode operation.

Photochemical processes	**Exposure time[a](s)**	**Inlet concentration (CFU mL^{-1}) [b]**	**Outlet concentration (CFU mL^{-1})**	**Log N_0/N**
UV-C	3.9	5.26×10^5	0	5
VUV	3.9	5.26×10^5	0	5
UV-C/VUV	3.9	5.26×10^5	0	5
VUV/UV-C	3.9	5.26×10^5	0	5
UV-C/H_2O_2	3.9	4.65×10^5	0	5
UV-C/H_2O_2	3.9	4.98×10^5	0	5

Notes:

a. Exposure time was set by a flow rate equals to 7 L min^{-1} (Max. capacity of the system)

b. A negative control was conducted on all samples to assured that only the bacterial strains of concern were present

By reducing the flow rate, the exposure time is increased, allowing more time for the UV radiation to damage the bacterial cells present in water. Since results at lower flow rates were the same, Table 4.1 only shows the results for the lowest exposure time studied. These results are consistent with those obtained during TOC removal, in which both processes showed similar removal rates. Although the mechanisms of disinfection were different, since

UV-C photolysis is absorbed by the DNA and VUV oxidation destroys the cell wall by producing $^{\bullet}OH$, both were highly effective with the inactivation goals set by the most stringent regulatory standards, like that of Germany, of approximately 4 logs (99.99%) of bacteria inactivation (Oppenlander, 2003).

4.4.2 Bacteria Inactivation in Synthetic Slaughterhouse Wastewater

One of the objectives of this study was to see whether different processes were able to inactivate pathogenic bacteria present in slaughterhouse wastewater. For this purpose, 5 L solutions of synthetic slaughterhouse wastewater and a mixed culture of the bacterial strains of concern, including *E. coli* O157:H7, *S. enterica* serovar Typhimurium, *S. flexneri*, and *P. aeruginosa*, were subjected to different photochemical processes. Experiments were performed on continuous operation mode. The flow rate was 1 L min^{-1}, resulting in a HRT of 4.6 minutes.

In previous experiments, 70 L working solutions of distilled water spiked with bacteria were used. Because no background bacteria were detected, no sterilization by autoclaving was necessary. However, the combined solution, synthetic wastewater in the presence of bacteria, was required sterilization by autoclaving at 121°C for 1 h to assure no background bacteria were present. In this case, 5 L working solutions were used, since the maximum capacity of the autoclave suited 5 L flasks; volumes beyond this capacity were difficult to process. Consequently, experiments with synthetic slaughterhouse wastewater in the presence of bacteria could be done in the lower flow rates of 0.1, 0.5, and 1 L min^{-1} only. Due to the limited volume used, 5 L, at higher flow rates the pump started to suck the water

too fast and air was introduced into the system, generating errors in the final result. For this reason, experiments at higher flow rates were omitted.

The water transmittance of the combined solution was measured with a spectrophotometer (Ultrospec™ *1100 pro* UV/visible) at 254 nm and showed values around 66%. Initial TOC concentration was 140 mg L^{-1}. According to Tchobanoglous *et al.* (2003), the transmittance of wastewater effluents after secondary treatment (filtration) can vary between 56% and 79%, which is in accordance with the values observed in this study. Initial bacteria concentrations were on the order of 10^5 CFU mL^{-1}. Table 4.2 describes the effectiveness of all the photochemical processes in reducing bacteria from the synthetic slaughterhouse wastewater.

Table 4.2. Logarithmic viability reduction of mixed culture bacterial strains: *S.* Typhimurium, *E.coli* O157:H7, *S. flexneri, and P. aeruginosa*, in synthetic slaughterhouse wastewater after photochemical treatment in continuous mode operation.

Photochemical processes	**Exposure time[a] (s)**	**Inlet concentration (CFU mL^{-1})**	**Outlet concentration (CFU mL^{-1})**	**Log N_0/N**
UV-C	27.6	2.8×10^5	0	5
VUV[b]	27.6	2.8×10^5	0	5
UV-C/VUV	27.6	2.6×10^5	0	5
VUV/UV-C	27.6	3.1×10^5	0	5
UV-C/H_2O_2	27.6	3.5×10^5	0	5
VUV/H_2O_2	27.6	3.3×10^5	0	5

Notes:

a. Exposure time was controlled by the flow rate. 5 L working solutions were used, which allowed a maximum flow rate of 1 L min^{-1} (HRT =27.6 s) during continuous mode operation.

b. Same solution was used for both UV-C and VUV.

Logarithmic reduction values were on the order of 5 logs inactivation in ~ 27 s of exposure time, which were in accordance with the results obtained on experiments with clear water. The present study has shown the germicidal effect that all the photochemical processes evaluated in inactivating highly virulent pathogens have. Photochemical treatment is becoming a proven alternative to conventional treatments for inactivating bacterial pathogens. AOPs are also effective in removing organic matter as shown by results obtained in this study. Moreover, different studies have shown that AOPs are effective in removing toxic and recalcitrant (non-biodegradable) constituents from source waters. Consequently, AOPs are positioned as a promising technology for implementation in water and wastewater treatment plants.

4.4.3 Photodegradation of Synthetic Slaughterhouse Wastewater in the Presence of Bacteria

The TOC removal efficacy from synthetic slaughterhouse wastewater was also tested in the presence of bacterial pathogens to determine any effect derived from the reduction of UV transmittance. The UV transmittance in the absence of bacteria was approximately 75% in comparison to 66% in the presence of bacteria. The results obtained showed a slight reduction in the TOC reduction when compared to results obtained in the absence of bacteria. To illustrate, UV alone achieved a TOC reduction of 5.1% in comparison to 5.5% obtained in the absence of bacteria. VUV alone achieved a TOC reduction of 5.4% from 6.2% in the absence of bacteria as shown in Figure 4.12. Similarly, TOC reduction values for the combined processes, UV-C/VUV and VUV/UV-C, were 5.3% and 5.2%, respectively, in

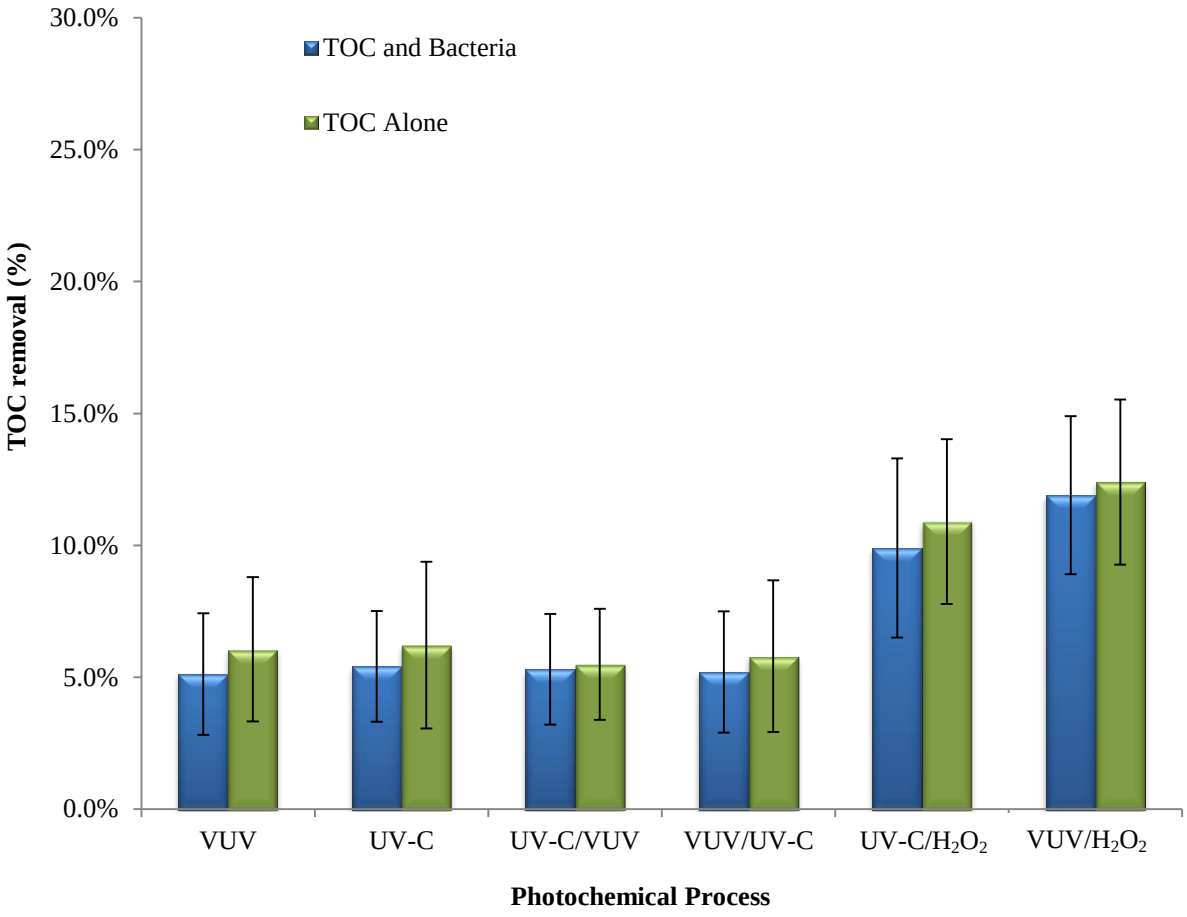

Figure 4.12. TOC removal (%) efficiency from synthetic slaughterhouse wastewater in the presence of bacteria (10^5 CFU mL^{-1}) and absence of bacteria (TOC alone) for all photochemical processes evaluated: VUV, UV-C, UV/VUV, VUV/UV, UV/H_2O_2, and VUV/H_2O_2. Continuous mode operation; flow rate = 0.1 L min^{-1}; HRT = 4.6 min. Errors bars represent the standard deviation for three experimental replicates.

contrast to 6.1% and 5.8% in the absence of bacteria. As for the UV-C/H_2O_2 and VUV/H_2O_2 processes, TOC removals were of 9.9% and 11.9% in contrast to 10.8% and 12.2% in the absence of bacteria.

It should be noted that the contribution of bacteria to the carbon content in the system was negligible. Different authors have reported carbon content values for a bacterial cell of approximately 2.11×10^{-10} mgC μm^{-3} once it reach stationary phase (Bratbak and Dundas, 1984; Loferer-Krößbacher *et al.,* 1998). The volume of an *E. coli* cell could reach around 3.5 μm^3, which when multiplied by the carbon content factor of 2.11×10^{-10} mgC μm^{-3}, yields a carbon content of about 7.38×10^{-10} mgC per cell (Loferer-Krößbacher *et al.,* 1998). Consequently, for a mixed culture population on the order of 10^9 CFU, the carbon content may reach values of about 1 mg of C. Given that the readings of initial TOC concentrations measured with the TOC analyzer varied within a range of 135 to 150 mg L^{-1}, the contribution of organic carbon by bacteria was hard to quantify and almost imperceptible by the system. This was confirmed when the TOC values — initial concentrations — in the inlet were measured for the experiments carried out in the absence and presence of bacteria, which showed no significant difference — all the TOC values readings were within the range of 135 to 150 mg L^{-1}.

As explained in Section 2.3.3, the transmittance of water determines the amount of UV radiation that is absorbed for the targeted compounds within the photoreactor. The lower the transmittance value, the less UV radiation passes through the solution. Therefore, not all targeted particles are reached by UV. It can be seen in Figure 4.12 that the efficiency for all

photochemical processes with regards to TOC degradation was reduced, although the difference is minimal. It is worth noting, however, that the only compounds present in the system were the targeted compounds — bacteria and TOC — which could explain why the difference was minimal in the case of UV-C alone, whereas in the case of the photo-oxidative processes ($^{\bullet}OH$ radicals' production) no radicals' scavengers, such as carbonates and chloride ions, were present. Consequently, the difference in UV transmittance between synthetic slaughterhouse in the presence and absence of bacterial pathogens (66% and 75%, respectively) did not dramatically affect the final TOC degradation results, and in fact TOC removal rates were very similar as previously shown in Figure 4.12.

4.5 Computational Fluid Dynamics (CFD) Modeling

Kinetic modeling is a good option to predict and understand the TOC reduction process that occurs within the photoreactor during a photochemical process. CFD is used to help describe and understand the behaviour of all chemical species that participate in a photodegradation reaction including, TOC, H_2O_2, $^{\bullet}OH$, and $HO_2^{\bullet}$ and UV radiation (photons) by making use of numerical techniques, in combination with a powerful sofware, to solve the fundamental governing fluid dynamics equations: the conservation of mass, the conservation of momentum, and the conservation of energy (Alpert *et al*., 2010; Wendt, 2009). These governing equations combined with boundary, and initial conditions, can describe the physical and chemical changes within a photoreactor.

4.5.1 Operating Conditions and Geometry of a Single Lamp Photoreactor

The TOC photodegradation of a synthetic slaughterhouse wastewater accomplished by a single lamp photoreactor was modeled using a commercial CFD software (COMSOL Multiphysics V3.5). The momentum, radiation energy, and mass balances contained in the chemical reaction module of the COMSOL package, were applied for the main components involved in the photochemical process including TOC, H_2O_2, $^{\bullet}OH$, and $HO_2^{\bullet}$ and UV radiation (photons). The photoreactor geometry, which is composed of two concentric cylinders with an annular laminar flow with a $Re \sim 27$, can be seen in Figure 4.13. The quartz sleeve with a radius R_i, contains the UV lamp, and represents the inner cylinder with a total length of 305 mm equal to that of the photoreactor. The photoreactor radius is R_t. Cylindrical coordinates were employed in the modeling of the photoreactors. The main operating condition and characteristics of the photoreactor are summarized in Table 4.3. It was assumed for the flow modeling an isothermal reaction at 25°C, steady state condition, laminar flow as well as the physical properties of water.

Table 4.3. Operating conditions and characteristics of the photoreactors.

Parameters	**UV-C lamp**
arc length (mm)	205
radius (mm)	13.3
type	Low pressure Hg
input Watts (W)	14
UV Output watts (W)	4
	Photoreactors
length (mm)	305
nominal radius R_t (mm)	51
	Quartz Sleeve
outer radius (R_i) (mm)	24.4
	Operating Conditions
volumetric flow rate (L min^{-1})	0.1
Reynolds number (R_e)	27.6
[TOC] (M)	0.0117
[H_2O_2] (M)	0.0294

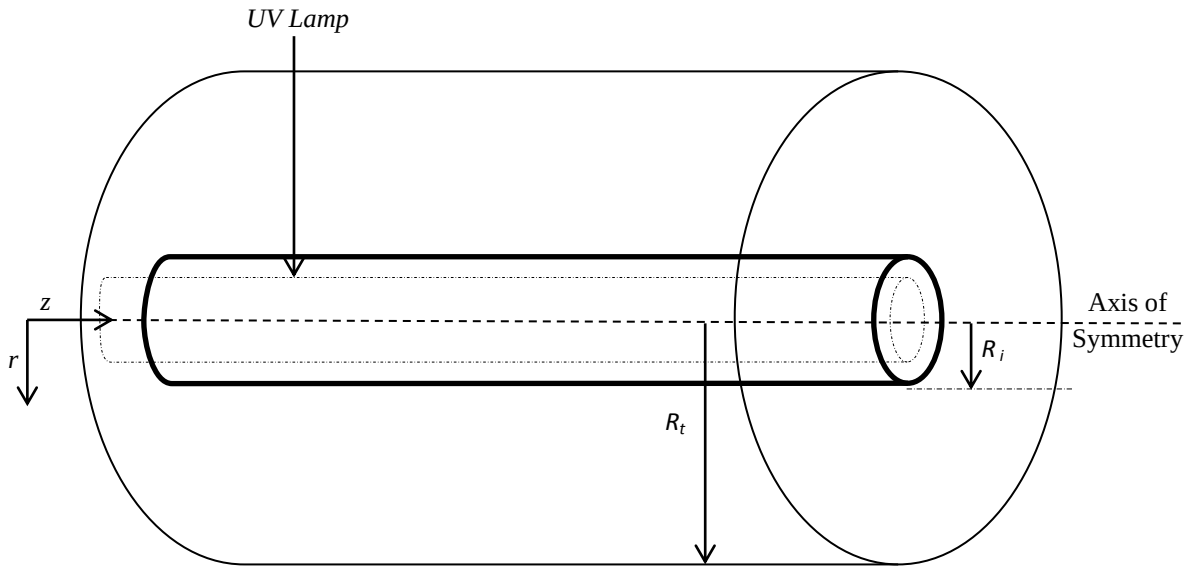

Figure 4.13. Schematic diagram of a single lamp photoreactor.

4.5.2 Reaction Mechanisms

The major photochemical and chemical reactions taking place in the UV-C/H_2O_2 process are described in Table 4.4.

Table 4.4. Reaction mechanisms in a UV-C/H_2O_2 process.

Reaction Number	Reaction	Reaction Rate Constant	References
(1)	$H_2O_2 + hv \xrightarrow{\phi_1} 2^{\bullet}OH$ ($\phi = 0.5$)		Buxton *et al.*, (1988)
(2)	$TOC + hv \xrightarrow{\phi_2}$ intermediates $\rightarrow CO_2 + H_2O$ ($\phi_2 = 0.032$)		This study
(3)	$H_2O_2 + {}^{\bullet}OH \xrightarrow{k_1} HO_2^{\bullet} + H_2O$	$k_1 = 2.7\times 10^7\ M^{-1}s^{-1}$	Cristensen *et al.*, (1982)
(4)	$2^{\bullet}OH \xrightarrow{k_2} H_2O_2$	$k_2 = 6.0 \times 10^9\ M^{-1}s^{-1}$	Staehelin *et al.*, (1984)
(5)	$2HO_2^{\bullet} \xrightarrow{k_3} H_2O_2 + O_2$	$k_3 = 1.5 \times 10^6\ M^{-1}s^{-1}$	Buxton *et al.*, (1988)
(6)	$HO_2^{\bullet} + {}^{\bullet}OH \xrightarrow{k_4} H_2O + O_2$	$k_4 = 6.6 \times 10^9\ M^{-1}s^{-1}$	Buxton *et al.*, (1988)
(7)	$TOC + {}^{\bullet}OH \xrightarrow{k_5}$ intermediates $\rightarrow CO_2 + H_2O$	$k_5 = 7 \times 10^5\ M^{-1}s^{-1}$	This study

Notes:
ϕ_1 = Quantum yield of H_2O_2 in aqueous solution.
ϕ_2 = Quantum yield of TOC degradation in aqueous solution.
k_5 was determined by parameter estimation (see Section 4.5.6)

According to Shemer *et al.* (2006) the quantum yield can be calculated by Equations (4.1) and (4.2) as follows:

$$\phi\,[M] = \frac{-d[M]/dt}{k_{s(\lambda)}} \qquad (4.1)$$

$$k_{s(\lambda)} = \frac{q_{0(\lambda)}\varepsilon_{\lambda}[1 - 10^{-\alpha_{\lambda}(r-R_i)}]}{\alpha_{\lambda}(r - R_i)} \qquad (4.2)$$

where $k_{s(\lambda)}$ is the specific rate of light absorption by TOC (Einstein mol^{-1} s^{-1}), ϕ is the quantum yield for TOC removal (mol $Einstein^{-1}$), q_o is the incident photon irradiance (Einstein cm^{-2} s^{-1}), $\varepsilon_{(\lambda)}$ is the molar absorption coefficient of TOC (M^{-1} cm^{-1}), $\alpha_{(\lambda)}$ is the absorption coefficient (cm^{-1}), r=R_t and R_i are the photoreactor nominal and inner radius (cm). The quantum yield for the present work was found to be 0.032 (mol $Einstein^{-1}$) (see Appendix E for details).

4.5.3 Momentum Balance

The momentum balance was performed for laminar flow with *Re* ~27. According to Bird *et al.* (2002), the governing equation for momentum balance for constant density, and viscosity, at steady state can be described as follows:

$$\nabla . V = 0 \qquad (4.3)$$

$$\rho V . \nabla V = -\nabla P + \nabla . \mu(\nabla V + (\nabla V)^T) \qquad (4.4)$$

where ρ, V, P, and μ are the density, velocity, pressure, and the dynamic viscosity respectively (see Appendix F for details).

There are three momemtum balances for each direction, including r, θ, and z, yet when r, and θ directions are considered, it leads to pressure variations at any cross section of these directions (Wilkes, 2006). Therefore, only the axial momemtum balance — in the z

direction — is considered to simplify the solution performed by the software. Equations (4.3) and (4.4), continuity and momentum balances respectively, were solved simultaneously for the following boundary conditions for the momentum balance:

1. Inlet of the photoreactor: the inflow velocity was given by the ratio of the volumetric flow rate to the surface area *(V=Q/S).*
2. No slip condition on solid boundary: velocity at the wall of the quartz sleeve and of the photoreactor ($r=R_t$) is zero.
3. A normal flow is assumed so the normal stress (pressure) in the outlet is zero.

4.5.4 Mass Balance

To find the concentration profile for each compound within the photoreactor, a mass balance for each component of the system was run at the same time. According to Bird *et al.*, (2002), the continuity equation for each componet of the system is given by

$$\nabla \cdot (V \cdot C_i) = \nabla(D\nabla C_i) + R_{rxn,i} \qquad (4.5)$$

where, D and V are the diffusivity of species i in the solution ($m^2\ s^{-1}$) and the laminar velocity ($m\ s^{-1}$), respectively. C_i and R_{rxni} represent the TOC (M) and reaction rate constant of the TOC and hydroxyl radicals ($M^{-1}\ s^{-1}$). Equation (4.5) represents the steady mass-transport equation that can be solved for a laminar flow regime. To solve the mass balance equation it was assumed a steady state and impermeable walls, which include three boundary conditions requiered as follows:

1. The inlet TOC is 10.83 mol m^{-3}
2. The diffusion of TOC at the quartz sleeve is zero, therefore, the concentration gradient at the quartz sleeve is zero.
3. There is no molar flux at the wall, therefore, the concentration gradient at the wall is zero.

4.5.5 Photon Irradiation Balance

To model the irradiation balance in the photoreactor, the local volumetric rate of energy absorption (LVREA) — the local rate of absorbed radiation per unit time and unit volume — was calculated. The LVREA is directly proportional to the rate of pollutant degradation taking place in the photoreactor. Nonetheless, this parameter is affected by the light attenuation caused by the radiation absorption of different species present in water. Therefore, the LVREA is not uniform within the photoreactor and will be dependent on the radiation field of the system. Equation (4.6) shows the fraction of incident light absorbed (*fi*) by a specific compound at any given position within the reactor:

$$f_i = \frac{\varepsilon_i C_i}{\mu_s} \qquad (4.6)$$

where ε_i and C_i are the molar absorptivity (M^{-1} cm^{-1}) and the concentration of species i (M), which in this study refers to TOC and H_2O_2. μ_s is the extinction coefficient of the solution being treated and may be defined as:

$$\mu_s = \mu_w + \varepsilon_{H_2O_2} C_{H_2O_2} + \varepsilon_{TOC} C_{TOC} \qquad (4.7)$$

where μ_w is the extinction coefficient of distilled water at 254 nm, taken to be 0.007 cm^{-1} (Gadgil, 1995). The molar absorption coefficient of H_2O_2, ε_{TOC}, was taken as 18.6 $M^{-1}cm^{-1}$ (Oppenlander, 2003); the molar absorption coefficient of the organic content, ε_{TOC}, was calculated using Equation (2.8) (see Appendix E for details).

As Johnson and Mehrvar (2008) suggested, the radiation balance for a single lamp photoreactor is given by:

$$\frac{1}{r}\frac{d\,(rq)}{dr} = -q(2.303\mu_s) \qquad (4.8)$$

where q is the radiant energy flux (Einstein $cm^{-2}\,s^{-1}$), $r=R_t$ is the photoreactor nominal radius (cm) and μ_s is the extinction coefficient (cm^{-1}) of the solution (base 10).

The integration of the irradiation governing Equation (4.8) yields:

$$q = q_o \frac{R_i}{r}\, e^{-2.303\mu_s(r-R_i)} \qquad (4.9)$$

where q_o and R_i are the energy flux on the sleeve wall before attenuation (Einstein cm^{-2} s^{-1}) and the inner reactor radius (cm), repectively.

Using Equations (4.7) and (4.9), The LAVREA *(A)* can be calculated as follows:

$$A = \mu_s q_o \frac{R_i}{r} e^{-2.303\mu_s(r-R_i)} \qquad (4.10)$$

Thus, base upon the UV-C/H_2O_2 reaction mechanisms categorized in Table 4.4, the reaction rates of the different species, which are the base for the kinetic model of the photochemical system, could be expressed as follows:

$$\frac{d[TOC]}{dt} = -k_5[TOC][^{\bullet}OH] - \phi_2 f_{TOC} A \qquad (4.11)$$

$$\frac{d[H_2O_2]}{dt} = -\phi_1 f_{H_2O_2} A - k_1[H_2O_2][^{\bullet}OH] + k_2[^{\bullet}OH]^2 + k_3[HO_2^{\bullet}]^2 \qquad (4.12)$$

$$\frac{d[^{\bullet}OH]}{dt} = 2\phi_1 f_{H_2O_2} A - k_5[TOC][^{\bullet}OH] - k_1[H_2O_2][^{\bullet}OH] - k_2[^{\bullet}OH]^2 - k_4[^{\bullet}OH][HO_2^{\bullet}] \qquad (4.13)$$

$$\frac{d[HO_2^{\bullet}]}{dt} = k_1[H_2O_2][^{\bullet}OH] - k_3[HO_2^{\bullet}]^2 - k_4[^{\bullet}OH][HO_2^{\bullet}] \qquad (4.14)$$

4.5.6 Model Calibration

To determine the reaction rate constant, k_5, for the TOC reaction with the $^{\bullet}OH$ radicals during the experiments performed in this study, a parameter estimation method was employed. This method consisted in giving different values to k_5 until reaching an absolute relative error of less than 10% between the model prediction and any experimental data. When the value of k_5 entered into the model over-estimated the TOC removal rate, the value was reduced. Conversely, if the value of k_5 entered into the model under-estimated the TOC removal rate, the value was increased. The data obtained during the batch recirculation mode values were used, along with a numerical computational software package (MATLAB® Version 7.11.0.584 R2010b), to solve the ordinary differential equations (ODEs) mentioned above. A predictor/corrector numerical method, ode15s, used to solve 'stiff' ODEs was employed for this specific set of equations; other methods such as the Runge-Kutta method were unable to solve these kinds of ODEs.

TOC and H_2O_2 initial concentrations were of 140 mg L^{-1} (0.0117 mol L^{-1}) and 1000 mg L^{-1} (0.0294 mol L^{-1}), respectively. The simulation used the reaction mechanisms in Table 4.4, which along with the parameter estimation technique previously mentioned, found the value for k_5 to be 7×10^5 M^{-1} s^{-1}. The calibrated model was able to predict the TOC removal rate obtained from the experimental data as shown in Figure 4.14. Furthermore, the model was able to predict the consumption of H_2O_2 over time, showing a steep decrease after 2000 s (33.3 min), eventually showing a total depletion of the H_2O_2 concentration after 5000 s (83.3 min) as shown in Figure 4.15. This result explains the low TOC removal rates obtained by

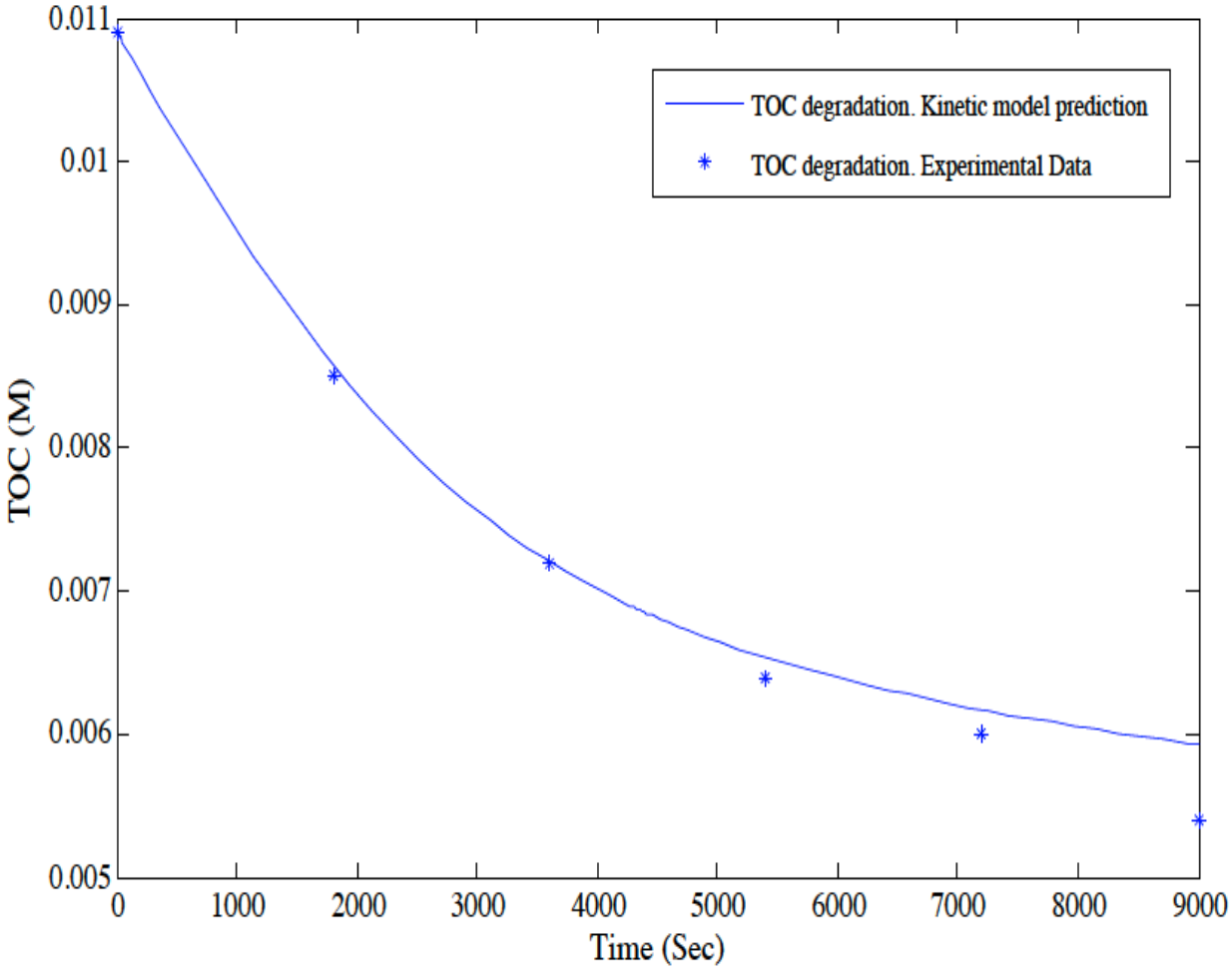

Figure 4.14. Calibrated model of TOC degradation against time under UV-C/H_2O_2 exposure in batch recirculation mode. The kinetic model prediction used a reaction rate constant value, k_5, of 7 x 10^5 $M^{-1}s^{-1}$. $[TOC]_{in}$ = 0.0117 M and $[H_2O_2]_{in}$ = 0.0294 M. All the other rate constants and quantum yield values are shown in Table 4.4.

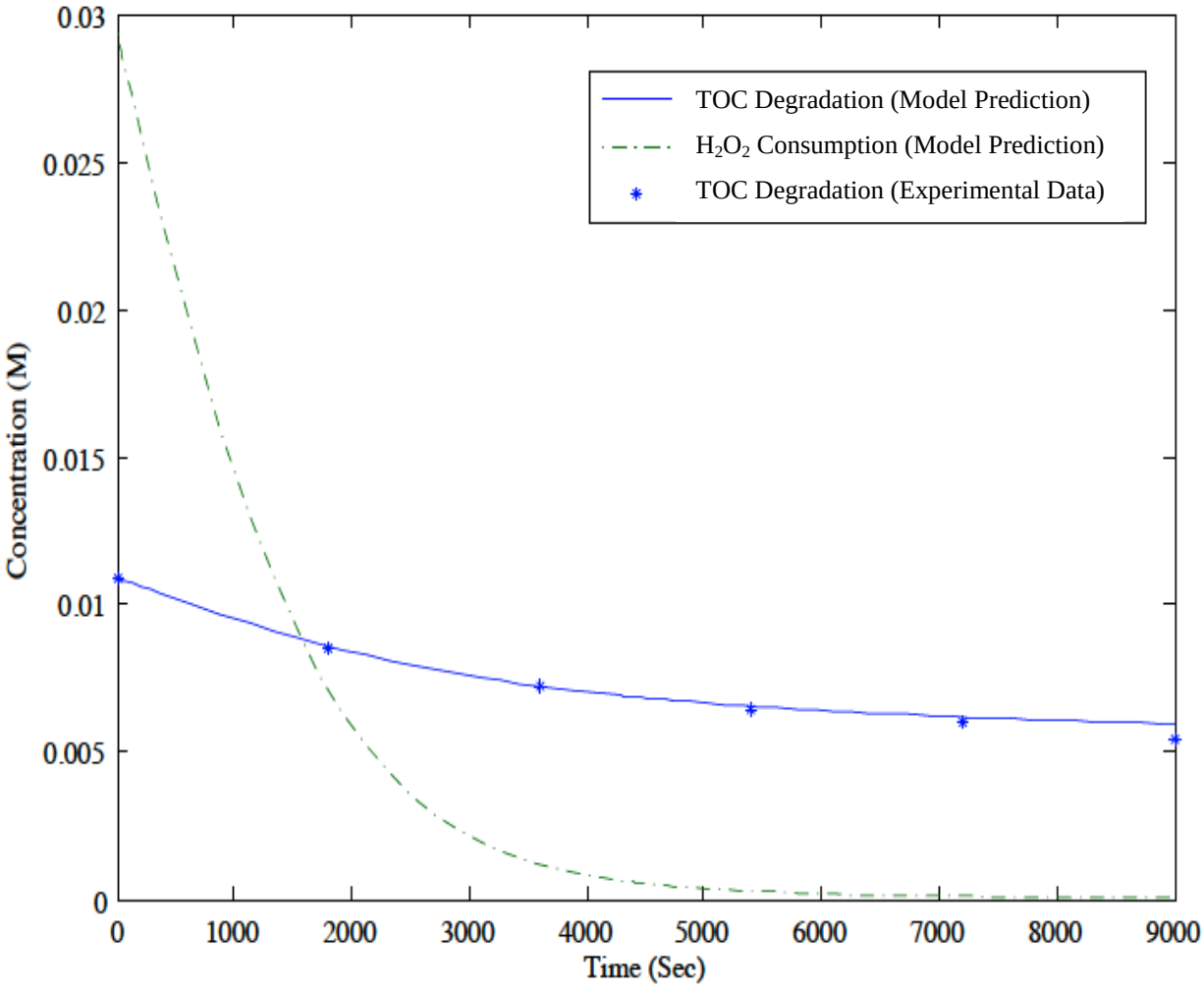

Figure 4.15. Calibrated model of TOC degradation and H_2O_2 depletion against time in batch recirculation mode; the kinetic model prediction used a reaction rate constant value, k_5, of 7 x 10^5 $M^{-1}s^{-1}$. $[TOC]_{in}$ =0.0117 M and $[H_2O_2]_{in}$ = 0.0294 M. All the other rate constants and quantum yield values are shown in Table 4.4.

the combined UV-C/H_2O_2 photolytic process during batch recirculation mode, which displays similar TOC removal rates to the UV-C photolysis process alone. Therefore, it is inferred that the ultimate TOC degradation was mainly carried out by the less efficient photolysis process instead of $^{\bullet}$OH radicals' oxidation, resulting in lower removal rates. However, the UV-C/H_2O_2 photolytic processes duplicated the TOC removal rate in the continuous mode operation, where it is assumed that the H_2O_2 concentration kept near optimum concentration values during the irradiation time.

4.6 CFD Modeling Results

The modeling of the TOC degradation in a single lamp photoreactor by UV-C/H_2O_2 was performed based on the experimental data obtained in this study, along with the main reaction rate constants, which were obtained from literature, for the different species, particularly the hydroxyl radicals ($^{\bullet}$OH) and hydroperoxyl radicals ($HO_2^{\bullet}$) species, present during the photochemical reaction. A kinetic model for a single lamp photoreactor was proposed by Johnson and Mehrvar (2008), and later modified by Mohajerani *et al*. (2010) using CFD simulation. The CFD modeling for the present study was based on the aforementioned works tailored for a laminar flow regime used in the present study. The reactions and rate constants that took place during experiments conducted in the present study as well as the reaction rate constant, k_5, between TOC and hydroxyl radicals and the system's quantum yield, ϕ, for the present study are summarized in Table 4.4.

Figure 4.16(a), illustrates the fluid layers moving over one another, in which the maximum velocity occurs somewhere near the center of the annular space, between the photoreactor wall and the quartz sleeve surface. Also, at the photoreactor wall, where no slip boundary condition applies ($r=R_t$), the velocity is close to zero. This means particles near the wall will receive more UV irradiation than particles in the center of the photoreactor since they tend to remain in the system longer. Similarly, Figure 4.16(b) shows that the velocity in the lighter blue region, in the center of the annular space, is much greater (around 1 m s^{-1}) than the velocity in the dark blue region near the walls, which is near zero. Also, the velocity in both inlet and outlet are much higher than in the reactor itself due to a smaller radious.

Figure 4.17 describes the velocity profile at the outlet radial cross section. The maximum velocity is reached at the center of the radial cross section, whereas near the walls the solution flows with a lower velocity. It should be noticed the velocity at the wall (bottom of the radial cross-section) where a lighter green color indicates a higher velocity (around 3.5 m s^{-1}) than the rest of the perimeter. This is caused by the kinetic energy that the solution carries when entering the oultet cross-section area, which at the moment of impacting this section is higher than the rest of the cross-sectional perimeter.

The TOC concentration profile in a single lamp photoreactor was modeled for a volumetric flow rate of 0.1 L min^{-1}, which followed a laminar regime. The residence time of the photoreactor was 4.6 min. Figure 4.18 illustrates the TOC concentration profile that is reduced as the mixture passes through the photoreactor from (a) top view. From the (b) side view, it can be observed that there is no change in the concentration in the radial direction

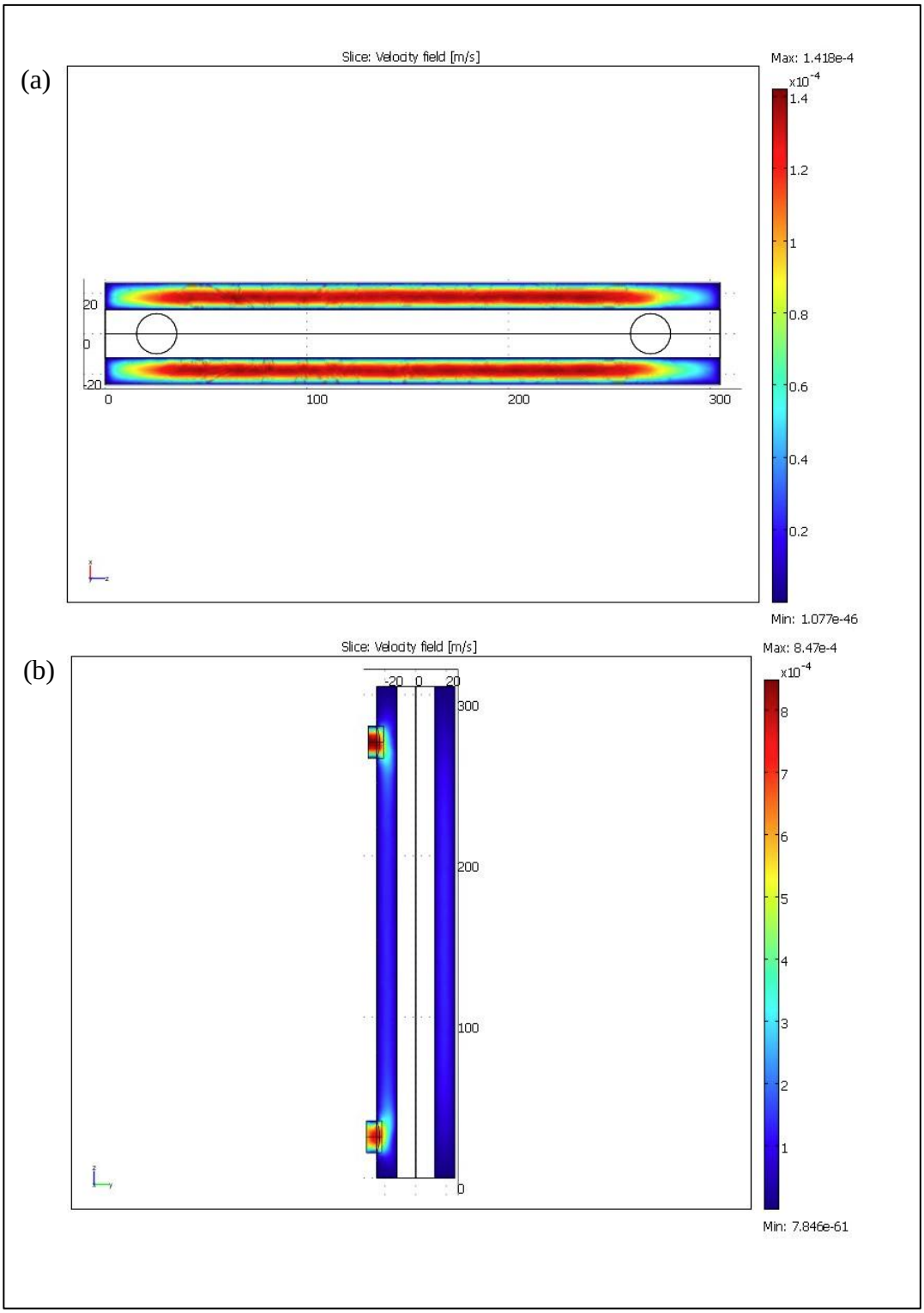

Figure 4.16. Axial velocity from (a) top view; and (b) side view; UV-C/H_2O_2 photolytic process; continuous mode operation; flow rate 0.1 L min^{-1}. HRT= 4.6 min.

along the photoreactor. However, in the inlet, once the flow comes into contact with the lamp, it causes a radial concentration, which dissipates as the mixture moves forward. Similarly, it is observed that there is no radial TOC concentration in the outlet. As Figure 4.19 shows, the difference between the minimum and maximum concentration at the outlet is negligible. While the TOC concentration in the higher region is about 10.167 mol m^{-3}, the TOC concentration in the lower region is about 10.165 mol m^{-3}.

When looking at the local volumetric rate of energy absorption (LVREA) illustrated in Figure 4.20, which describes the radiant energy distribution within the photoreactor, it can be seen that the region near the lamp's quartz sleeve has the highest radiant energy absorption. The magnitude of the LVREA value decreases as the radiation travels to the photoreactor wall. In this sense, the LVREA value near the quartz sleeve's wall is four orders of magnitude higher than that at the photoreactor's wall (1.202×10^{-6} against 7.333×10^{-6} Einstein m^{-3} s^{-1}, respectively). As a result, a large number of photons will be available near the quartz sleeve, where, it is inferred, the majority of TOC degradation takes place.

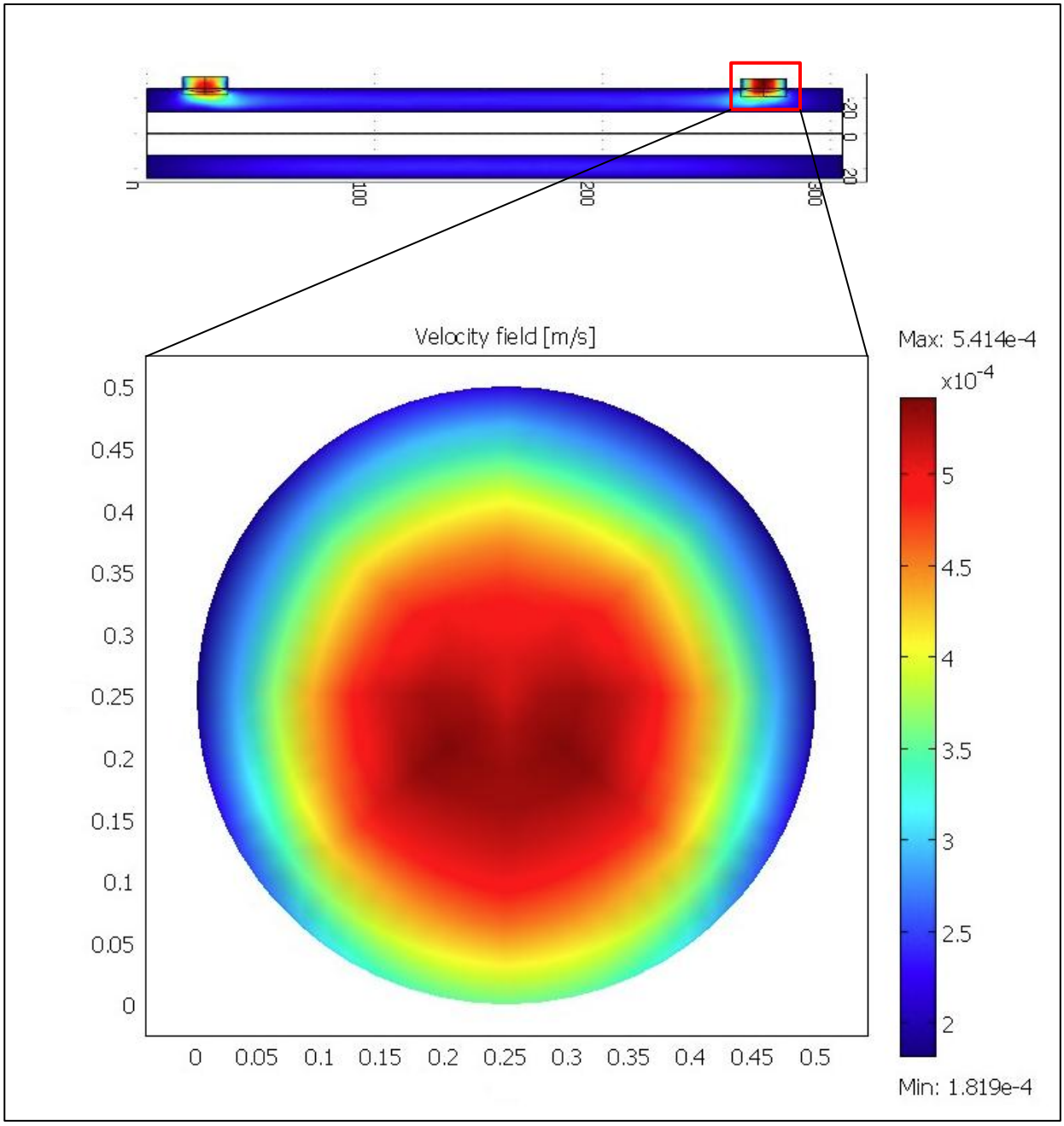

Figure 4.17. Velocity profile at the outlet radial cross section; UV-C/H_2O_2 photolytic process; continuous mode operation; flow rate 0.1 L min^{-1}. HRT= 4.6 min. The *y* and *x* axes are dimensions.

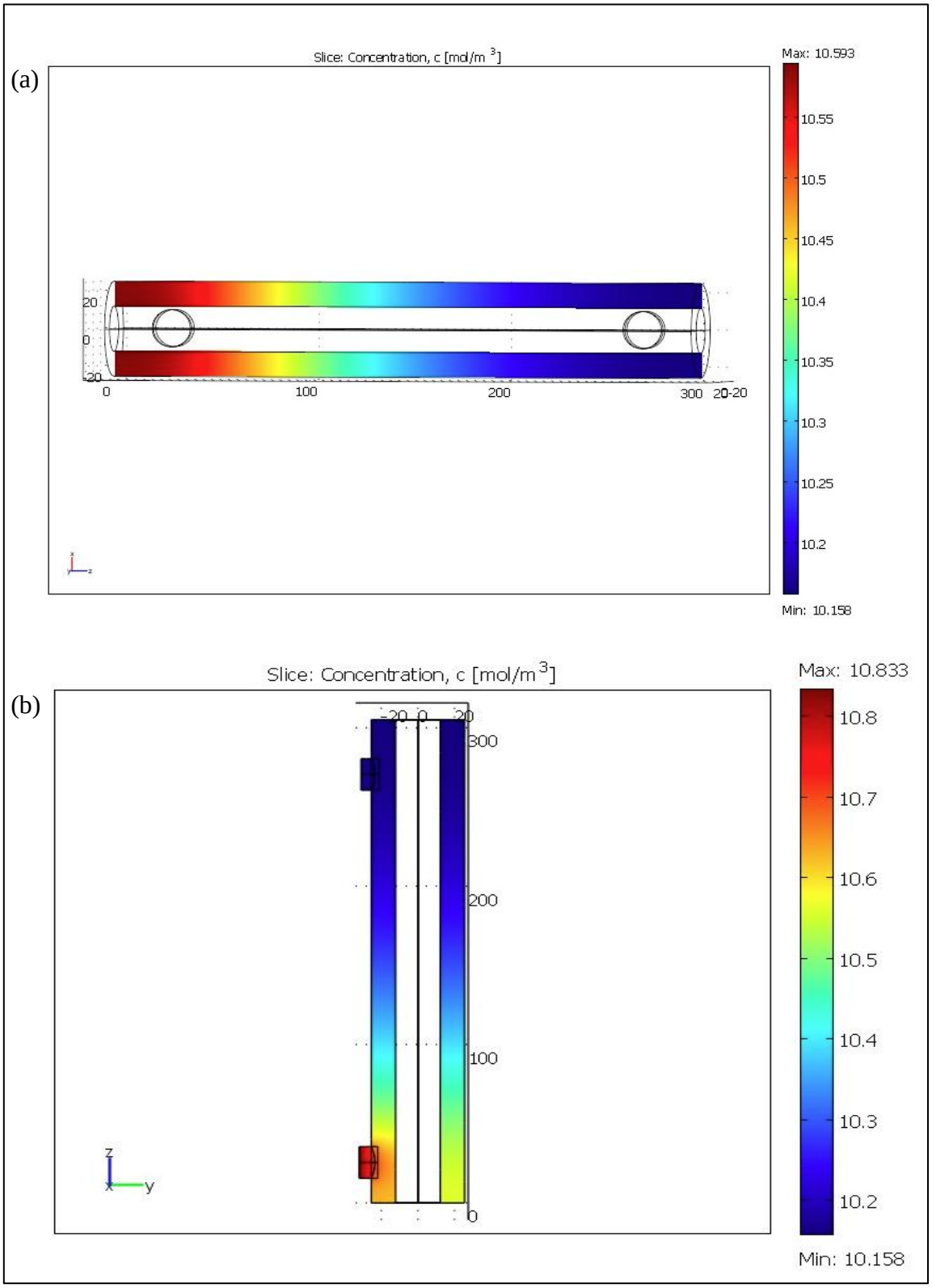

Figure 4.18. TOC concentration profile from (a) top view and (b) side view; UV-C/H_2O_2 photolytic process; continuous mode operation; flow rate 0.1 L min^{-1}. HRT= 4.6 min.

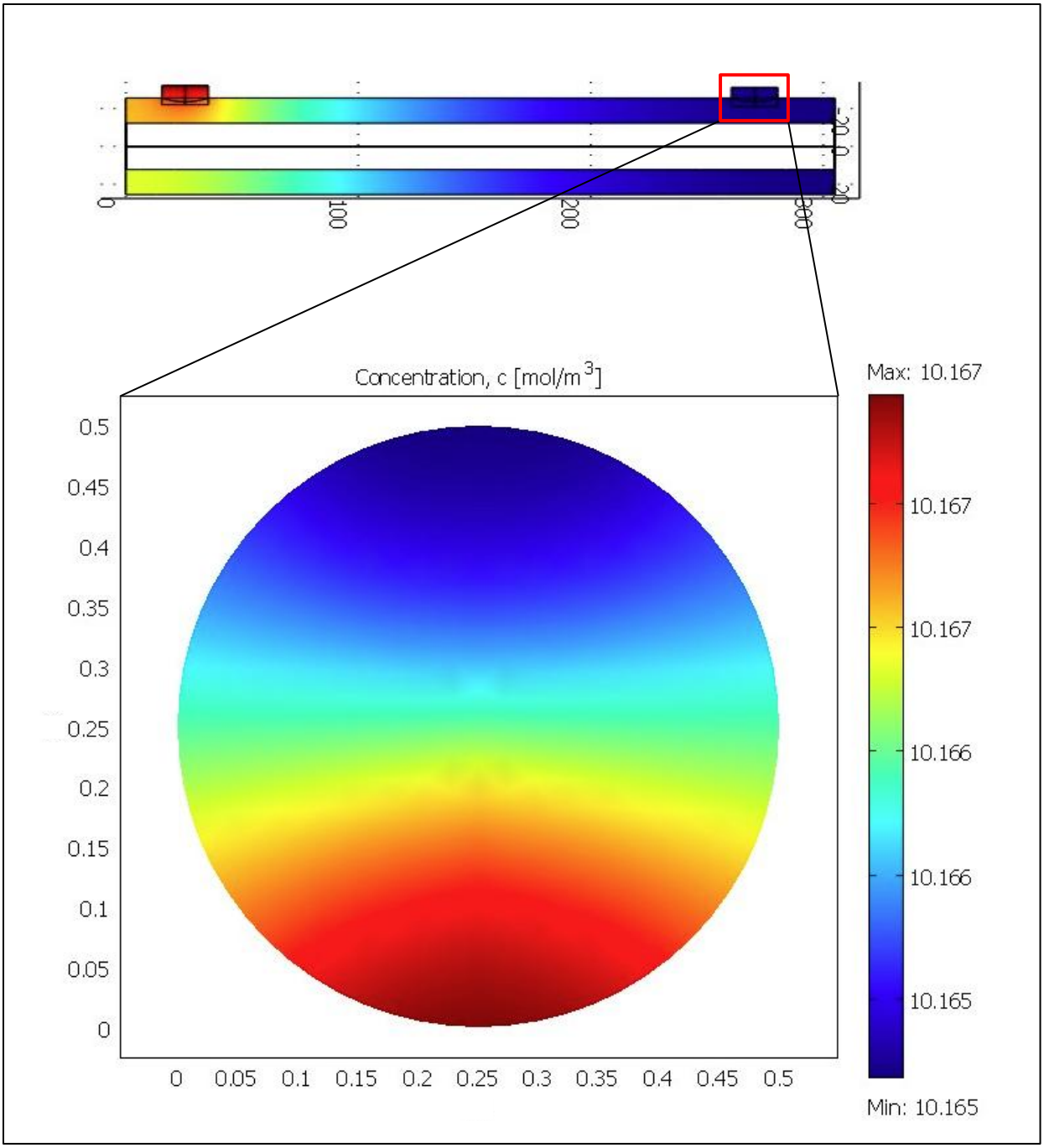

Figure 4.19. Radial TOC concentration in the outlet: maximum $[TOC]_{in}$=10.167 mol m^{-3}; UV-C/H_2O_2 photolytic process; continuous mode operation; flow rate 0.1 L min^{-1}. HRT= 4.6 min. The *y* and *x* axes are dimensions.

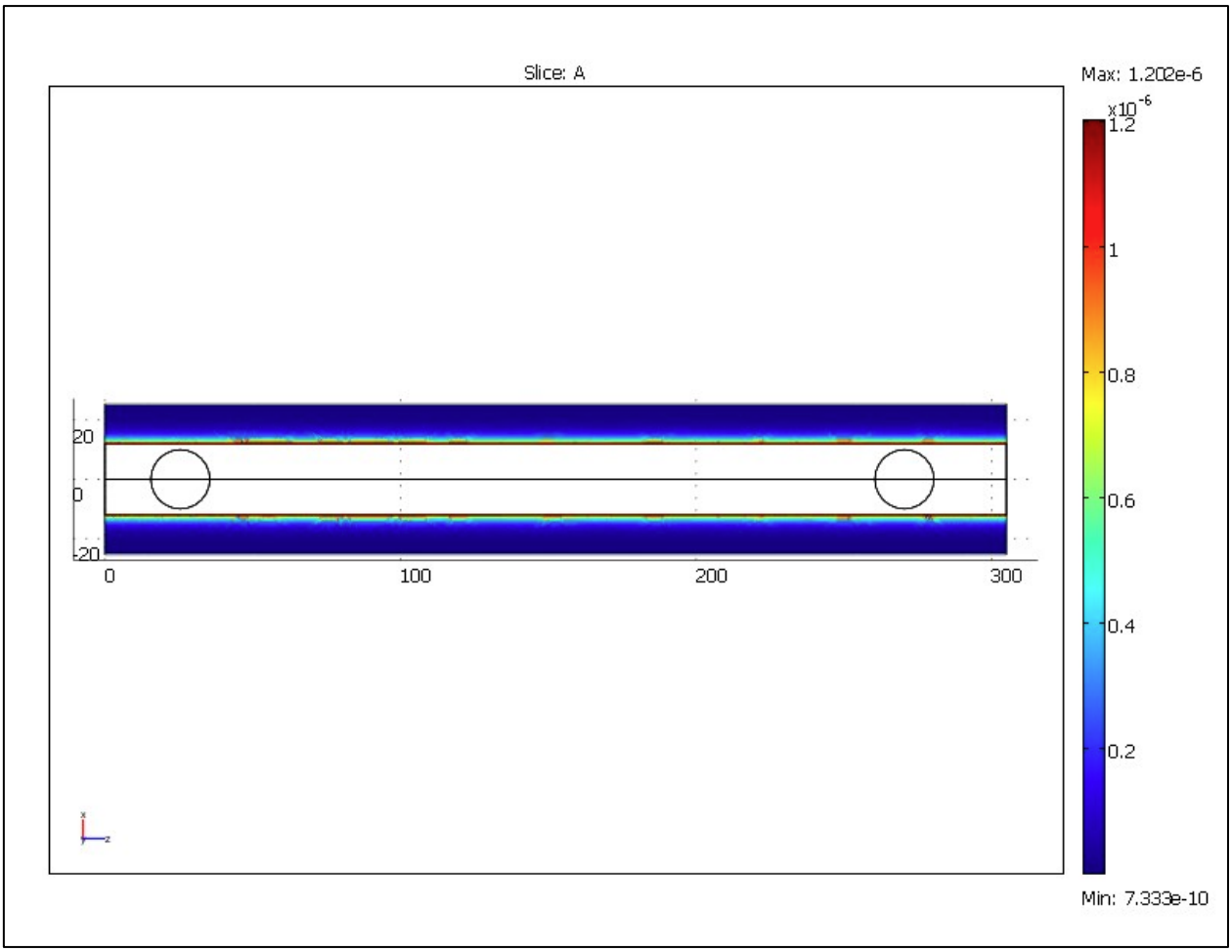

Figure 4.20. Axial local volumetric rate of energy absorption — LVREA — (*A*) (Einstein m^{-3} s^{-1}) from top view: maximum *A*: 1.202×10^{-6}; minimum *A*: 7.333×10^{-6}; UV-C/H_2O_2 photolytic process; continuous mode operation; flow rate 0.1 L min^{-1}. HRT= 4.6 min.

CHAPTER 5

CONCLUSIONS AND RECOMMENDATIONS

5.1 Conclusions

The following conclusions can be drawn from this thesis:

1. It was determined that VUV oxidation (λ=185 nm) alone achieved slightly better TOC removal rates for slaughterhouse effluents than UV-C (λ=254 nm) photolysis alone in both, batch recirculation and continuous mode operations. In batch recirculation mode, the TOC removal rates were 55.4% and 48.1% for VUV and UV-C respectively, for 2.5 h of exposure time, whereas in continuous mode, the TOC removal rates were 6.2% and 5.5% for a HRT of 4.6 min. The combination of these two processes, UV-C/VUV and VUV/UV-C in batch recirculation mode achieved better TOC removal rates, 57.6% and 55.1 %, respectively, than that of UV-C photolysis alone and very similar to that of VUV alone during batch recirculation mode.
2. TOC removal rates in continuous mode operation for combined UV-C/VUV and VUV/UV-C were of 5.8% and 6.1%, respectively, which were very similar to that of the VUV and UV-C individual processes of 6.2, and 5.5%, respectively. In both batch recirculation and continuous mode, the UV-C individual process is the least efficient, whereas VUV alone and combined UV-C/VUV and VUV/UV-C, showed higher TOC removal efficiencies. It is inferred that the production of $^{\bullet}OH$ radicals by the VUV process is the factor increasing the TOC removal efficiency in the combined processes.

3. The addition of hydrogen peroxide to both processes UV-C/H_2O_2 and VUV/H_2O_2 in batch recirculation mode showed no improvements in TOC removal rates, 50.9% and 48.6%, respectively, from that of the processes alone or combined. Nonetheless, when both processes were tested on the continuous mode operation, there was an improvement in TOC removal rates from 6.2% to 10.8% for UV-C/H_2O_2 and from 6.0% to 12.2% for VUV/H_2O_2. The difference between batch recirculation and continuous flow mode could be due to the fact that the hydrogen peroxide was a one-time addition at the beginning of the process in batch recirculation mode, and after a period of time, H_2O_2 concentration decayed due to the photolytic mechanism — H_2O_2 was broken down — under UV-C and VUV irradiation as was confirmed by the mathematical model. Therefore, the production of hydroxyl radicals was hindered reducing the ability of the system to oxidized organic matter.

4. VUV at 185 nm removed half of the TOC as the UV-C/H_2O_2 process did. Therefore, VUV at 185 nm is not a viable alternative to avoid the addition of auxiliary oxidants in AOPs application on wastewater treatment. However, it should be noted that the VUV lamp emission efficiency was 5% of that of the UV-C lamp.

5. The optimum H_2O_2 dose required in the photochemical oxidation of organic matter was found to be 1,000 mg L^{-1} for the UV-C/H_2O_2 process, and 600 mg L^{-1} for the VUV/H_2O_2 process. It was observed that a lower H_2O_2 concentration is needed when using VUV, due to a higher energy emitted at this band of the electromagnetic spectrum, which the H_2O_2 absorbs in large quantities producing more $^{\bullet}OH$ species. A larger quantity of $^{\bullet}OH$ radicals in the system means a better ability for the oxidation of organic matter.

6. Molar ratios of H_2O_2 to organic matter ([H_2O_2]/[TOC]) for both processes UV-C/H_2O_2 and VUV/H_2O_2 were assessed in this study. A molar ratio of 2.5 moles H_2O_2 per mole of TOC worked well for the UV-C/H_2O_2 process. Likewise, 1.5 moles of H_2O_2 per mole of TOC showed a good TOC removal efficiency in the case of VUV/H_2O_2. These values are in accordance with the literature that expressed molar ratio values should be between 0 and 100.
7. All photochemical processes evaluated were shown to be effective in inactivating bacteria from synthetic slaughterhouse wastewater. The concentrations of a mixed culture of pathogenic bacteria were reduced in the order of 5 logs in just 4.6 min of hydraulic residence time in clear water and in 27.6 sec from synthetic slaughterhouse wastewater. These results considerably surpassed the most stringent regulatory standards, which set bacteria inactivation standards at 4 logs.

5.2 Recommendations for Future Research

The following recommendations can be suggested to guide future research on photochemical processes:

1. It is suggested to conduct experiments at lower wavelengths within the vacuum-UV region of the electromagnetic spectrum. The lower the wavelength, the higher the energy and the higher the concentration of $^{\bullet}OH$ radical's produced. Modern lamps such as xenon excimer (Xe_2*) lamps, which generate VUV radiation from the excitation of xenon gas, can emit VUV radiation at 172 nm. These lamps have higher efficiencies than mercury lamps, reaching VUV outputs efficiencies of 60% and higher. As a result, the ability of

the system to oxidize organic and refractory constituents present in water will be greatly enhanced without the need to add any auxiliary oxidant, namely H_2O_2.

2. Further studies should use actual slaughterhouse wastewater in both UV-C/H_2O_2 and VUV (λ =172 nm) processes in order to examine the applicability of AOPs technologies to real situations.
3. It is recommended to broaden the experimental data for various molar ratios of hydrogen peroxide to organic matter ([H_2O_2]/[TOC]) by increasing the ranges of TOC concentration. This will help to confirm or improve the optimum ratio value to maximize the TOC removal rate from the system and minimize overuse of the auxiliary oxidant.
4. It is of interest to ensure a constant concentration of hydrogen peroxide within the photoreactor at all times during the batch recirculation operation by using an automated system that provides an optimum H_2O_2 concentration at all times. In this way, a better correlation between irradiation time and pollutant degradation could be established.
5. Further work is needed on testing the VUV processes in the removal of not only organic matter and pathogenic bacteria, but also emerging contaminants of concern such as veterinary pharmaceutical compounds like antibiotics, and anti-inflammatories, particularly in the case of livestock rearing, which are discharged in significant concentrations from slaughterhouses. In a more broad perspective, it is also suggested to apply the photochemical processes in the removal or personal care products, endocrine disruptors, corrosion inhibitors, plasticizers, fluorinated surfactants, among other hazardous compounds, entering our source waters on a daily basis, which are not presently targeted by conventional treatments.

REFERENCES

Abramovic, B., Banic, N.D, and Sokic, D.V. (2010). Degradation of thiacloprid in aqueous solution by UV and UV/H_2O_2 treatments. *Chemosphere, 81*(1), 114–119.

Aga, D.S. (Ed.) (2008). *Fate of Pharmaceuticals in the Environment and in Water Treatment Systems*. Boca Raton, FL: CRC Press.

Afzal, A., Oppenländer, T., Bolton, J.R, and El-Din, M.G. (2010). Anatoxin-a degradation by Advanced Oxidation Processes: Vacuum-UV at 172 nm, photolysis using medium pressure UV and UV/H_2O_2. *Water Res., 44*(1), 278–286.

Alpert, S.M., Knappe, D.R.U, and Ducoste, J.J. (2010). Modeling the UV/hydrogen peroxide advanced oxidation process using computational fluid dynamics. *Water Res., 44*(6), 1797–1808.

APHA (1998). *Standard Methods for the Examination of Water and Wastewater* (20th ed.). American Water Works Association. Baltimore, Maryland: United Books Press Inc.

Arslan-Alaton, I., Cokgor, E.U, and Koban, B. (2007). Integrated photochemical and biological treatment of a commercial textile surfactant: Process optimization, process kinetics and COD fractionation. *J. Hazard. Mater., 146*(3), 453–458.

Asano, T., Burton, F, and Leverenz, H. (2007). *Water Reuse: Issues, Technologies, and Applications.* New York, NY: McGraw-Hill Professional.

Baeza, C., Rossner, A., Jardim, W.F., Litter, M.I, and Mansilla, H.D. (2003). Removal of EDTA by UV-C/hydrogen peroxide. *Environ. Technol., 24*(10), 1277–1281.

Bali U., Catalkaya, E, and Sengul, F. (2004), Photodegradation of reactive black 5, direct red 28 and direct yellow 12 using UV, UV/H_2O_2 and UV/ H_2O_2/Fe^{2+}: A comparative study. *J. Hazard. Mater., 114*(1–3), 159–166.

Barcelo, D. and Petrovic, M. (Eds.). (2008). *Emerging Contaminants from Industrial and Municipal Waste: Occurrence, Analysis and Effects*. The Handbook of Environmental Chemistry Vol. 5/S/1. Berlin, GER: Springer-Verlag Berlin Heidelberg.

Baruth, E.E. (Ed.). (2005) *Water Treatment Plant Design* (4th ed.). American Water Works Association. New York, NY: McGraw-Hill.

Batzing, B.L. (2002). *Microbiology: An Introduction*. Pacific grove, CA: Brooks Cole.

Beltran, F.J., Gonzalez, M., Rivas, J, and Jaramillo J. (1995). Application of photochemical reactor models to UV radiation of trichloroethylene in water. *Chemosphere, 31*(3), 2873–2885.

Benka-Coker, M.O. and Ojior, O.O. (1995) Effect of slaughterhouse wastes on the water quality of Ikpoba River, Nigeria. *Bioresour. Techno., 52*(1), 5–12.

Benson, H.J. (2001). *Microbiological Applications Lab Manual* (8th ed.). New York, NY: McGraw-Hill Professional.

Bigda R.J. (1995). Consider Fenton's Chemistry for Wastewater Treatment. *Chem. Eng. Progr., 91*(12), 62–66.

Bird, R.B., Stewart, W.E, and Lightfoot, E.N. (2002). *Transport Phenomena* (5th ed.). New York, NY: John Wiley and Sons.

Birkett, J.W. and Lester, J.N. (2003). *Endocrine Disrupters in Wastewater and Sludge Treatment Processes*. Boca Raton, FL: CRC Press LLC.

Bitton, G. (2005). *Wastewater Microbiology* (3rd ed.). Hoboken, NJ: John Wiley and Sons.

Black and Veatch. (2010). *White's Handbook of Chlorination and Alternative Disinfectants* (5th ed.). Hoboken, New Jersey: John Wiley and Sons.

Bolton, J.R. (2000). Terms and Definitions in Ultraviolet Disinfection in: Proceedings, Disinfection 2000: Disinfection of Wastes in the New Millennium, 15–18 March, New Orleans, LA, Water Environment Federation, Alexandria, VA.

Bolton, J.R., Bircher, K.G., Tumas, W, and Tolman, C.A. (2001). "Figures-of-merit for the technical development and application of advanced oxidation technologies for both electric- and solar-driven systems." *Pure Appl. Chem.*, *73*(4), 627–637.

Bolton, J.R. and Cotton, C.A. (2008). *The Ultraviolet Disinfection Handbook* (1st ed.). American Water Works Association. Denver, TX: AWWA.

Bolton, J.R. (2010). *Ultraviolet Application Handbook* (3rd ed.). Edmonton, Alta: Bolton Photosciences Inc.

Bratbak, G. and Dundas, I. (1984). Bacterial Dry Matter Content and Biomass Estimations. *Appl. Environ. Microbiol.*, *48*(4), 755–757.

Braun A.M, Maurette M.T, and Oliveros E. (1991). *Photochemical Technology*. New York, NY: John Wiley and Sons.

Braun, A.M. and Oliveros, E. (1997). How to Evaluate Photochemical Methods for Water Treatment. *Wat. Sci. Tech., 35*(4), 17–23.

Buxton, G. V., Greenstock, C. L., Helman, W. P, and Ross, A. B. (1988). Critical review of rate constants for reactions of hydrated electrons, hydrogen atoms and hydroxyl radicals in aqueous solutions. *J. Phys. Chem. Ref. Data., 17*, 513.

Cao, W. (2009). *Combined anaerobic baffle reactor and UV/ H_2O_2 process for the treatment of synthetic slaughterhouse wastewater*. M.A.Sc Thesis. Ryerson University.

Cao, W. and Merhvar, M. (2010). Slaughterhouse wastewater treatment by combined anaerobic baffled reactor and UV/H_2O_2. *Chem. Eng. Res. Des.(In press).*

Chelikani, P. Fita, I, and Loewen, P.C. (2004). Diversity of structures and properties among catalases. *Cell. Mol. Life Sci., 61*(2), 192–208.

Christensen, H.S., Sehested, K, and Corftizan, H. (1982). Reaction of hydroxyl radicals with hydrogen peroxide at ambient temperatures and elevated temperatures. *J. Phys. Chem., 86*(9), 1588–1590.

Christensen, J. and Linden, K.G. (2003). How particles affect UV light in the UV disinfection of unfiltered drinking water. *J. Am. Water Works Assn., 95*(4), 179–189.

Comninellis, C., Kapalka, A., Malato, S., Parsons, S.A., Poulios, I, and Mantzavinos, D. (2008). Perspective Advanced oxidation processes for water treatment: advances and trends for R&D. *Chem. Technol. Biotechnol., 83*(6), 769–776.

Correctional Service Canada. (2003). *Environmental Guidelines: Management of Wastewater Treatment Systems* (EG 318-6), Ottawa.

Crittenden, J.C., Rhodes, R., Hand, D.W,. Howe, K.J, and Tchobanoglous, G. (2005). *Water Treatment: Principles and Design* (2nd ed.). Hoboken, NJ: John Wiley and Sons.

Council of the European Communities. (1991). Urban Wastewater Treatment Directive 91/271/EEC. Off. J. Eur. Comm., 1991, L135/40-52.

De Laat, J., Berger, P., Poinot, T., Karpel Vel Leitner, N, and Dore, M. (1997). Modeling the oxidation of atrazine by H_2O_2/UV. Estimation of kinetic parameters. *Ozone. Sci. Eng., 19*(5), 395–408.

Del Pozo, R. and Diez, V. (2005). Integrated aerobic-anaerobic fixed-film reactor for slaughterhouse wastewater treatment. *Water Res., 39*(6), 114–1122.

Eckenfelder, W., Ford, D, and Englande, A. (2009). *Industrial Water Quality* (4th ed.). New York, NY: McGraw-Hill Professional.

Environment Canada. (2001). Threats to Sources of Drinking Water and Aquatic Ecosystems Health in Canada. Retrieved on October 10, 2010, from http://www.ec.gc.ca/inre-nwri/default.asp?lang=En&n=235D11EB-1.

Environmental Commissioner of Ontario. (2010). "Sewage Treatment: Not Good Enough." *Redefining Conservation, ECO Annual Report, 2009/10*. Toronto: The Queen's Printer for Ontario. 80.

Environmental Management Act. (2008). Code of Practice for the Slaughter and Poultry Processing Industries. B.C. Reg. 246/2007. Vancouver: B.C Ministry of Environment.

FAO. (2010). Food Outlook: Meat and Meat Products. Rome, Italy: Food and Agriculture Organization of the United Nations.

Flynn, D. (2009). *The Nalco Water Handbook*. (3rd ed.). New York, NY: McGraw-Hill Professional

Fogler, H.S. (2006). *Elements of Chemical Reaction Engineering* (4th ed.). Upper Saddle River. NJ : Pearson Education.

Gadgil, A. (2005). *UV Waterworks 2.0: Answers to Ten Commonly Asked Questions about the Design, Operation, and Economics*. Berkeley, CA: Energy & Environment Division Lawrence Berkeley National Laboratory.

Gerardi, M.H. (2006). *Wastewater Bacteria*. Hoboken, NJ: John Wiley and Sons.

Glaze, W.H., Kang, J.W, and Chapin, D.H. (1987). The chemistry of water treatment processes involving ozone, hydrogen peroxide and ultraviolet radiation. *Ozone Sci. Eng.*, *9*(4), 335–352.

Greenbaum, A. and Wellington, A. (2008). *Environmental Law and Policy: Canadian Perspectives*. Concord, Ontario: Captus Press Inc.

Gonzalez, M.C., Braun, A.M., Prevot, A.B, and Pelizzetti, E. (1994). Vacuum-Ultraviolet (VUV) photolysis of water: mineralization of atrazine. *Chemosphere, 28*(12), 2121–2127.

Goslan, E.H., Gurses, F., Banks, J., Parsons, S.A. (2006). An investigation into reservoir NOM reduction by UV photolysis and advanced oxidation processes. *Chemosphere, 65*(7), 1113–1119.

Gyles, C. L., Prescott, J. F., Songer, G, and Thoen, C.O. (Eds.). (2010). *Pathogenesis of Bacterial Infections in Animals* (4th ed.). Ames, IA: Wiley-Blackwell.

Halweil, B. (2008). *Vital Signs: Meat Production Continues to Rise*. Washington, D.C: World Watch Institute.

Health Canada. (2006). Guidelines for Canadian Drinking Water Quality: Guideline Technical Document — Bacterial Waterborne Pathogens — Current and Emerging Organisms of Concern. Ottawa, Ontario. Water Quality and Health Bureau, Healthy Environments and Consumer Safety Branch, Health Canada.

Henry, G. and Heinke, GW. (1996). *Environmental Science and Engineering* (2nd ed.). Upper Saddle River, NJ: Prentice Hall College Div.

Jing, P. and Yongquian, C. (2010). Oxidative Degradation of Bisphenol A (BPA) by UV/H2O2 Process. Bioinformatics and Biomedical Engineering (iCBBE), 4th International Conference, 1–4.

International Finance Corporation (IFC). (2007). Environmental, Health, and Safety Guidelines for Meat Processing. World Bank. Retrieved on October 5, 2010, from

http://www.ifc.org/ifcext/enviro.nsf/AttachmentsByTitle/gui_EHSGuidelines2007_Meat Processing/$FILE/Final+-+Meat+Processing.pdf.

IJC. (2009). Fourteenth Biennial Report on Great Lakes Water Quality. International Joint commission.

Johnson, M.B. and Mehrvar, M. (2008). Aqueous metronidazole degradation by UV/H_2O_2 process in single- and multi-lamp tubular photoreactors: Kinetics and reactor design. *Ind. Eng. Chem. Res.*, *47*(17), 6525–6537.

Kiepper, B. (2001). A Survey of Wastewater Treatment Practices in the Broiler Industry. The University of Georgia. U.S. Poultry and Egg Association. Presented at WEFTEC 2001.

Kim, I., Yamashita, N, and Tanaka, H. (2009a). Performance of UV and UV/ H_2O_2 processes for the removal of pharmaceuticals detected in secondary effluent of a sewage treatment plant in Japan. *J. Hazard. Mater.*, *166*(2–3), 1134–1140.

Kim, I., Yamashita, N, and Tanaka, H. (2009b). Photodegradation of pharmaceuticals and personal care products during UV and UV/ H_2O_2 treatments. *Chemosphere*, *77*(4), 518–525.

Kumar, K., Gupta, S.C., Chander, Y, and Singh, A.K. (2005). Antibiotic use in agriculture and its impacts on the terrestrial environment. *Adv. Agron.*, *87*, 1–54.

Lawley, R., Curtis, L, and Davis, J. (2008).*The food safety hazard guidebook*. Cambridge, UK: Royal Society of Chemistry.

Lemarchand, K., Masson, L, and Brousseau, R. (2004). Molecular biology and DNA microarray technology for microbial quality monitoring of water. *Crit. Rev. Microbiol., 30*(3), 145–172.

Li, K., Stefan, M.I, and Crittenden, J.C. (2007). Trichloroethene Degradation by UV/H_2O_2 Advanced Oxidation Process: Product Study and Kinetic Modeling. *Environ. Sci. Technol., 41*(5), 1696–1703.

Liao, C.H., Kang, S.F, and Wu, F.A. (2001). Hydroxyl radical scavenging role of chloride and bicarbonate ions in the H_2O_2/UV process. *Chemosphere, 44*(5), 1193–1200.

Loferer-Krößbacher, M., Klima, J, and Psenner, R. (1998). Determination of bacterial cell dry mass by transmission electron microscopy and densitometric image analysis. *Appl. Environ. Microbiol., 64*(2), 688–694.

López-Peñalver, J.J., Sánchez-Polo, M., Gómez-Pacheco, C.V, and Rivera-Utrilla, J. (2010) Photodegradation of tetracyclines in aqueous solution by using UV and UV/H2O2 oxidation processes. *J. Chem. Technol. Biotechnol., 85*(10), 1325–1333.

Lorenzo-Lorenzo, M.J., Ares-Mazas, M.E., Maturana, I.V, and Duran-Oreiro, D. (1993). Effect of ultraviolet disinfection of drinking water on the viability of cryptosporidium parvum oocysts. *The Journal of Parasitology, 79*(1), 67–70.

Luo, Y.R. (2007). *Comprehensive Handbook of Chemical Bond Energies*. Boca Raton, FL. CRC press.

Luiz, D.B., Genena, A.K., José, H.J., Moreira, R.F.P.M, and Schröder, H.F. (2009). Tertiary treatment of slaughterhouse effluent: Degradation kinetics applying UV radiation or H_2O_2/UV. *Water Sci. Technol., 60*(7), 1869–1874.

Maier, R., Pepper, I.L, and Gerba, C.P. (2009). *Environmental Microbiology*. 2ed. Burlington, MA: Academic Press.

Manitoba Water Stewardship. (2005). Chlorine and Alternative Disinfectants Guidance Manual. Office of Drinking Water. Retrieved on January 5, 2009, from http://www.gov.mb.ca/waterstewardship/odw/reg-info/approvals/odw_chlorine_ and _alternative_disinfectants.pdf.

Martin, E.J. and Martin, E.T. (1991). *Technologies for Small Water and Wastewater Systems*. New York, NY: Van Nostrand Reinhold.

Maruani, J. (1988). *Molecules in Physics: Topics in Molecular Organization and Engineering, Chemistry and Biology* (1st ed.). Amsterdam, The Netherlands: Kluwer Academic Publishers.

McMurry, J. and Fay, R.C. (1998). *Chemistry* (5th ed.). Upper Saddle River, NJ: Pearson Prentice-Hall.

Meulemans, C.C.E. (1987). The Basic Principles of UV–Disinfection of Water. *Ozone Sci. Eng., 9*(4), 299–313.

Mohajerani, M., Mehrvar, M, and Ein-Mozaffari, F. (2010). CFD modeling of metronidazole degradation in water by the UV/H_2O_2 process in single and multilamp photoreactors. *Ind. Eng. Chem. Res., 49*(11), 5367–5382.

Morris, D., Sung, S, and Dague, R.R. (1998). "ASBR treatment of beef slaughterhouse wastewater." In Proceedings of the 52nd Purdue Industrial Waste Conference, Purdue University, West Lafayette, IN.

Muller, L.P. and Jekel, M. (2001). ''Comparison of Advanced Oxidation Processes in Flow-Through Pilot Plants (Part I)". *Water. Sci. Technol., 44*(5), 303–309.

Muruganandham, M., Selvam, K, and Swaminathan, M. (2006). A comparative study of quantum yield and electrical energy per order (EEo) for advanced oxidative decolourisation of reactive azo dyes by UV light. *J. Hazard. Mater.,144*(1–2), 316–322.

Nemerow, N.L. (2007). *Industrial Waste Treatment*. Burlington, MA: Elsevier Science & Technology.

Nieuwenhuijesen, M.J., Toledano, M.B., Eaton, N.E., Fawell, J, and Elliott, P. (2000). Chlorination disinfection by-products in water and their association with adverse reproductive outcomes: A review. *Occup. Environ. Med., 57*(2), 73–85.October 10, 2008, from ProQuest Science Journals database. (Document ID: 30353845).

Nollet, M.L. (Ed.). (2007). *Handbook of Water Analysis* (2nd ed.). Boca Raton, FL: CRC press a Taylor and Francis group.

Olmez-Hanci, T., Imren, C., Arslan-Alaton, I., Kabdash, I, and Tunay, O. (2009). H_2O_2/UV-C oxidation of potential endocrine disrupting compounds: a case study with dimethyl phthalate. *Photochem. Photobiol. Sci., 8*(5), 620–627.

Oppenländer, T. (2003). *Photochemical Purification of Water and Air, Advanced Oxidation Processes (AOPs): Principles, Reaction Mechanisms, Reactor Concepts*. Winheim, GER: Wiley-VCH.

Ontario Drinking Water Standards, Objectives and Guidelines. (June 2003, revised June 2006). PIBS 4449e01. Technical support document of the Safe Drinking Water Act, 2002. Retrieve on November 13, 2008, from http://www.ontario.ca/drinkingwater/stel01_046947.pdf .

Percival, S., Chalmers, R., Embrey, M., Hunter, P., Sellwood, J, and Wyn-Jones, P. (2004). *Microbiology of Waterborne Diseases.* London, UK: Elsevier Academic Press.

Pereira, V.J., Linden, K.G, and Weinberg, H.S. (2007). Evaluation of UV irradiation for photolytic and oxidative degradation of pharmaceutical compounds in water. *Water Res., 41*(19), 4413–4423.

Qasim, S. R., Motley, E.M, and Zhu, G. (2000). *Water Works Engineering – Planning, Design & Operating*., Upper Saddle River, NJ:Prentice Hall.

Quinete, N., Orata, F., Maes, A., Gehron, M., Bauer, K.H., Moreira, I, and Wilken, R.D. (2010). Degradation studies of new substitutes for perfluorinated surfactants. *Arch. Environ. Contam. Toxicol., 59*(1), 20–30.

Reynolds, T.D. and Richards, P.A. (1996). *Unit Operations and Processes in Environmental Engineering* (2nd ed.). Boston, MA: PWS Publishing Company.

Rietbergen-McCracken, J. and Abaza, H, (2000). *Economic Instruments for Environmental Management: A Worldwide Compendium of Case Studies*. London, UK: Earthscan Publications Ltd.

Rosario, F.L., Wert, E.C, and Snyder, S.A. (2010). Evaluation of UV/H_2O_2 treatment for the oxidation of pharmaceuticals in wastewater. *Water Res., 44*(5), 1440–1448

Rose, L.J. and O'Connel, H. (2009). UV light inactivation of bacterial biothreat agents. *Appl. Environ. Microbiol., 75*(9), 2987–2990.

Salvato, J.A., Nemerow, N.L, and Agardy, F.J. (2003). *Environmental Engineering* (5th ed.). Hoboken, NJ: John Wiley and Sons.

Sawyer, C., McCarty, P, and Martin, G. (2002). *Chemistry for Environmental Engineering and Science* (5th ed.). New York, NY: McGraw-Hill Science.

Secondary Treatment. Title 40 Code of Federal Regulations, Part 122. (1989).

Sharpless, C.M. and Linden, K.G. (2003). Experimental and model comparisons of low- and medium-pressure Hg lamps for the direct and H_2O_2 assisted UV photodegradation of N-Nitrosodimethylamine in simulated drinking water. *Environ. Sci. Technol. 37*(9), 1933–1940.

Shemer, H., Kacar, Y.K, and Linden, K.G. (2006). Degradation of the pharmaceutical metronidazole via UV, Fenton and photo-Fenton processes. *Chemosphere, 63*(2), 269–276.

Shu, H.Y. and Chang, M.C. (2005). Pilot Scale Annular Plug Flow Photoreactor by UV/H_2O_2 for the Decolorization of Azo Dye Wastewater. *J. Hazard. Mater., 125*(1–3), 244–251.

Shugar, G.J, Bauman S.L, Drum, D.A, and Lauber, J. (2001). *Environmental Field Testing and Analysis Ready Reference Handbook*. New York, NY: McGraw-Hill.

Sommer, R., Cabaj A., Hirschmann, G, and Haider T. (2008). Disinfection of Drinking Water by UV Irradiation: Basic Principles - Specific Requirements - International Implementations. *Ozone Sci. Eng., 30*(1), 43–48.

Sosnin, E.A., Oppenlander, T, and Tarasenko, F.V. (2006). Applications of capacitive and barrier discharge excilamps in photoscience. *J Photochem. Photobiol. C: photchem. Reviews, 7*(4), 145–163.

Spellman, F.R. (2008). *The Science of water: Concepts and Applications.* Boca Raton, FL: CRC Press.

Spellman, F.R. (2009). *Handbook of Water and Wastewater Treatment Plant Operations* (2nd ed.). Boca Raton, FL: CRC Press.

Staehelin, J., Buehler, R.E, and Hoigne, J. (1984).Ozone decomposition in water studied by pulse radiolysis. 2. Hydroxyl and hydrogen tetroxide (HO_4) as chain intermediates. *J. Phys. Chem., 88*(24), 5999–6004.

Stephenson, T. and Lester, J.N. (1986). Evaluation of startup and operation of four anaerobic processes treating a synthetic meat waste. *Biotechnol. Bioeng.*, 28(3), 372–380.

Sullivan, P., Agardy, F.J, and Clark, J.J. (2005). *The Environmental Science of Drinking Water*. Elsevier Science & Technology Books.

Tabrizi, G.B. and Mehrvar, M. (2004). Integration of Advanced Oxidation Technologies and Biological Processes: Recent Developments, Trends, and Advances. *J. Environ. Sci. Health., 39*(11–12), 3029–3081.

Tabrizi, G.B. and Mehrvar, M. (2006). Pilot-plant study for the photochemical treatment of aqueous linear alkylbenzene sulfonate. *Sep. Purif. Technol., 49*(2), 115–121.

Tang, W.Z. (2004). *Physicochemical Treatment of Hazardous Wastes*. Boca Raton, FL: CRC Press.

Tarr, M.A. (Ed.). (2003). *Chemical Degradation Methods for Wastes and Pollutants: Environmental and Industrial Applications*. New York, NY: Marcel Dekker.

Tchobanoglous, G., Burton, F.L, and Stensel. H.D. (2003). *Wastewater Engineering: Treatment and Reuse* (4th ed.). New York, NY: McGraw Hill.

Thomas, O. and Burgess, C. (2008). *UV Visible Spectrophotometry of Water and Wastewater*. Amsterdam, The Netherlands: Elsevier.

UNEP. (2000). Cleaner production in meat processing. COWI Consulting Engineers/UNEP/Danish Environmental Protection Agency, 2000.

U.S EPA. (1992). Manual - Guidelines for Water Reuse. Environmental Protection Agency and U.S Agency for International Development (U.S EPA), EPA/625/R-92/004-017, Washington, D.C.

U.S EPA. (1998). Handbook of Advanced Photochemical Oxidation Processes, EPA/625/R-98/004.

U.S EPA. (1999). Alternative Disinfectants and Oxidants Guidance Manual. Office of Water, EPA 815-R-99-014. Retrieved on January 4, 2009 from http://www.epa.gov/OGWDW/mdbp/alternative_disinfectants_guidance.pdf.

U.S EPA. (2006). Ultraviolet Disinfection Guidance Manual for the final long term 2 enhanced surface water treatment rule. Office of Water, EPA 815-R-06-007. Retrieved on December 6, 2008, from: http://www.epa.gov/safewater/disinfection/lt2/pdfs/guide_lt2_uvguidance.pdf.

Vilhunen, S., Rokhina, E.V, and Virkutyte, J. (2010). Evaluation of UV LEDs Performance in Photochemical Oxidation of Phenol in the Presence of H_2O_2. *J. Environ. Eng., 136*(3), 274–280.

Verhoeven, J.W. (1996). Glossary of Terms Used in Photochemistry *Pure & Appl. Chem., 68*, 2223. IUPAC.

Wang, L.K., Hung, Y.T., Lo, H.H, and Yapijakis, C. (Eds.). (2004). *Handbook of industrial and hazardous wastes treatment* (2nd ed.). New York: NY, Marcel Dekker.

Wang, L.K., Hung, Y, and Shammas, N.K. (Eds.). (2005). *Physicochemical Treatment Process: Volume 3 (Handbook of Environmental Engineering)*. Totowa, NJ: Humana Press.

Wang, L.K., Hung, Y, and Shammas, N.K. (Eds.). (2006a). *Advanced Physicochemical Treatment Process: Volume 4 (Handbook of Environmental Engineering)*. Totowa, NJ: Humana Press.

Wang, L.K., Hung, Y.T., Lo, H.H, and Yapijakis, C. (Eds.). (2006b). *Waste Treatment in the Food Processing Industry*. Boca Raton, FL: CRC press.

Wang, L.K, Shammas, N.K, and Hung, Y. (Eds.). (2008). *Advanced Biological Treatment Processes: Volume 9 (Handbook of Environment Al Engineering)* (1st ed.). New York, NY: Humana Press.

Wang L.K., Hung, Y.T, and Shammas, N.K. (Eds.). (2010). *Handbook of Advanced Industrial and Hazardous Wastes Treatment*. Boca Raton, FL: CRC Press.

Water Environment Federation. (2008). *Industrial Wastewater Management, Treatment, and Disposal*. New York, NY: McGraw-Hill.

Water Environment Federation. (2009). *Manure pathogens: manure management, regulation, and water quality protection*. New York, NY: McGraw-Hill.

Weissman, U., Choi, I.S, and Dombrowski, E.M. (2007). *Fundamentals of Biological Wastewater Treatment*. Weinheim, GER: Wiley-VCH Verlag GmbH & Co.

Wendt, J.F. (2009). *Computational Fluid Dynamics: An Introduction* (3rd ed.). Berlin, GER: Springer-Verlag Berlin Heidelberg.

WHO. (2003). Emerging issues in water and infectious disease. Retrieved on January 5, 2009, from http://www.who.int/water_sanitation_health/emerging/emerging.pdf

WHO. (2006). Guidelines for Drinking-water Quality [electronic resource]. incorporating first addendum. Vol. 1, Recommendations (3rd ed.). Retrieved on January 5, 2009, from http://www.who.int/water_sanitation_health/dwq/gdwq0506.pdf

WHO. (2008). Guidelines for Drinking-water Quality, third edition incorporating the first and second addenda Volume 1 Recommendations. Retrieved on March 15, 2009, from http://www.who.int/water_sanitation_health/dwq/gdwq3rev/en/

Wilkes, J.O. (2006). Fluid Mechanics for Chemical Engineers with Microfluidics and CFD (2nd ed.).Upper Saddle River, NJ: Prentice Hall.

World Bank. (1999).*Pollution Prevention and abatement handbook toward cleaner production*. Washington, DC: The International Bank for Reconstruction and Development/THE WORLD BANK.

World Bank. (2005). Managing the Livestock Revolution: Policy and Technology to Address the Negative Impacts of a Fast-Growing Sector. Washington, DC: The World Bank Agriculture and Rural Development Department Report No. 32725-GLB.

Yasar, A, Ahmad, N, and Khan, A.A. (2006). Energy requirement of ultraviolet and AOPs for the post-treatment of treated combined industrial effluent. *Color. Technol*., *122*(4), 201–206.

Zhang, C., (2007). *Fundamentals of Environmental Sampling and Analysis*. Hoboken, New Jersey: John Wiley and Sons.

APPENDICES

APPENDIX A: Determination of the theoretical TOC

The following compounds were used in the synthetic slaughterhouse wastewater: commercial meat extract powder (Oxoid Lab Lemco LP0029, Oxoid Ltd.), 1950 mg L^{-1}; glycerol ($C_3H_8O_3$), 200 mg L^{-1}; ammonium chloride (NH_4Cl), 360 mg L^{-1}; sodium chloride (NaCl), 50 mg L^{-1}. 5, 15, and 25% fractions of the original aforementioned concentrations were used.

Based on the composition of the Oxoid meat extract provided by manufacturer Oxoid Ltd. shown on Table A.2, the theoretical TOC can be calculated as follows:

Taking alanine (AL) as example,

Theoretical Total Organic Carbon:

$$TOC_{AL}\left(\%w/_w\right) = \frac{Carbon\ Molar\ Mass}{AL\ Molar\ Mass} \times \frac{\%\ w_{\ AL}}{w_{meat\ extract}}$$

$$TOC_{AL}\left(\%w/_w\right) = 89.01 mgAL \times \frac{5.85\ mgAL}{100\ mg\ Meat\ Extract} = \frac{2.37\ mgC}{100\ mg\ Meat\ Extract}$$

Only meat extract and glycerol are contributing organic carbon to the system; thus, the amount added to the system for a TOC residual of 15% after anaerobic is:

a) Fraction of original meat extract concentration

$$=1950\,\frac{mg}{L}\times 0.15 = 292\,\frac{mg}{L}$$

b) Fraction of original Glycerol concentration

$$=200\,\frac{mg}{L}\times 0.15 = 30\,\frac{mg}{L}$$

From these values the theoretical TOC concentration can be calculated for the different fractions of the original TOC values as shown in Table A.1.

Table A.1. Theoretical TOC for the different TOC fractions from the original concentration.

Theoretical TOC fraction from original concentration (%)	**TOC (mg L^{-1})**
5	34.7
15	105
25	173

Example of theoretical TOC calculation for the 15% TOC residual fraction:

$$TOC\ Meat\ extract\left(\frac{mgC}{L}\right) = \frac{292\ mg\ Meat\ Extract}{L}\times\frac{31.5\ mgC}{100\ mg\ Meat\ Extract} = 92.0$$

$$TOC\ Glycerol\left(\frac{mgC}{L}\right) = \frac{33.0\ mg\ C_3H_8O_3}{L}\times\frac{36.0\ mg\ C_3H_8O_3}{92.1\ mg\ C_3H_8O_3} = 13.0$$

$$Theoretical\ TOC = 105\,\frac{mg}{L}$$

Table A.2. TOC and TN values contained in the Oxoid Meat Extract based on information provided by the manufacturer (Oxoid Ltd.).

Symbol	Typical Amino Acid	% w of chemical/ w of meat extract	Molar mass (g mol^{-1})	Carbon Molar Mass (g mol^{-1})	% w of TOC/ w of meat extract
AL	ALANINE ($C_3H_7NO_2$)	5.85	89.1	36.03	2.37
AR	ARGININE ($C_6H_{14}N_4O_2$)	7.1	174.2	72.06	2.94
AS	ASPARTIC ACID ($C_4H_7NO_4$)	5.1	133.1	48.04	1.84
CY	CYSTEINE ($C_4H_7NO_4$)	0.68	121.2	36.03	0.2
G.A	GLUTAMlC ACID ($C_3H_7NO_2S$)	10.71	147.1	60.05	4.37
GL	GLYCINE ($C_2H_5NO_2$)	10.85	75.1	24.02	3.47
IS	ISOLEUCINE ($C_6H_{13}NO_2$)	3.17	131.2	72.06	1.74
LE	LEUCINE ($C_6H_{13}NO_2$)	3.15	131.2	72.06	1.73
LY	LYSINE ($C_6H_{14}N_2O_2$)	4.78	1462	72.06	2.36
ME	METHIONINE $C_5H_{11}NO_2S$	2.61	149.2	60.05	1.05
PH	PHENYLALANIN ($C_9H_{11}NO_2$)	2.34	165.2	108.09	1.53
PR	PROLINE ($C_5H_9NO_2$)	7.79	115.1	60.05	4.06
SE	SERINE ($C_3H_7NO_3$)	1.87	105.1	36.03	0.64
TH	THREONINE ($C_4H_9NO_3$)	2.54	119.1	48.04	1.02
TR	TRYPTOPHAN ($C_{11}H_{12}N_2O_2$)	0.34	204.2	132.11	0.22
TY	TYROSINE ($C_9H_{11}NO_3$)	0.66	181.2	108.09	0.39
VA	VALINE ($C_5H_{11}NO_2$)	3.06	117.2	60.05	1.57
	Total	72.6	3620.5	1104.9	31.5

APPENDIX B: Determination of the molar concentration and molar ratio calculations for the UV/ H_2O_2 and VUV/H_2O_2 photochemical processes.

Calculation for 600 mg L^{-1} assuming a molar mass H_2O_2 (g mol^{-1}) = 34.01:

$$600\ \frac{mg\ H_2O_2}{L}\ \times\ \frac{1\ gH_2O_2}{1000\ mgH_2O_2}\times\ \frac{1\ molH_2O_2}{34.01\ gH_2O_2} = 0.0176\ \text{M}\ \ H_2\ O_2$$

Calculation for 1000 mg L^{-1} assuming a molar mass H_2O_2 (g mol^{-1}) = 34.01:

$$1000\ \frac{mg\ H_2O_2}{L}\ \times\ \frac{1\ gH_2O_2}{1000\ mgH_2O_2}\times\ \frac{1\ molH_2O_2}{34.01\ gH_2O_2} = 0.0294\ \text{M}\ \ H_2\ O_2$$

Table B.1. Molar ratios for the UVC/H_2O_2 and VUV/ H_2O_2.

TOC concentration (mg L^{-1})	**Carbon molar mass (g mol^{-1})**	**Molar concentration (mol L^{-1})**	**UV/H_2O_2 Molar ratio [H_2O_2]/[TOC]**	**VUV/H_2O_2 Molar ratio [H_2O_2]/[TOC]**
230	12	0.0192	0.92	1.53
140	12	0.0117	1.51	2.52
22	12	0.0018	9.62	16.04

Example of TOC molar concentration calculation for meat extract

$$140\frac{mg\ C}{L}\ \times\ \frac{1gC}{1000mgC}\times\frac{1\ mol\ C}{12\ gC} = 0.0117\frac{mol\ C}{L}$$

APPENDIX C: Determination of the reactor effective volume

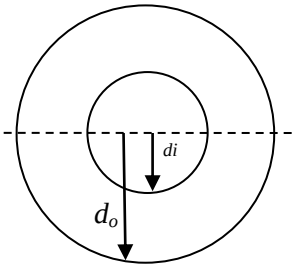

Figure C.1. Reactor cross section.

The effective volume of each photoreactor can be calculated by Equation (C.1), where *V*, d_o, d_i and h are the photoreactor volume, volumetric flow rate, inner diameter of annular photoreactor, outer diameter of quartz sleeve (Figure C.1) and photoreactor length, respectively.

$$V = \frac{\pi}{4}(d_0^2 - d_i^2)h \qquad (C.1)$$

Therefore,

$$V = \frac{\pi}{4}(\,51^2 - 24.4^2) \times 305\ mm$$

$$V = 4.8 \times 10^5 mm^3 \times \frac{1\ cm^3}{10^3\ mm^3} = 4.6 \times 10^2 cm^3$$

$$V = 4.6 \times 10^2 cm^3 \times \frac{1\ L}{1000\ cm^3} = 0.46\ L$$

Therefore, the volume of each photoreactor is 0.46 L.

The cross-sectional area is

$$A = \frac{(D_0^2 - D_i^2)\pi}{4} \qquad (C.2)$$

$$A = \frac{(51^2 - 24.4^2\ mm)\ \pi}{4}$$

$$A = 1.6\ \times 10^3\ mm^2\ \times \frac{1\ m^2}{1000^2\ mm^2}\ = 1.6 \times 10^{-3}\ m^2$$

Thus, the irradiation time *t* can be calculated from volume *V* and flow rate *Q* as shown in Equation (D.1)

$$t = \frac{V}{Q} \qquad (D.1)$$

APPENDIX D: Determination of the Reynolds number for the different flow rates during bacteria inactivation

For flow in a pipe the Reynolds number is determined by Equation (E.1)

$$R_e = \frac{uD}{v} \qquad (E.1)$$

where *Re* is Reynolds number, *u* is average velocity of the fluid, *D* is equivalent diameter of the pipe, and *v* is kinematic viscosity. A kinematic viscosity for water at 30°C is $1.004 \times 10^{-6}\ m^2\ s^{-1}$

The velocity of the fluid was obtained from:

$$u = \frac{Q}{A} \qquad (E.2)$$

From Equation (E.3) we obtained

$$A = \frac{(D_o^2 - D_i^2)\pi}{4} \qquad (E.3)$$

Since flow rate *(Q)* value is given by the system configuration, the Reynolds number can be obtained as follow

$$A = 1.6 \times 10^{-3} m^2$$

$$Q = 1\frac{L}{min} \times \frac{1m^3}{1000\ L} \times \frac{1\ min}{60\ s} = 1.7 \times 10^{-5}\ \frac{m^3}{s}$$

$$u = \frac{1.7 \times 10^{-5}\ \frac{m^3}{s}}{1.6 \times 10^{-3}\ m^2} = 0.0106\frac{m}{s}$$

Thus, the Reynolds number for Q= *1 L min*$^{-1}$ at 20°C is

$$R_e = \frac{0.0106\ \frac{m}{s}\ (0.051 - 0.0244)\text{m}}{1.004 \times 10^{-6}\frac{m^2}{s}} = \ 276$$

Table (D.1) groups the Reynolds number used during experiments on recirculation and continuous operation.

Table D.1. Reynolds number for different flow rates

Flow rate (Q) (L min^{-1})	**Flow rate (Q) (m^3 s^{-1})**	**Area (A) (m^2)**	**Velocity (u=Q/A) (m s^{-1})**	**Reynolds number* (Re = uD/v)**
0.1	1.7×10^{-6}	1.6×10^{-3}	1.1×10^{-3}	27.6
0.2	3.3×10^{-6}	1.6 × 10-3	2.1×10^{-3}	55.63
0.3	5.3×10^{-6}	1.6 × 10-3	3.3×10^{-3}	87.8
0.5	8.3×10^{-6}	1.6×10^{-3}	5.2×10^{-3}	138
1	1.7×10^{-5}	1.6×10^{-3}	1.1×10^{-2}	276
Upper limit				
5.5	9.2×10^{-5}	1.6×10^{-3}	5.8×10^{-2}	1518
6	1.0×10^{-4}	1.6×10^{-3}	6.3×10^{-2}	1656
6.5	1.1×10^{-4}	1.6×10^{-3}	6.8×10^{-2}	1794
7	1.2×10^{-4}	1.6×10^{-3}	7.5×10^{-2}	1932

Notes:
*D= (Do – Di)
D_o = outside diameter
D_i = inside diameter

APPENDIX E: Determination of the quantum yield (ϕ)

The quantum yield can be calculated by Equations (E.1) and (E.2) as follows (Shemer *et al.*, (2006); Sharpless and Linden, 2003):

$$\phi\,[M] = \frac{-d[M]/dt}{k_{s(\lambda)}} \qquad (E.1)$$

$$k_{s(\lambda)} = \frac{q_{0(\lambda)}\varepsilon_\lambda[1 - 10^{-\alpha_\lambda(r-R_i)}]}{\alpha_\lambda(r - R_i)} \qquad (E.2)$$

Equation (E.1) may be rearranged as:

$$\phi\, k_{s(\lambda)} dt = \frac{-d[M]}{[M]} \qquad (E.3)$$

Rearranging Equation (E.3) for integration gives

$$\int_{t_0}^{t_f} \phi\, k_{s(\lambda)} dt = -\int_{M_0}^{M_f} \frac{d[M]}{[M]} \qquad (E.4)$$

which after integration becomes

$$\phi\, k_{s(\lambda)}(t) = \ln\left[\frac{M_{intial}}{M_{final}}\right] \qquad (E.5)$$

Solving for ϕ it is obtained

$$\phi_{(254nm)} = \frac{ln\left[\frac{M_{initial}}{M_{final}}\right]}{(t)k_{s_{(254\ nm)}}} \qquad (E.6)$$

where M is the TOC concentration, *mol* L^{-1}, $k_{s(\lambda)}$ is the specific rate of light absorption by TOC (Einstein mol^{-1} s^{-1}), q_o is the radiant energy flux on the sleeve wall (Einstein m^{-2} s^{-1}), α_λ is the decadic absorption coefficient (cm^{-1}) and r and R_i are the outer and inner radius respectively

Initial and final TOC concentrations $[TOC]_{in}$ and $[TOC]_f$ (mol L^{-1}) are obtained by

$$[TOC]_{initial} = 140\frac{mg\ TOC}{L} \times \frac{1g\ TOC}{1000mgTOC} \times \frac{1mol\ TOC}{12gTOC} = 1.17 \times 10^{-2}\frac{\text{moles TOC}}{L}$$

$$[TOC]_{final} = 65\frac{mg\ TOC}{L} \times \frac{1g\ TOC}{1000mgTOC} \times \frac{1mol\ TOC}{12gTOC} = 5.41 \times 10^{-3}\ \frac{\text{moles TOC}}{L}$$

According to Oppenlander (2003), the energy (E) of a single photon at 254 nm is calculated by

$$E_{(254\ nm)} = \frac{hc}{\lambda} \qquad (E.7)$$

where (h) is the plank's constant (6.626×10^{-34} s/J), (c) is the speed of light 2.998×10^{8} (m/s), and (λ) is the wavelength in (nm)

Thus, when replacing the aforementioned values into Equation (E.7) the energy of a photon at 254 nm is:

$$E_{(254\ nm)} = \frac{6.626\ \times 10^{-34} s/J\ \times 2.998 \times 10^{8} m/s}{254 \times 10^{-9} m} = 7.82\ \times 10^{-19}\ \frac{J}{photon}$$

Energy of a mol of photons can be calculated by using Avogadro's number (N_A):

$$E_{(254\ nm)} = 7.82\ \times 10^{-19}\ \frac{J}{photon} \times \frac{6.023 \times 10^{23}\ photons}{1\ mol\ of\ photons} = 4.71 \times 10^{5}\ \frac{\text{J}}{\text{mol of photons}}$$

The energy E is used to calculate the incident light flux, q_o, (Einstein $cm^{-2}\ s^{-2}$) in the quartz sleeve is calculated by dividing the power of the lamp by the surface area, S, (cm^2) of the quartz sleeve as follows

$$S = 2\pi R_i L \qquad (E.8)$$

$$S = 2\pi(1.24\ cm^2)(30.5\ cm) = 229.9\ cm^2$$

Therefore,

$$q_o = \frac{14\ W}{229.9\ cm^2} \times \frac{1J/S}{1W} \times \frac{1\ \text{mol of photons}}{4.71 \times 10^5\ J} = 1.29 \times 10^{-7}\ \frac{\text{mol photon}}{cm^2.s}$$

The molar absorption coefficient $\varepsilon_{TOC_{(254\ nm)}}$ is calculated as follows

$$\varepsilon_{TOC_{(254\ nm)}} = \frac{A}{c.l}$$

where *A* is absorbance determined by a spectrophotometer ((Ultrospec™ *1100 pro* UV/visible) at 254 nm. *C* is the TOC concentration (mol L^{-1}), and *l* is the pathlength (cm), which is 1 cm — given by the spectrophotometer cuvette.

$$\varepsilon_{TOC_{(254nm)}} = \frac{0.120}{0.0117\ \frac{mol}{L} \times 1cm} = 10.34\ \frac{L}{mol.cm}$$

$$\alpha_{TOC_{(254\ nm)}} = \frac{0.120}{1cm} = 0.120\ \frac{1}{cm}$$

By inserting the values of q_o , $\varepsilon_{TOC_{(254nm)}}$, $\alpha_{TOC_{(254nm)}}$, and the pathlength (r-R_i), the specific rate of light absorption, $k_{s_{(254\ nm)}}$, by TOC can be determined as follows:

$$k_{s_{(254nm)}} = \frac{1.29 \times 10^7\ \frac{mol\ photons}{cm^2.s} \times 10.34\ \frac{L}{molTOC.cm} \times \frac{1000\ cm^3}{1L}[1 - 10^{-0.120(1.33)}]}{0.120\ \frac{1}{cm} \times 1.33\ cm}$$

$$k_{s_{(254nm)}} = 2.56 \times 10^{-3}\ \frac{mol\ photons}{molTOC.s}$$

Inserting all values into Equation (E.6), the quantum yield $\phi_{(254\,nm)}$ for the TOC photodegradation is

$$\phi_{(254\,nm)} = \frac{ln\left[\frac{TOC_{initial}}{TOC_{final}}\right]}{(t)k_{s_{(254nm)}}} = \frac{ln\left[\frac{1.17\times10^{-2}\,\frac{\text{moles TOC}}{L}}{5.41\times10^{-3}\,\frac{\text{moles TOC}}{L}}\right]}{9000\ s\times 2.56\times10^{-3}\,\frac{mol\ photons}{molTOC.s}} = 0.032\,\frac{mol\ TOC}{Einstein}$$

Note that 1 Einstein= 1 mol of photons

APPENDIX F: Momentum and mass balance equations

Momentum Balance

Equations (4.3) and (4.4) are the simplified form of the continuity and governing equations for the momentum balance

$$\nabla.V = 0 \qquad (4.3)$$

$$\rho V.\nabla V = -\nabla P + \nabla.\mu(\nabla V + (\nabla V)^T) \qquad (4.4)$$

where the del operator ∇ represents the gradient of the velocity ,*v*, in the difference axis *r*, *θ*, and *z* expressed in terms of derivatives with respect to *r*, *θ*, and *z* (Bird *et al.*, 2002)

$$\nabla . V = v_r \frac{\partial}{\partial r} + \frac{v_\theta}{r}\frac{\partial}{\partial \theta} + v_z \frac{\partial}{\partial z} \qquad (F.1)$$

For simplification purposes the velocity , *v*, in the *r*, and θ directions is omitted ($v_r = v_\theta = 0$) since it leads to pressure variations at any cross section of these directions (Wilkes, 2006). Therefore, only the axial momemtum balance — in the *z* direction — is considered to simplify the solution performed by the CFD software. According to Wilkes (2006), the continuity Equation (4.3) can be stated as

$$\frac{\partial \rho}{\partial t} + \frac{1}{r^2}\frac{\partial(\rho r^2 v_r)}{\partial \theta^2} + \frac{1}{r \sin\theta}\frac{\partial(\rho v_\theta \sin\theta)}{\partial \theta} + \frac{1}{r \sin\theta}\frac{\partial(\rho v_z)}{\partial z} = 0 \qquad (F.2)$$

With constant density and $v_r = v_\theta = 0$ the continuity equation becomes:

$$\frac{\partial v_z}{\partial z} = 0 \qquad (F.3)$$

Equation (4.4) that represents the governing equation for the momentum balance can be stated as follows:

$$\rho\left(\frac{\partial v_z}{\partial t} + v_r\frac{\partial v_z}{\partial r} + \frac{v_\theta}{r}\frac{\partial v_z}{\partial \theta} + v_z\frac{\partial v_z}{\partial z}\right) = -\frac{\partial p}{\partial z} + \mu\left(\frac{1}{r}\frac{\partial}{\partial r}\left[r\frac{\partial v_z}{\partial r}\right] + \frac{1}{r^2}\frac{\partial^2 v_z}{\partial \theta^2} + \frac{\partial^2 v_z}{\partial z^2}\right) - \rho g_z \; (F.4)$$

where ρ, *V*, *P*, and μ are the density, velocity, pressure, and the dynamic viscosity, respectively.

With $v_r = v_\theta = 0$ and continuity $\partial v_z / \partial z = 0$ (from Equation (F.3)). Since gravity, g, acts vertically downwards in z $g_z = 0$ Equation (F.4) becomes

$$\mu\left(\frac{1}{r}\frac{d}{dr}\left[r\frac{dv_z}{dr}\right]\right) = \frac{\partial p}{\partial z}$$

Mass Balance:

The continuity equation in cylindrical coordinates for a compound with constant density, ρ, and diffusivity D_{AB}, is given by

$$\nabla \cdot (V \cdot C_i) = \nabla(D\nabla C_i) + R_{rxn,i} \qquad (4.5)$$

Equation (4.5) can be stated as follows:

$$\left(v_r\frac{\partial C_i}{\partial r} + v_\theta\frac{1}{r}\frac{\partial C_i}{\partial \theta} + v_z\frac{\partial C_i}{\partial z}\right) = D_{AB}\left(\frac{1}{r}\frac{\partial}{\partial r}\left[r\frac{\partial C_i}{\partial r}\right] + \frac{1}{r^2}\frac{\partial^2 C_i}{\partial \theta^2} + \frac{\partial^2 C_i}{\partial z^2}\right) - R_{rxn,i}$$

where C_i is the concentration of species i (M), v_r, v_θ, v_z are the velocities (m/s) in the r- θ-, and z-directions, respectively, D_{AB} is the diffusivity of the species in the aqueous solution (m^2/s) an $R_{rxn,i}$ is the reaction of species i (M/s). only axial velocity is considered — in the z direction. The governing equations for momentum, mass balance and radiation balance were solved simultaneously by the CFD software (COMSOL Multiphysics V3.5).